eL15 and eL22 proteins and their functional environments during ribosome assembly in *Saccharomyces cerevisiae*

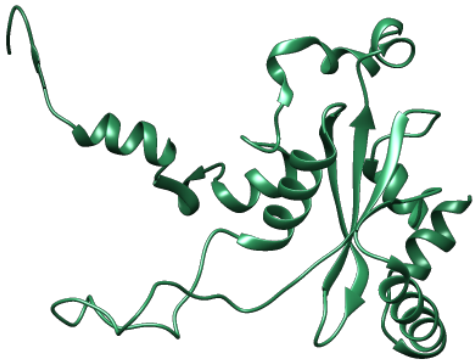

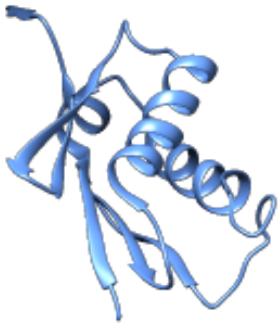

José Fernández Fernández

DOCTORAL THESIS 2023

Departamento de Genética
Universidad de Sevilla

eL15 and eL22 proteins and their functional environments during ribosome assembly in *Saccharomyces cerevisiae*

Memoria presentada para aspirar al grado de Doctor en Biología Molecular, Biomedicina e Investigación Clínica

V.° B.°: El director de la Tesis **El doctorando**

Jesús de la Cruz Díaz **José Fernández Fernández**

This work was funded by an FPI fellowship (BES-2017-080876), project grants from the Spanish Government (BFU2016-75352-P and PID2019-103850GB-I00) and the Andalusian Regional Government (P20_00581), and by an EMBO short-term fellowship (8468).

A Vane y Nico,

que me robaron el corazón

INDEX

RESUMEN

Los ribosomas son complejos ribonucleoproteicos encargados de la traducción de proteínas. La traducción es un proceso esencial en todos los organismos mediante el cual, la información contenida en el mRNA (RNA mensajero) se descodifica generando proteínas. El proceso de biogénesis ribosómica presenta igualmente una importancia crucial en todas las células. Los ribosomas se componen de dos subunidades diferenciadas, una llamada subunidad grande y otra llamada pequeña, también denominadas 60S y 40S en *Saccharomyces cerevisiae*, el organismo modelo usado en esta tesis. Como la biogénesis de los ribosomas está muy conservada entre los distintos eucariotas, *S. cerevisiae* es un organismo perfectamente adecuado para este estudio. Los ribosomas de *S. cerevisiae* están compuestos por 79 proteínas ribosómicas y 4 RNAs ribosómicos (rRNAs), tres de ellos en la subunidad grande (25S, 5.8S y 5S) y uno en la pequeña (18S).

La biogénesis de los ribosomas es un proceso extraordinariamente complejo en el que intervienen los cuatro rRNAs y las 79-80 proteínas ribosómicas, del orden de 100 RNAs pequeños nucleolares (snoRNAs) y más de 300 factores proteicos de ensamblaje, que al no formar parte de las subunidades maduras también son llamados factores de actuación en *trans*. La síntesis de ribosomas es un proceso secuencial altamente regulado y organizado que empieza en el nucleolo y progresa ordenadamente a través del nucleoplasma; las partículas pre-ribosómicas prácticamente completas son exportadas al citoplasma donde los últimos pasos de maduración tienen lugar antes de ser reclutadas al proceso de traducción. El papel de los distintos componentes que participan en la biogénesis de las subunidades ribosómicas ha sido ampliamente estudiado en las ultimas décadas. Sin embargo, aún quedan numerosos factores de ensamblaje y algunas proteínas ribosómicas por ser caracterizadas en detalle. Este era el caso de las proteínas ribosómicas eL22 y eL15 durante el ensamblaje de la subunidad 60S antes del estudio realizado en esta tesis doctoral.

Con respecto a la proteína ribosómica eL22, en esta tesis, hemos demostrado que, aunque en condiciones de laboratorio, esta proteína no es esencial para la supervivencia celular, el crecimiento celular y la síntesis de ribosomas desprovistos de eL22 se encuentran afectados. Así, hemos demostrado que la síntesis de ribosomas carentes de eL22 se encuentra ligeramente bloqueada en el núcleo. Nuestros resultados

indican que la presencia de eL22 es necesaria para el correcto procesamiento del pre-rRNA 27S. Además, hemos observado que eL22 juega un papel importante en el citoplasma, donde su presencia es probablemente necesaria para el reciclaje eficaz de los factores de ensamblaje Arx1 y Alb1.

Con respecto a la proteína ribosómica eL15, en esta tesis se demuestra que esta proteína es esencial para la producción de ribosomas maduros y, por tanto, para la supervivencia y el crecimiento celular. En concreto, hemos demostrado que eL15 es necesaria para el correcto procesamiento de los pre-rRNAs 27SA_3 y 27SB en el nucleolo. Esto a su vez se debe al papel de eL15 en la estabilización de partículas ribosómicas tempranas que permitan la unión estable de diversas proteínas ribosómicas de su propio grupo funcional (eL8, eL36 y eL13) y numerosos factores de ensamblaje, denominados factores A_3 y B que son necesarios para el procesamiento de los pre-rRNAs 27SA_3 y 27SB, respectivamente.

SUMMARY

Ribosomes are ribonucleoprotein complexes in charge of protein translation. Translation is an essential process in all organisms that involves decoding the information contained in mRNAs (messenger RNAs) to generate proteins. Similarly, the process of ribosome biogenesis represents a critical pathway for all cells. Ribosomes are comprised of two different subunits, one large and one small, also named 60S and 40S, respectively, in eukaryotes, among them *Saccharomyces cerevisiae,* which is the model organism employed in this thesis. As ribosome biogenesis is well conserved among different eukaryotes, *S. cerevisiae* is a perfectly appropriate organism for this study. Ribosomes of *S. cerevisiae* are composed of 79 ribosomal proteins and 4 ribosomal RNAs (rRNAs), three of them in the large (25S, 5.8S y 5S) and one in the small ribosomal subunit (18S).

The biogenesis of ribosomes is an extraordinarily complex process, in which in addition of the four rRNAs and the 79-80 ribosomal proteins, take part about 100 small nucleolar RNAs (snoRNAs) and more than 300 assembly protein factors, which are not present in the mature subunits and therefore are also known as *trans*-acting factors. The synthesis of ribosomes is a sequential process highly regulated and organized that starts in the nucleolus and orderly progresses through the nucleoplasm; almost mature ribosomal particles are exported to the cytoplasm, where the last steps of maturation take place, previously to their involvement in the translation process. The role of the different components participating in the biogenesis of the ribosomal subunits has been broadly studied through last decades. However, there are numerous assembly factors and some ribosomal proteins which still await characterization. This was the case for the ribosomal proteins eL22 and eL15 during the assembly of the 60S ribosomal subunit before the study performed in this doctoral thesis.

With respect to the eL22 ribosomal protein, in this thesis, we have observed that, although, in laboratory conditions, this protein is not essential for survival, cell growth and ribosome production are mildly affected in strains lacking eL22. In this context, we have proved that the synthesis of ribosomes lacking of eL22 is partially blocked in the nucleus. Thus, our results indicate that the presence of eL22 is necessary for the correct processing of the 27S pre-rRNAs. Moreover, we have observed that eL22 performs an

important role in the cytoplasm, where its presence is likely needed for the efficient recycling of assembly factors Arx1 and Alb1.

With respect to the eL15 ribosomal protein, in this thesis, we have shown that this protein is essential for the production of mature ribosomes and, thus, for the cell survival and cell growth. Specifically, we have demonstrated that eL15 is necessary for the precise processing of the $27SA_3$ and 27SB pre-rRNAs in the nucleolus. This is due to the role of eL15 in the stabilization of early ribosomal particles which permits the stable assembly of proteins of its own functional cluster (eL8, eL36 y eL13) and association of numerous assembly proteins, known as A_3- and B-factors, which are necessary for the processing of the $27SA_3$ and 27SB pre-rRNAs, respectively.

INTRODUCTION

Structure, function and evolution of the ribosome

The ribosome is the macromolecular ribonucleoprotein complex responsible for catalysis of the translation process. During translation, ribosomes decode the information contained in messenger RNAs (mRNAs) in order to synthesize the corresponding proteins. Therefore, ribosomes are essential players in the process of gene expression [1].

Ribosomes are constituted of 54-80 ribosomal proteins (r-proteins) and 3-4 specific RNAs known as ribosomal RNAs (rRNA) distributed in two ribosomal subunits (r-subunits), a large subunit (LSU) and a small one (SSU). These subunits are named according to their sedimentation coefficient; the LSU is termed 50S in prokaryotes and 60S in eukaryotes. In turn, the SSU is named 30S in prokaryotes and 40S in eukaryotes. Both subunits together form the 70S ribosome in prokaryotes and the 80S in eukaryotes [2,3]. There are also specific ribosomes in mitochondria and chloroplasts [4,5]. Both subunits exert different functions; the LSU catalyses the formation of peptide bonds in the peptidyl-transferase centre (PTC), while the SSU is responsible for decoding mRNAs by base pairing of their codons with the transfer RNAs (tRNAs) in the decoding centre [6]. Translation initiates when an SSU, an LSU and an mRNA come together building an active ribosome. In the subunit interface, the A (acceptor), P (peptidyl) and E (exit) sites are formed. The A-site is the first binding site for tRNAs in the ribosome while the P-site is the second and the E-site the last one. The A-site is the place in the ribosome where the charged aminoacyl-tRNAs enters. The P-site holds a tRNA with the growing polypeptide chain for peptide bond formation. The E-site is the site at which the deacylated tRNAs bind before they dissociate from the ribosome. The mRNA moves along the groove of the SSU as it is being decode while the nascent protein in formation exits through the polypeptide exit tunnel (PET) that is located in the LSU [6].

In this work, we have used the budding yeast *Saccharomyces cerevisiae* as a model organism. This is an eukaryotic organism with the advantages of low complexity, fast growth and available powerful biochemical, genetic and molecular tools. The process of ribosome biogenesis has been studied in several other eukaryotes, including humans, but most of our current knowledge in this process comes from yeast. In *S.*

cerevisiae, the LSU is composed of 46 r-proteins and 3 rRNAs named 25S, 5.8S and 5S. The SSU is composed of 33 r-proteins and one rRNA named 18S [3].

Regarding the structure of ribosomes, a repertoire of techniques such as cryogenic electron microscopy (cryo-EM) and X-ray crystallography has provided the field with detailed models at atomic or subatomic resolution **(Figure 1)**. Although rRNAs and r-proteins are distributed all intertwined along the r-subunits, proteins are more commonly situated at the solvent exposed surface while rRNAs are mainly in the subunit interface, where play crucial role in the functional centres. Several structural domains can be highlighted in the r-subunits **(Figure 1)**. In the SSU, it can be distinguished the domains named beak, head, platform and body. The groove of mRNA is formed between the head and the body and platform, where the mRNA moves while is being decoded. In the LSU, the main domains are the central protuberance (CP), where is situated the PTC, the L1-stalk and the P-stalk [7-9].

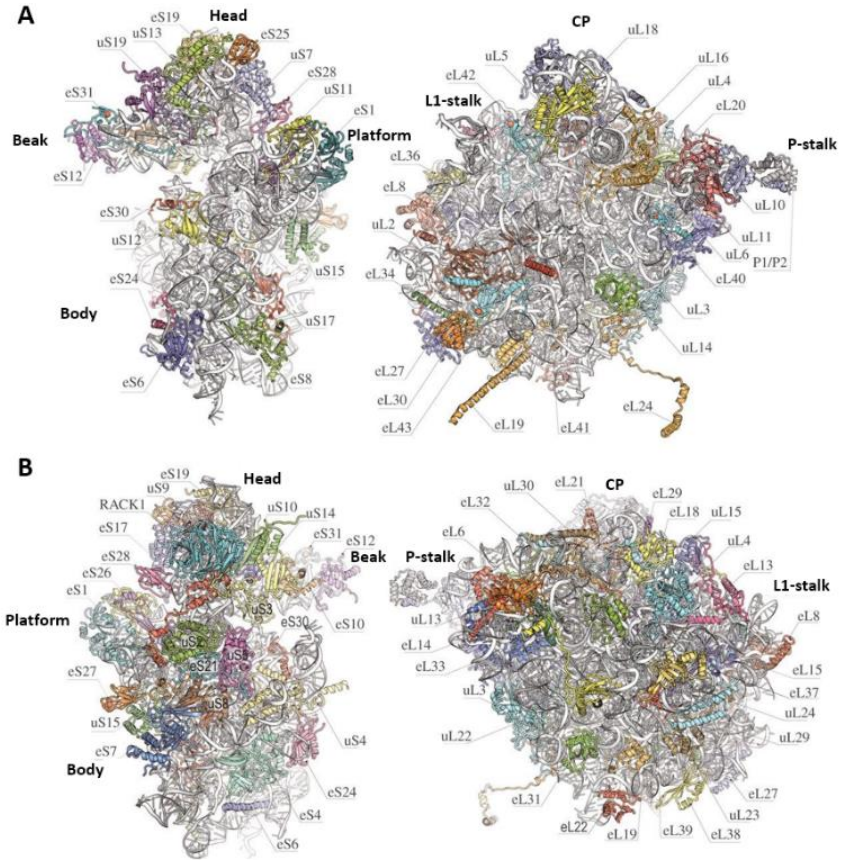

Figure 1. **Architecture of the yeast r-subunits.** The figure shows the small r-subunit or SSU (left) and the large r-subunit or LSU (right). The model shows the location of the different r-proteins. Main structural features are highlighted: head, beak, platform and body in the small r-subunit; central protuberance (CP), L1-stalk and P-stalk in the large r-subunit. **(A)** Interface view. **(B)** Solvent exposed view. Adapted from [10].

Ribosomes are well conserved in evolution. However, it can be appreciated an increase in complexity and size from prokaryotes to eukaryotes **(Figure 2)**. There is a conserved common core, which involves the functional centres and that corresponds mainly to the prokaryote ribosome. Over this core, evolution has added a "shell", layer that is formed by some expansion segment (ES) of rRNA, r-proteins, and eukaryote-specific r-protein extensions. This layer is distributed towards the periphery of the ribosome, mainly in the solvent exposed surface. Although the biological function of rRNA ESs is not fully understood, their accessibility on the surface of the LSU raises the possibility that they could play a role in the recruitment of ribosome assembly factors and r-proteins during assembly. Most of the r-protein extensions interact with other eukaryote-specific r-proteins and rRNA ESs, suggesting that extensions of the conserved proteins may facilitate the assembly of eukaryote-specific ribosome components. These specific elements also provide new interactions with elements involved in translation; indeed, translation initiation presents several differences between kingdoms and therefore, many eukaryotic specific components have been found to participate in this process [7,11].

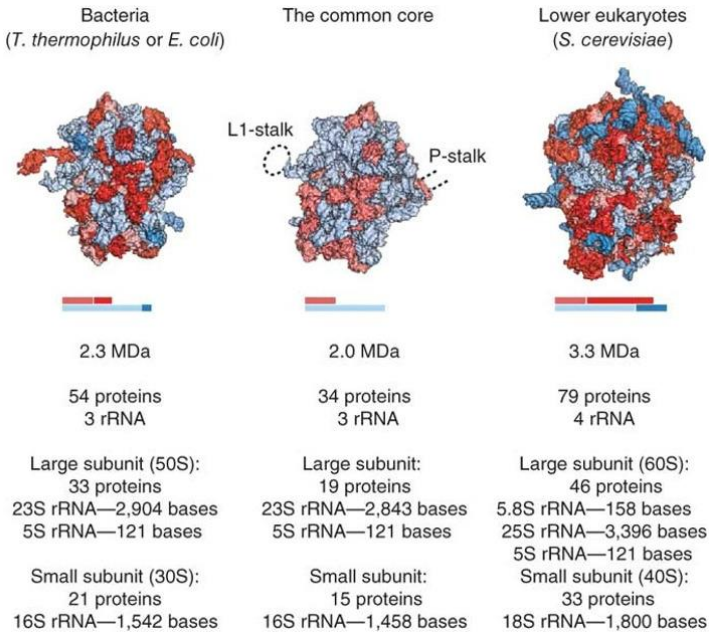

Figure 2. Comparative composition of bacterial and eukaryotic ribosomes. The common core between bacteria and eukaryotes is shown in light red (proteins) and light blue (rRNA). Both, bacteria and eukaryotes contain specific r-proteins and/or extensions and insertions in those r-proteins that are conserved (both in red). The expansion segments of rRNA are shown in blue. Dashed lines around the common core represent the position of the stalks that are used to be flexible in X-ray structures. Adapted from [11].

Ribosomal proteins

Most r-proteins are characterized for their basic nature, small size and the presence of intrinsically disordered domains **(Figure 3)**.

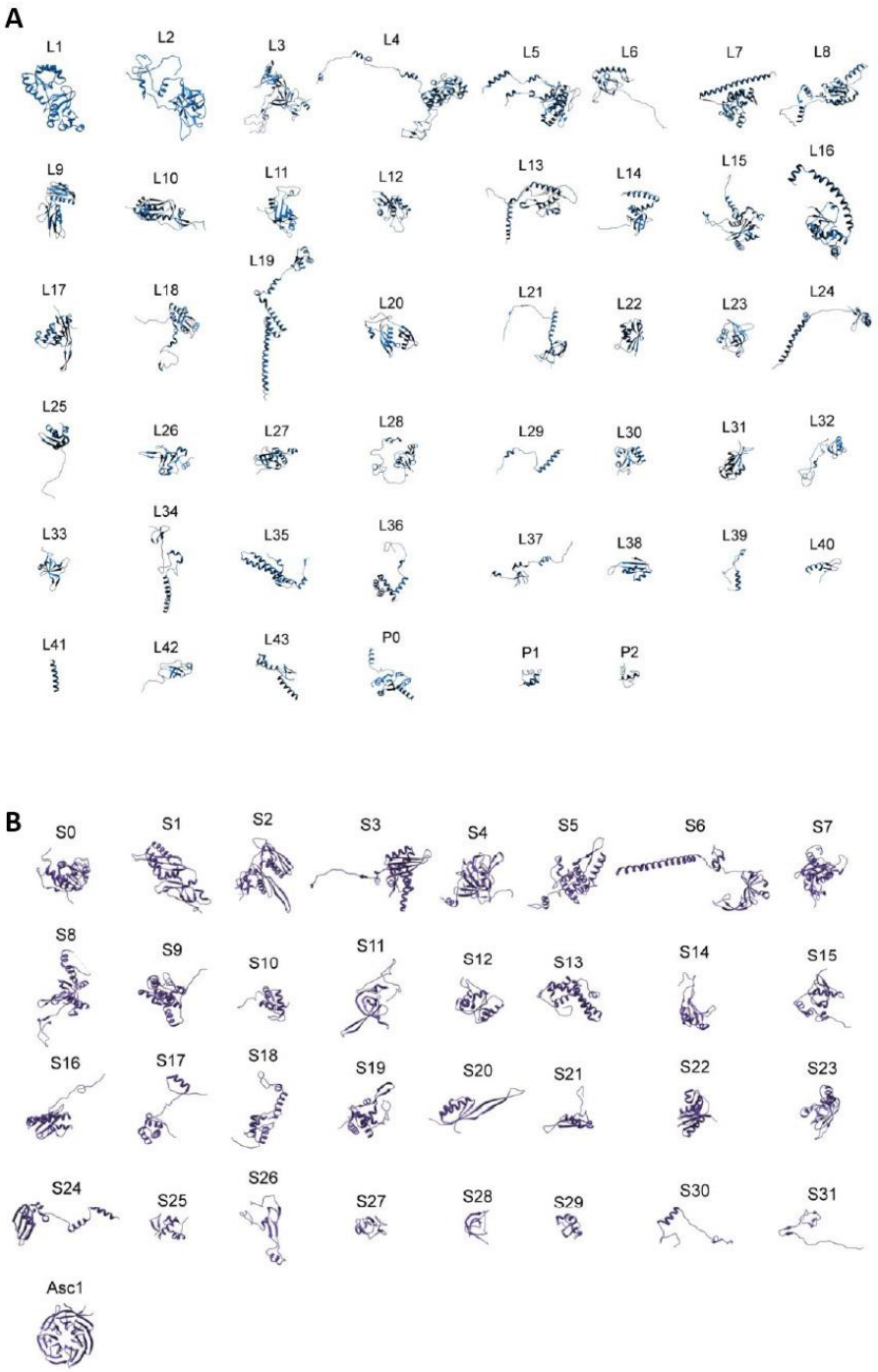

Figure 3. Ribosomal proteins from *S. cerevisiae*. All yeast r-proteins are shown. These usually present terminal or internal extensions that spreads from their globular regions. **(A)** Structure of r-proteins from the large r-subunit. **(B)** Structure of r-proteins from the small r-subunit. Note that r-proteins are named using a former, non-updated nomenclature system. Adapted from Espinar-Marchena, F. J., Doctoral thesis. 2017.

The small size feature of r-proteins has been interpreted as a fitness required for the high cellular demand of ribosomes and the necessity of limiting the time that ribosomes spend on their own production, thus allowing them to be involved in the translation of the non-ribosomal proteome. In this context, it has been speculated that it could be more effective to produce more and smaller r-proteins than less but larger ones, minimizing the time that growing peptides are been translated. On the contrary, rRNAs are few and particularly large, likely due to the fact that the assembly of rRNAs with r-proteins is mainly a co-transcriptional process. Furthermore, rRNA contributes to an extraordinary part of the ribosome mass, not only in catalytic regions but also developing structural tasks. Production of proteins costs at least twice than RNA in terms of time and energy so it has also been rationalised the use of RNA when this is chemical and functionally possible. The adaptation to a high growth rate has been suggested as the reason to explain the compositional differences between ribosomes from prokaryotes, eukaryotes or mitochondria that evolved upon different selective pressure [12].

The r-proteins are mainly basic because they interact with rRNA, thus, acting to neutralise the negative charge of the latter. However, this feature, together with the tendency of r-proteins to display intrinsically disordered domains, causes that free r-proteins are prone to interact with other cellular components and aggregate resulting in proteotoxicity. To avoid this, selection has arisen general chaperones able to fold the r-proteins even co-translationally and rapidly transport them to the nuclear assembly sites. Furthermore, there is a specific group of proteins named dedicated chaperones that assist folding, transport into the nucleus and delivery of selected r-proteins into the maturing r-subunit intermediates [13,14]. To avoid proteotoxicity, excess of free r-proteins is efficiently degraded by the proteasome; this system, known as ERISQ (excess ribosomal protein quality control), involves the ubiquitin ligase Tom1, which adds ubiquitin moieties to r-protein regions normally masked when they are integrated in the r-subunits [15,16]. Regarding the degradation of mature r-subunits and pre-ribosomal particles, several different mechanisms have been described. In the cytoplasm, these complexes are degraded by the non-functional rRNA decay (NRD) pathway. This pathway is different for each r-subunit [17]. SSU degradation is located in the P-bodies

and shares components with the no-go-decay (NGD) pathway used to degrade mRNAs containing a structural barrier into their open reading frames that causes ribosome stalling [18,19]. Degradation of LSUs is dependent on ubiquitination, involves the proteasome and is located in a perinuclear compartment [20,21]. Moreover, the degradation of ribosomes is dependent on the growth condition. Upon starvation, the excess of LSUs is selectively marked for degradation by a specific type of autophagy pathway known as ribophagy that also involves ubiquitination. SSUs are also subjected to ribophagy but the mechanisms for this process are still unknown [22,23].

Many r-proteins, especially in eukaryotes, have long terminal extensions or internal loops that extend from the globular structured domains and which have a variety of functions. These extensions are normally disordered when the r-proteins are not incorporated into ribosomes. Extensions penetrate deep into the ribosome to stabilize rRNA junctions [24]. Extensions can also act as binding sites for chaperones and biogenesis factors or harbour nuclear localization signals (NLSs) for the import of r-proteins to the nucleus [25,26]. In some cases, extensions have been described to provide extra-ribosomal functions [27,28].

In *S. cerevisiae*, most r-proteins are encoded by two paralogs in the genome, their sequences usually being identical or very similar to each other. Deletion of each paralog displays different phenotypes [29,30]. This diversity has been explained by different means. First, different paralogs have different expression levels [31]. Second, some extra-ribosomal functions for r-proteins are paralog-dependent [32]. Finally, assembly of different paralogs can generate heterogeneous ribosomes that could play specific roles, for example, translating preferentially subsets of mRNAs. Ribosome specialisation is a very exciting field and additional sources of ribosome heterogeneity as modifications of r-proteins or rRNA, alternative forms of rRNAs and changes in ribosomal-associated proteins have also been proposed to be relevant [33].

The nomenclature for the r-proteins has been subjected to some changes through the last years. Unfortunately, the fact that prokaryotes and eukaryotes orthologs were not always named similarly has generated some confusion in the past. A recent effort to solve this problem has carried out with the establishment of an universal nomenclature system. **Table 1** summarises standard and novel names to bacterial, yeast

and human r-proteins [34]. When possible, this novel nomenclature system will be used in this thesis work.

Nomenclature for proteins from the large ribosomal subunit				
New name	Taxonomic range	Bacteria name	Yeast name	Human name
uL1	B A E	L1	L1	L10A
uL2	B A E	L2	L2	L8
uL3	B A E	L3	L3	L3
uL4	B A E	L4	L4	L4
uL5	B A E	L5	L11	L11
uL6	B A E	L6	L9	L9
eL6	E	–	L6	L6
eL8	A E	–	L8	L7A
bL9	B	L9	–	–
uL10	B A E	L10	P0	P0
uL11	B A E	L11	L12	L12
bL12	B	L7/L12	–	–
uL13	B A E	L13	L16	L13A
eL13	A E	–	L13	L13
uL14	B A E	L14	L23	L23
eL14	A E	–	L14	L14
uL15	B A E	L15	L28	L27A
eL15	A E	–	L15	L15
uL16	B A E	L16	L10	L10
bL17	B	L17	–	–
uL18	B A E	L18	L5	L5
eL18	A E	–	L18	L18
bL19	B	L19	–	–
eL19	A E	–	L19	L19
bL20	B	L20	–	–
eL20	E	–	L20	L18A
bL21	B	L21	–	–
eL21	A E	–	L21	L21
uL22	B A E	L22	L17	L17
eL22	E	–	L22	L22
uL23	B A E	L23	L25	L23A
uL24	B A E	L24	L26	L26
eL24	A E	–	L24	L24
bL25	B	L25	–	–
bL27	B	L27	–	–
eL27	E	–	L27	L27
bL28	B	L28	–	–
eL28	E	–	–	L28
uL29	B A E	L29	L35	L35
eL29	E	–	L29	L29
uL30	B A E	L30	L7	L7
eL30	A E	–	L30	L30
bL31	B	L31	–	–
eL31	A E	–	L31	L31
bL32	B	L32	–	–
eL32	A E	–	L32	L32
bL33	B	L33	–	–
eL33	A E	–	L33	L35A
bL34	B	L34	–	–
eL34	A E	–	L34	L34
bL35	B	L35	–	–
bL36	B	L36	–	–
eL36	E	–	L36	L36
eL37	A E	–	L37	L37
eL38	A E	–	L38	L38
eL39	A E	–	L39	L39
eL40	A E	–	L40	L40
eL41	A E	–	L41	L41
eL42	A E	–	L42	L36A
eL43	A E	–	L43	L37A
P1/P2	A E	–	P1/P2 (AB)	P1/P2 (αβ)
b: bacterial, e: eukaryotic, u: universal				
B: bacteria, A: archaea, E: eukaryotes				

Nomenclature for proteins from the small ribosomal subunit				
New name	Taxonomic range	Bacteria name	Yeast name	Human name
bS1	B	S1	–	–
eS1	A E	–	S1	S3A
uS2	B A E	S2	S0	SA
uS3	B A E	S3	S3	S3
uS4	B A E	S4	S9	S9
eS4	A E	–	S4	S4
uS5	B A E	S5	S2	S2
bS6	B	S6	–	–
eS6	A E	–	S6	S6
uS7	B A E	S7	S5	S5
eS7	E	–	S7	S7
uS8	B A E	S8	S22	S15A
eS8	A E	–	S8	S8
uS9	B A E	S9	S16	S16
uS10	B A E	S10	S20	S20
eS10	E	–	S10	S10
uS11	B A E	S11	S14	S14
uS12	B A E	S12	S23	S23
eS12	E	–	S12	S12
uS13	B A E	S13	S18	S18
uS14	B A E	S14	S29	S29
uS15	B A E	S15	S13	S13
bS16	B	S16	–	–
uS17	B A E	S17	S11	S11
eS17	A E	–	S17	S17
bS18	B	S18	–	–
uS19	B A E	S19	S15	S15
eS19	A E	–	S19	S19
bS20	B	S20	–	–
bS21	B	S21	–	–
bTHX	B	THX	–	–
eS21	E	–	S21	S21
eS24	A E	–	S24	S24
eS25	A E	–	S25	S25
eS26	E	–	S26	S26
eS27	A E	–	S27	S27
eS28	A E	–	S28	S28
eS30	A E	–	S30	S30
eS31	A E	–	S31	S27A
RACK1	E	–	Asc1	RACK1
b: bacterial, e: eukaryotic, u: universal				
B: bacteria, A: archaea, E: eukaryotes				

Table 1. Novel and former nomenclatures for r-proteins. Former and current names are indicated. The r-proteins from bacteria (B), archaea (A) and eukaryotes (E) are shown. Taken from [34].

Ribosome biogenesis

The synthesis of ribosomes is one of the most important processes for cellular growth and consumes a vast amount of all cellular resources. In this regard, yeast cells growing exponentially produce about 2000 ribosomes per minute. To achieve this production, 60% of total transcription is dedicated to rRNAs, and about 50% of the overall transcription from RNA polymerase II (RNAPII) and approximately 90% of all splicing reactions correspond to pre-mRNAs of r-proteins [35]. Furthermore, during ribosome biogenesis, in addition to rRNAs and r-proteins, about 80 small nucleolar RNAs (snoRNAs) and more than 200 *trans*-acting proteins, also known as ribosomal assembly factors, take part. These protein factors assist the assembly of r-proteins with the precursors of rRNAs (pre-rRNAs) and are involved in a variety of tasks as folding, modification and processing of rRNA, and transport, modification and assembly of r-proteins. These factors also provide speed, accuracy, directionality and regulation to the overall process [36].

In *S. cerevisiae*, ribosome assembly initiates in the nucleolus, where a subset of the repeats of rDNA are transcribed. Each active repeat unit is transcribed by RNAPI and RNAPIII to respectively synthesize the 35S and 5S primary pre-rRNA transcripts **(Figure 6)**. There are about 150 tandem repeats of 35S/5S rDNA in yeast but not all of them are simultaneously engaged in transcription; instead, there are active and inactive copies, normally 50% each in normal growth conditions. The 35S rDNA unit encodes for 18S, 5.8S and 25S rRNAs and is transcribed by RNAPI. The 5S rDNA is transcribed separately by RNAPIII [37]. The pre-rRNAs associate co-transcriptionally with factors and r-proteins to form pre-ribosomal particles. Along the maturation path of these pre-ribosomes from the nucleolus to the nucleoplasm and from there to the cytoplasm, r-proteins and factors are sequentially assembled in an orchestrated manner. In the same way, once the factors have completed their function, they are released and recycled back. These reactions take place in a specific spatiotemporal manner **(Figure 4)**. Moreover, the process is highly regulated and many steps of proofreading and checkpoints have been described [38].

Ribosome assembly is coordinated through different layers that distribute in a coaxial mode from the rDNA. The assembly of pre-40S particles (mainly in the SSU

processome state) starts in the inner nucleolar layer while the assembly of the pre-60S particles does in the outer nucleolar layer and in the nucleoplasm. The driving force for relocation of maturing pre-subunit is known as “vectorial two-phase partitioning” and is related to the different characteristics of the protein assembly factors that guide their location from one layer or another [39].

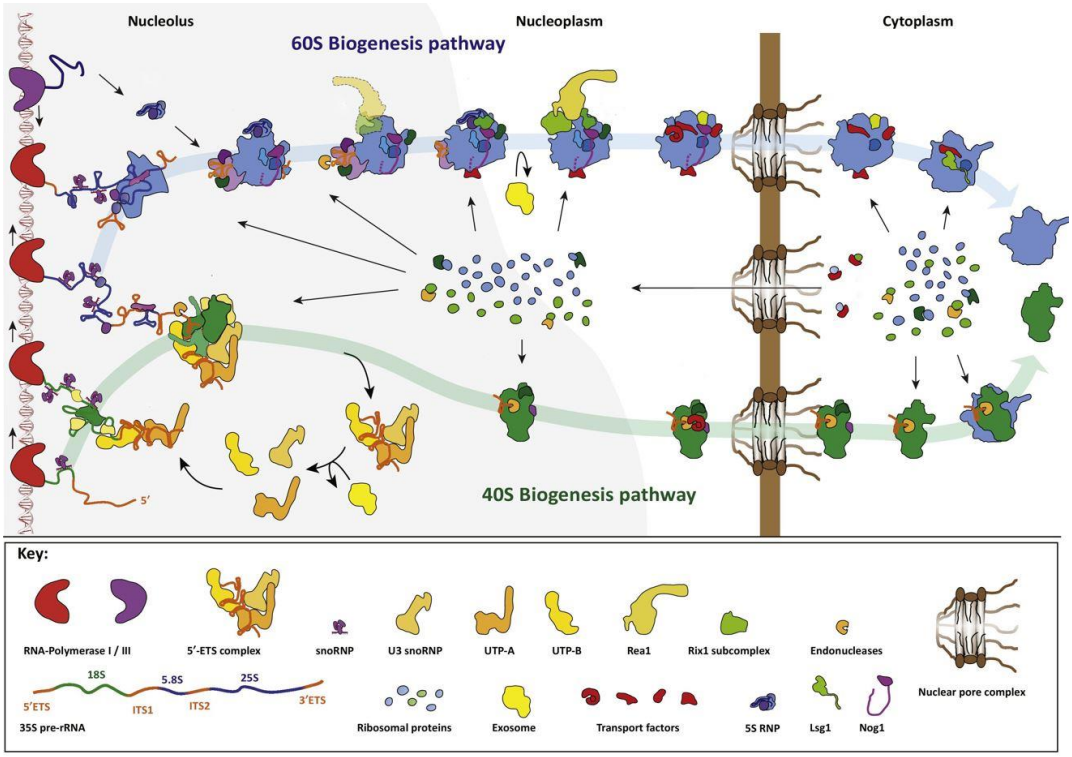

Figure 4. The assembly pathway of ribosomes in *S. cerevisiae*. Transcription of the 35S pre-rRNA and co-transcriptional association of r-proteins and assembly factors produce the 90S pre-ribosomal particle in the nucleolus. As the maturation process progresses, the 90S particle is first separated by cleavage at site A_2 in early pre-60S and pre-40S particles, whose maturation is therefore independent. Different processes occur in the transition from the nucleolus to the nucleoplasm. The pre-ribosomal particles are exported to the cytoplasm where the last steps of maturation take place to form mature r-subunits. Adapted from [40].

Moreover, the production of ribosomes depends on the growth rate, especially stimulated by nutrients availability and repressed by different stress conditions. It is also important that different ribosome components and factors maintain an appropriate concentration to permit ribosome stoichiometry. Basically, ribosome biogenesis is mainly controlled at the transcriptionally and post-transcriptionally level by TORC1 and Protein kinase A (PKA) signalling pathways **(Figure 5)** [41]. Due to the importance of ribosome biogenesis and function, failures on the assembly pathway have drastic cellular consequences. In humans, the dysfunction of ribosome synthesis and translation

results in a group of inherited pathologies known as ribosomopathies, which are linked to mutations affecting r-proteins and rRNA processing and assembly factor genes, or regulatory elements. In addition, mutation and misregulation of r-proteins genes are common features in several types of cancer [42,43].

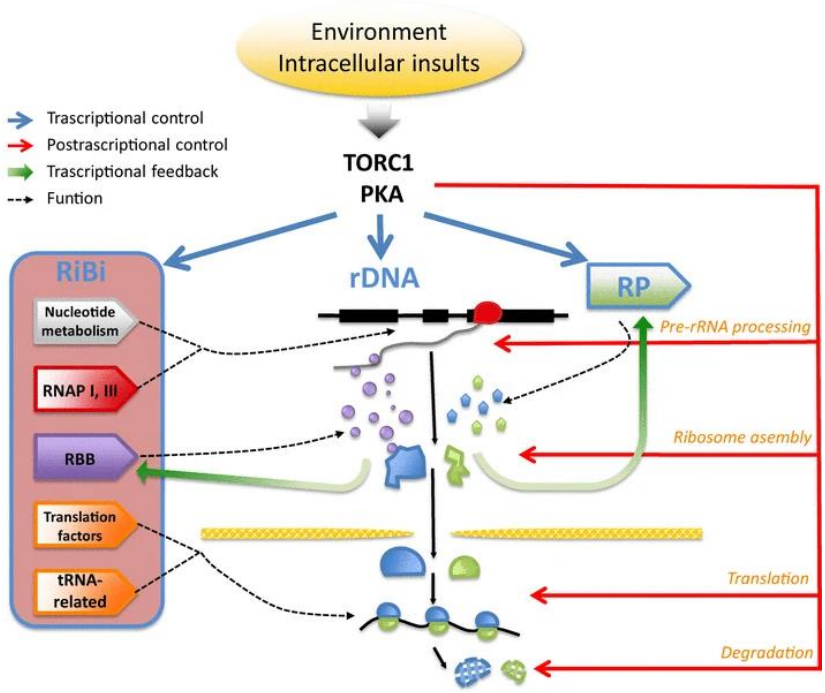

Figure 5. Regulation of ribosome biogenesis in *S. cerevisiae*. The TORC1 and PKA pathways regulate the synthesis of ribosomes. These signalling pathways control the transcription levels of r-proteins, protein assembly factors and rDNA. Post-transcriptionally, they also regulate pre-rRNA processing, ribosome assembly, translation and degradation at different levels. Besides, the process itself provides feedback regulation at different steps during the expression of pre-rRNAs, r-proteins and assembly factors. Adapted from [41].

Processing of precursor rRNAs

The yeast 35S pre-rRNA is the first detectable precursor transcribed by RNAPI. This harbours internal transcribed spacers (ITS1 and ITS2) and external transcribed spacers (5' ETS and 3' ETS). The 5S rRNA is transcribed by RNAPIII as a short precursor extended few nucleotides in its 3' end. These precursors (pre-rRNAs) undergo a complex stepwise process of modification and processing to produce the mature 18S, 5.8S, 25S and 5S rRNAs. The modification and processing reactions occur in the context of pre-ribosomal particles on the road of maturation [44]. **Figure 6** summarises the primary structure of the 35S and pre-5S pre-rRNAs and the different pre-rRNA processing steps in yeast.

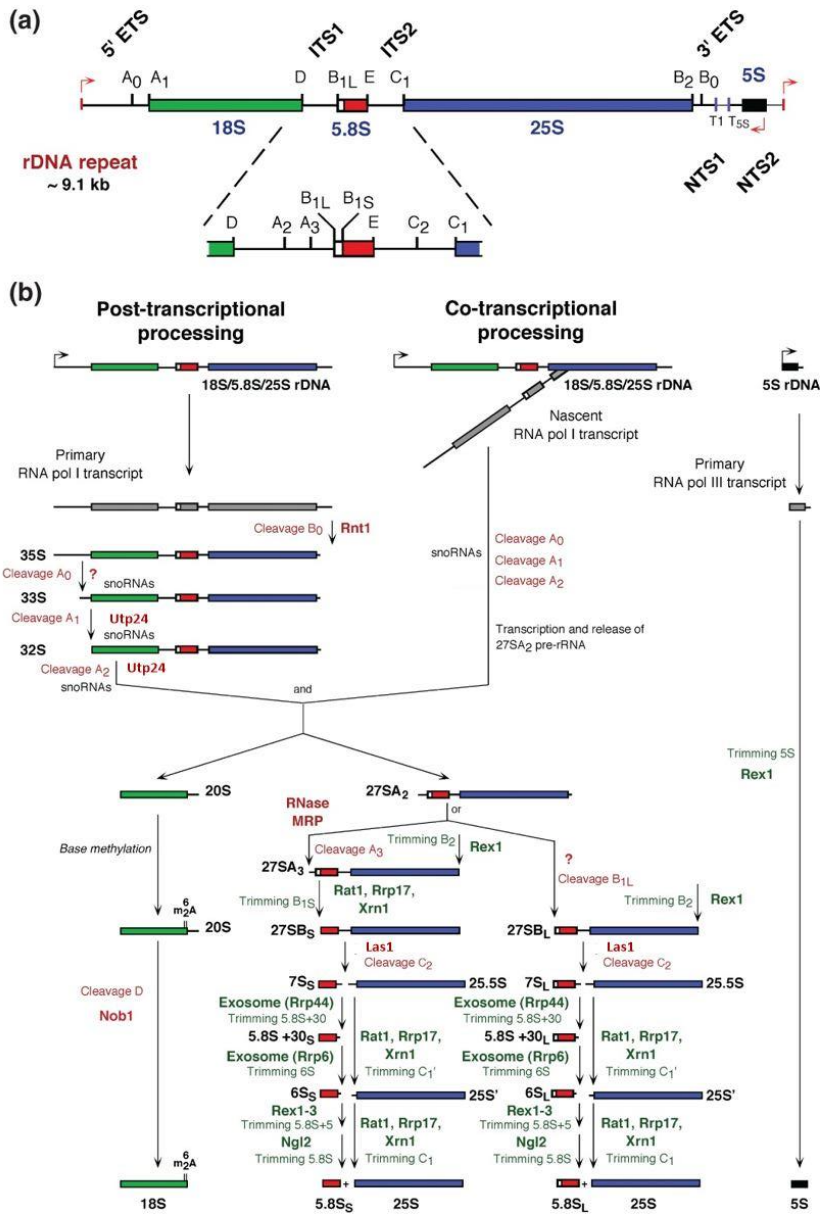

Figure 6. rRNAs maturation pathway. (**A**) Representation of a repeat unit of rDNA containing the two independently transcribed genes, the 35S rDNA is transcribed by RNA polymerase I into a polycistronic pre-rRNA, which encodes the 18S, 5.8S and 25S rRNAs whereas the 5S rDNA is transcribed by RNA polymerase III. Internal and external spacers (ETSs and ITSs) are indicated. Mature rRNAs are represented with bars and spacers with lines. The start of transcription is indicated by red arrows and the location of different processing sites are shown. (**B**) Pre-rRNA processing pathway. The 35S transcript is subjected to co- or post-transcriptional processing generating the 20S and $27SA_2$ pre-rRNAs, which are part of pre-40S or pre-60S r-particles, respectively. These pre-rRNAs are processed into the mature 18S, 5.8S and 25S rRNAs. The 5S pre-rRNA is processed into the mature 5S rRNA, which is a component of the LSU. Different steps, pre-rRNAs intermediaries and nucleases involved are indicated. Note that some cleavages still remain unassigned to specific nucleases. Adapted from [44].

Regarding pre-rRNA processing, the 35S pre-rRNA could be processed co- or post-transcriptionally. In rapidly growing cells, about 70% of the 35S pre-rRNA processing occurs in a co-transcriptional manner [45]. The 35S pre-rRNA processing initiates in the context of the particle called SSU processome. The first reactions remove the 5' ETS segment by cleavage at site A_0 and immediately after, at site A_1. It is not known the nuclease responsible for the cleavage at site A_0 but Utp24 has been suggested to be the endonuclease that cleaves at sites A_1 and A_2, although some authors had previously given this role to the Rcl1 endonuclease [46-48]. At its 3' end, processing of 35S pre-rRNA is poorly understood but seems to occur concomitantly to the processing reactions at sites A_0 and A_1 when processing is occurring post-transcriptionally. It seems that the endonuclease Rnt1 cleaves at the site B_0 and then, the 3'-5' exonuclease Rex1 trims from this site to the site B_2, which is the 3' end of mature 25S rRNA [49].

The cleavage at site A_1 is coupled and triggers that at site A_2 to generate the 20S and the $27SA_2$ pre-rRNAs [47]. This cleavage permits the separation of the SSU processome into the pre-40S and pre-60S r-particles that will undergo apparently independent maturation. Cleavage at site A_2 could occur co- or post-transcriptionally, so in the case of the co-transcriptional process, the early pre-60S r-particles is formed on nascent 27S pre-rRNA. In the cytoplasm, the 20S pre-rRNA is cleaved at site D to produce the mature 18S rRNA by the endonuclease Nob1 [50,51]. This is one of the last steps of maturation of pre-40S particles and occurs in the context of proofreading 80S-like particles, which are non-translating ribosomal particles formed by the association between a pre-40S r-particle and a mature LSU [52-54]. In slowly growing cells, cleavage at site A_3 is favoured *versus* cleavage at site A_2. This step is carried out by the MRP endonuclease and results in the formation of a 23S pre-rRNA. Whether or not processing of 23S pre-rRNA is productive (leading to a functional 18S rRNA) is still controversial [44,55].

The processing of the $27A_2$ pre-rRNA can be achieved in two ways. In about 85% of cases, this precursor is cleaved by MRP in the A_3 site, producing $27SA_3$ pre-rRNA that is then trimmed until the B_{1s} site to generate the $27SB_s$ pre-rRNA by 5'-3' exonucleases Rrp17, Rat1 and Xrn1 [56-58]. In the remaining 15% of the cases, $27SA_2$ pre-rRNA is cleaved by a still unknown endonuclease at the B_{1L} site producing the $27SB_L$ pre-rRNA.

The two isoforms of 27SB pre-rRNAs are processed in an identical way, being cleaved at the C_2 site in the middle of ITS2 by the endonuclease Las1. This reaction separates the 27SB pre-rRNAs in 25.5S and $7S_S$ or $7S_L$ pre-rRNAs [59,60].

In the nucleus, the 25.5S pre-rRNA is 5'-3' trimmed to mature 25S rRNA by the exonucleases Rrp17, Rat1 and Xrn1. In contrast, $7S_{L/S}$ pre-rRNAs are processed in a sequential and multistep process. First, the 3' end of $7S_{L/S}$ pre-rRNAs is trimmed in the nucleus by an exonucleolytic multi-protein complex named exosome to generate first the $5.8S_{L/S}$+30 pre-rRNAs and then the $5.8S_{L/S}$+8 pre-rRNAs, which are better known as $6S_{L/S}$ pre-rRNAs. In the cytoplasm, the Rex1-3 exonucleases trim the $6S_{L/S}$ pre-rRNAs generating the $5.8S_{L/S}$+5 pre-rRNAs, which are finally processed by the nuclease Ngl2 into mature $5.8S_S$ or $5.8S_L$ rRNAs [60-64].

On the other hand, the pre-5S rRNA is only subjected to minor processing. It is trimmed at the 3' end by 3'-5' exonucleases Rex1-3 to produce the mature 5S rRNA [65].

Concomitantly to processing, specially at very early steps, the pre-rRNAs are subjected to an extensive process of modification. Most of these modifications are conversions of uridines into pseudouridines and 2'-O-ribose methylations [66,67], which are executed by specific enzymes (Cbf5 and Nop1, respectively) that are specifically guided to their targets by a subset of about 80 snoRNAs. These snoRNAs are in complex with proteins forming small nucleolar ribonucleoproteins (snoRNPs). However, some other modifications are independent of snoRNAs. Interestingly, modifications are clustered in strategical regions of the rRNAs comprising the functional centres in the subunit interface; this fact clearly suggests that rRNA modifications play important role during translation [68,69].

Formation of the SSU processome or 90S pre-ribosomal particle

Co-transcriptional assembly of 35S pre-rRNA forms the primordial SSU processome, also known as 90S pre-ribosomal particle. Advances in cryo-EM have identified different r-particles that are typically referred as 90S, pre-40S or pre-60S r-particles, leading to the wrong idea of static snapshots and well-defined complexes. However, each of them encompasses a wide variety of maturation states. These states

present differences in the presence/absence of r-proteins and, which is more informative, protein assembly factors. These factors have been broadly identified in systematic compositional studies by co-immunoprecipitation with different r-proteins and selected assembly factors. In turn, the information obtained in these compositional studies has been the base to perform further cryo-EM studies of selected complexes, whose comparison has permitted to deeply know the structure and sequence of the maturation events. However, it has to still be considered that the study of these static particles has allowed to deduce certain dynamics of ribosome maturation.

The SSU processome is a cryo-EM particle that includes 5' ETS and a pre-rRNA precursor fragment containing 18S rRNA. The rest of the regions of the 35S pre-rRNA were not resolved in the structure as likely they are still flexible and unstructured at this point. In this particle, the sequence comprising 18S rRNA is organised in four topological domains: 5', central, 3' major and 3' minor domains, which are formed in a hierarchical 5' to 3' manner **(Figure 7)**. Prior folding, 35S pre-rRNA must be extensively modified by pseudouridylation and 2'-O-ribose methylation reactions, which are carried out by selected snoRNPs. These complexes must be released for further folding of the pre-rRNA and optimal r-protein assembly. Release of snoRNPs involves several enzymes including RNA helicases [40,70].

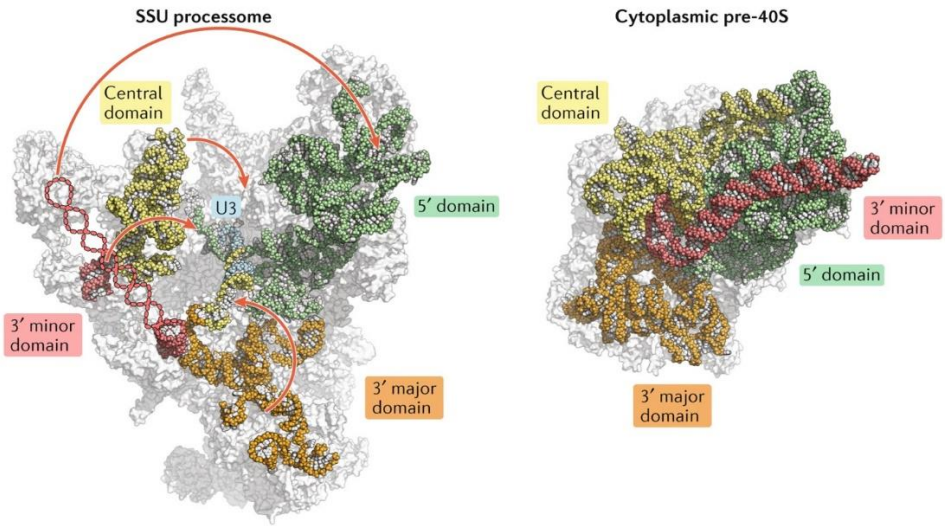

Figure 7. Arrangement of the 18S rRNA domains in the structured pre-rRNA in the SSU processome. Relative orientation of the different 18S rRNA domains in the yeast SSU processome and in the cytoplasmic pre-40S particle. The 5', central, 3' major and 3' minor domains and the U3 snoRNA are indicated. Adapted from [38].

The analysis of the SSU processome structure indicates the formation of different sub-complexes. The transcription of the 5' ETS permits the recruitment of two large modules: UTP-A (Utp4, Utp8, Utp9, Utp10, Utp15, Pol5 and Nam1) and UTP-B (Utp6, Utp13, Utp18, Utp21, Dip2 and Pwp2) sub-complexes. These modules form an scaffold where the nascent particle can continue formation by the recruitment of the U3 snoRNP, the Mpp10 complex (Mpp10-Imp3-Imp4) and other factors such as Utp3 [71-74]. After this, each domain of the 18S rRNA is independently associated with a subset of r-proteins and assembly factors **(Figure 8)**. At this moment, the U3 snoRNP plays a crucial role as central structural organiser. U3 snoRNP seems not to display any modification function, although the methyltransferase Nop1 is part of this complex. Instead, U3 snoRNP makes interactions with the UTP-A and UTP-B modules and other factors and contacts with the 5' ETS and regions of 18S rRNA within 35S pre-rRNA to bring them together. Besides, U3 snoRNP forms an heteroduplex with 18S rRNA, protecting the site A_1 from being prematurely cleaved. By this way, U3 snoRNP locks the 90S pre-ribosomal particle in an intermediary state, permitting ulterior events to take place [48,75,76].

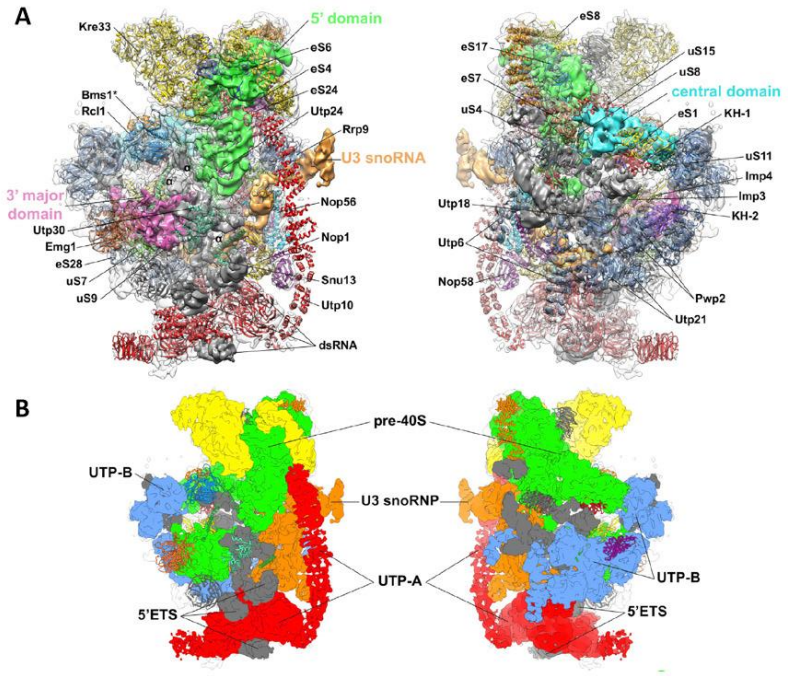

Figure 8. Structure of the SSU processome. (**A**) Two views of the cryo-EM model of the SSU processome from *Chaetomium thermophilum* with most identified factors, r-proteins and pre-rRNA in their assigned location. (**B**) Simplified representation of the SSU processome highlighting the main modules of pre-rRNA differently coloured, as well as the position of the UTP-A and UTP-B complexes, the U3 snoRNP and the 5' ETS region of 35S pre-rRNA. Adapted from [75].

Disassembly of the SSU processome

The SSU processome is not just a static particle. Instead, the earliest particle must go through a complex assortment of maturation states to allow cleavage at the A_1 site. These steps require folding and high compaction of the pre-rRNA **(Figure 7)** [77]. Among the different structural rearrangements compacting the pre-rRNA is included the formation of the so-called H1 stem loop in the 5' domain of the nascent 18S rRNA. The formation of this loop allows the A_1 site to get close to the endonuclease Utp24, thus favouring its cleavage. After this reaction, the SSU processome is dismantled, however, this does not occur as a block event but in a stepwise manner **(Figure 9)**. The accepted model suggests that first the Sfa1 module and Utp6 are removed, later UTP-A, U3 snoRNP and part of UTP-C, and finally the UTP-B and the remaining UTP-C factors [48]. The 5' ETS region of 35S pre-rRNA is further processed by the exosome, whose binding to the particle provides the remodelling force necessary for the release of this 5' ETS region and most assembly factors that will be recycled to form a new SSU processome [78]. Once Utp24 has cleaved at the site A_1, the partial disassembly of the particle permits this nuclease to reach the A_2 site in the flexible ITS1 region. Cleavage at site A_2 leads to the disassembly of the rest of the SSU processome leading to the generation of the initial pre-40S particles [48].

As the SSU processome does not contain components of the LSUs, it is assumed this structure correspond to ribosomes being matured through the co-transcriptional processing of pre-rRNA, thus, the corresponding initial pre-60S particle will be formed on the nascent 27S pre-rRNA. Recently, the isolation of a primordial pre-60S particle, composed by a specific set of assembly factors and snoRNAs has been reported. This particle, which still lacks of the enough atomic resolution, seems to reflect a 90S particle with a bipartite pre-40S-pre-60S structure, thus, being related to post-transcriptional processing of pre-rRNA [79].

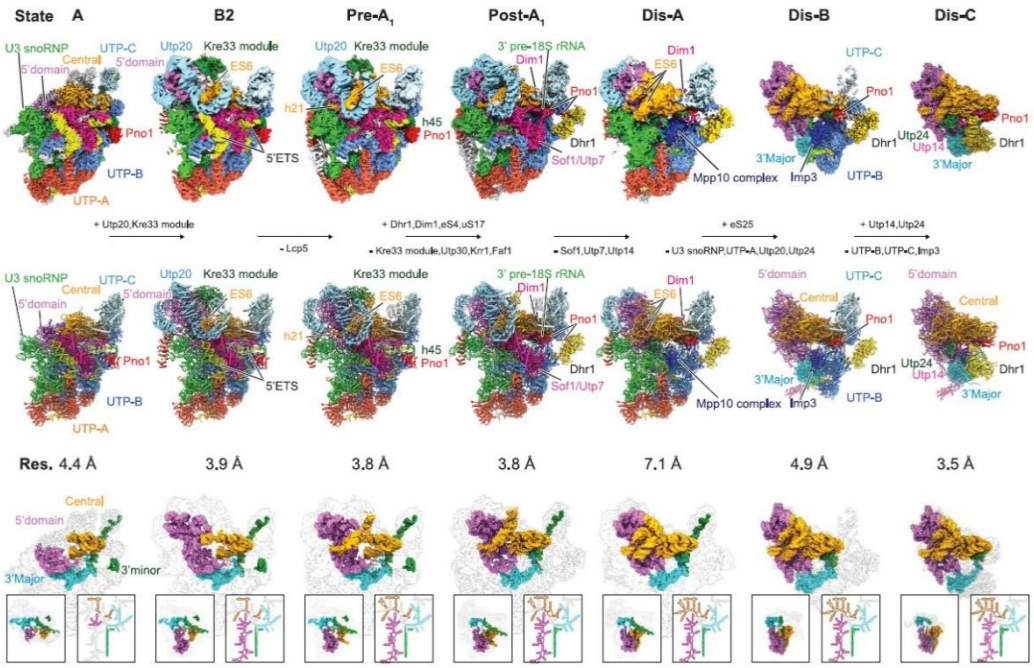

Figure 9. Dismantling of the yeast SSU processome. The figure shows the current model for the conversion of the SSU processome in an early pre-40S intermediate based on the structure of different identified cryo-EM particles. **Top panel**: Cryo-EM maps of distinct states of SSU processome to pre-40S particle transition. The main assembly factors and modules are indicated. Changes in the different proposed steps are depicted. **Middle panel**: Different view of the top panel, showing the molecular models and the resolution obtained for the different particles. **Bottom panel**: Representation of the pre-18S rRNA density within the models. The different domains of the 18S rRNA, represented as its secondary structure, are shown in the boxes. Adapted from [48].

Maturation of pre-40S ribosomal particles

Once the SSU processome has been disassembled, the primordial pre-40S r-particle emerges. This earliest pre-40S r-particle contains a defined composition, incorporating some additional assembly factors such as Tsr1, Rio2, Ltv1 or Dim1 and keeping other factors such as Pno1, Enp1 or Rrp12 that were already present in the 90S r-particle. Differently to the complex pre-60S r-particle maturation, the pre-40S r-particle shows a conformation almost close to the mature state that does not need extensive rearrangements. Soon after formation, nucleoplasmic pre-40S r-particles are rapidly exported to the cytoplasm where they acquire translation competence [80].

In early nucleoplasmic pre-40S r-particles, the 5' and central domains of the pre-rRNA are in a conformation almost mature. However, the 3' domains still need of certain remodelling, mainly related to the head formation and the beak completion. Once the

head is formed, it presents a highly rotated state when compared to mature SSU and only acquires its mature conformation in final steps in the cytoplasm. Functional sites as the mRNA binding groove and the decoding centre are not constructed yet. Instead, some factors as Tsr1, Enp1, Rio2, and Pno1 control their maturation, preventing premature formation until particles reach the cytoplasm **(Figure 10)** [81-83].

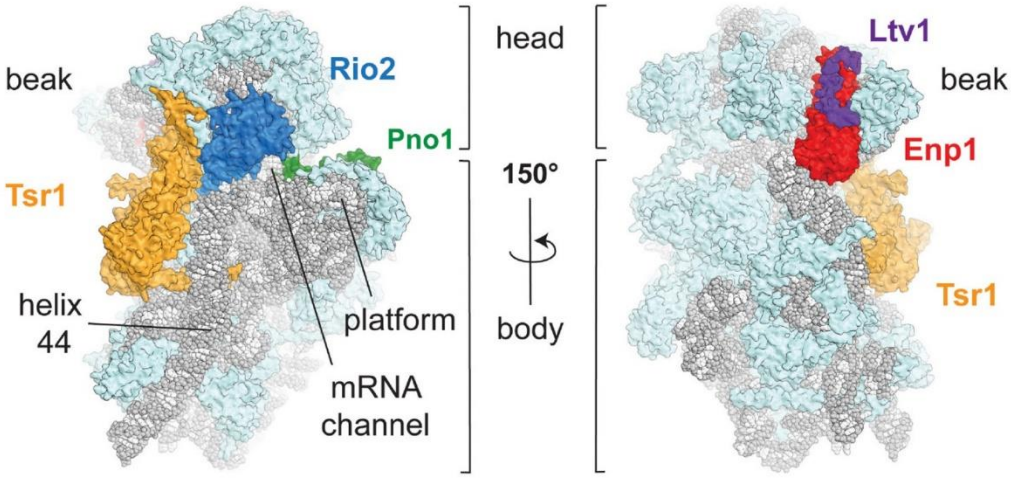

Figure 10. Structure of the cytoplasmic pre-40S particle. Representation of the structure of the pre-40S particle from the intersubunit interface (left) and solvent exposed interface (right). The 20S pre-rRNA is shown in grey and the r-proteins in light blue. Tsr1, Rio2, Pno1, Enp1 and Ltv1 are highlighted in different colours. The different structural domains, typical of SSUs, are also indicated. Adapted from [83].

Transport of the pre-40S r-particles from the nucleus to the cytoplasm through the nuclear pore complex (NPC) is facilitated by several and overlapping mechanisms. This redundancy provides efficiency for a rapid export. Different assembly factors such as Rio2, Pno1 and Ltv1 harbour nuclear export signals (NESs) that are recognized by selected exportins. Ltv1 and Rio2 are associated to nuclear pre-40S r-particles while Pno1 is present in the 90S particle but in a conformation that makes its NES still not accessible, thus, preventing premature export [80]. The most relevant exportin is Crm1 that binds to NES containing proteins, Ran-GTP and nucleoporins [80,84]. Besides, the heterodimer formed by Mex67 and Mtr2 and the Rrp12 factor, which are also important during export of pre-60S r-particles, also play a role in the export of pre-40S r-particles [85,86].

Once pre-40S r-particles reach the cytoplasm, the 3' major domain still requires maturation, in part due to the presence of Enp1 and Ltv1. These factors occupy the binding site of the eS10 r-protein in the still immature beak and stabilize the pre-rRNA in a conformation that impedes the stably association of the uS3 r-protein. Therefore, the correct association and completion of the beak depends on the release of Enp1 and Ltv1 in the cytoplasm [82,83]. Furthermore, the dissociation of these factors is thought to trigger several additional conformational changes in the 3' major rRNA, such as the head rotation. Besides, the presence of ribosomal assembly factors in cytoplasmic pre-40S particles has been postulated to be a quality control mechanism that impedes immature particles to engage prematurely in translation [82,83,87].

The head rotation induces the release of Rio2 and Tsr1 from the functional sites [83]. Then, Rio1 binds to the particle in a similar way than Rio2 and mediates the formation of the so-called 80S-like particle, which involves a transient union with a mature LSU. The formation of the 80S-like particle has been interpreted as part of a proofreading mechanism to ensure that only properly matured SSUs gain translation competence [52,88,89]. Furthermore, the release of Rio2 and Tsr1 results in some conformational changes that ultimately generates the displacement of Pno1 that releases the site D in 20S pre-rRNA to allow the endonucleolytic reaction by Nob1 to form the mature 18S rRNA [82,83].

Assembly of pre-60S ribosomal particles

The maturation of LSUs is much more elaborated than that of SSUs as the subunits themselves are also more complex. Within LSUs, the 25S rRNA forms six RNA domains (I-VI) of secondary structure that are more intertwined that those present in the 18S rRNA [3,90]. In general, domains I, II and the 5.8S rRNA form the solvent exposed face of the LSU while domains IV and V form the subunit interface. Domains III and VI mainly act as bridges between the former ones. The 5S rRNA docks to domains II and V. The assembly of different LSU domains does not follow a clear 5' to 3' pattern as occurring for those of SSU, although certain 5' to 3' order can be envisaged **(Figure 11)** [38]. As for SSUs, the incorporation of the different r-proteins to pre-60S r-particles

seems to be sequential and hierarchical, starting with weak interactions that in later steps of maturation become more stable [91]. In order to facilitate the comprehension of this complex process, most steps of LSU maturation have been organised in selected sections following spatial and temporal criteria.

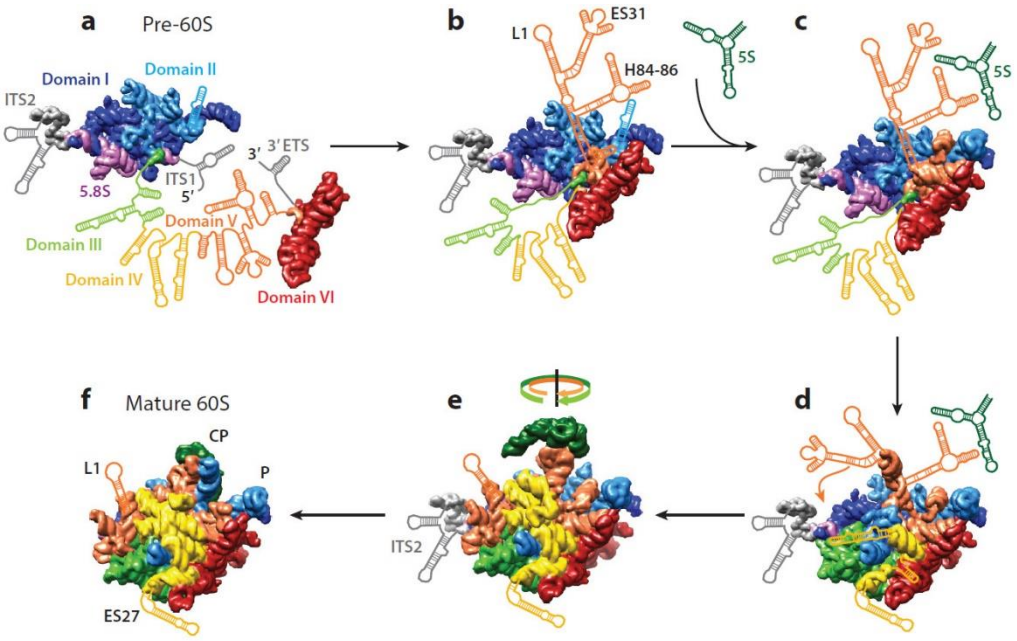

Figure 11. Maturation of pre-60S r-particles. (**a**) The first intermediary of pre-60S r-particles contains the $27SA_2$ pre-rRNA. Only few parts of the particle are stable enough to provide structural information. Most regions of pre-rRNA remain unstructured. (**b**) Removal of ITS1 and 3' ETS leads 27SB pre-rRNA to form some domains (domains I, II, VI, 5.8S and ITS2) into stable particles. (**c**) Part of domain V is formed, and 5S RNP incorporates (**d**) Incorporation of structured elements corresponding to domain III, IV and V. (**e**) Relocation of the L1-stalk stabilised by the completion of domain IV. At this step, the 5S RNP rotates 180° to reach its final conformation. (**f**) Removal of ITS2 and final rearrangements lead to the conformation of the functional sites in domain IV and V of mature LSUs. Adapted from [77].

Very early nucleolar assembly of pre-60S r-particles

The earliest pre-60S r-particle must be formed upon cleavage of pre-rRNA at site A_2 but its structure is unknown, reflecting its flexible state. The main pre-rRNA present in this stage is the $27SA_2$ pre-rRNA, which is co-transcriptionally subjected to modifications. Cryo-EM analysis of different early pre-60S particles has provided different snapshots for LSU maturation; during this process, the different RNA domains first independently associate with assembly factors in a modular fashion and then are sequentially brought together [92-94]. Most of the very early factors, such as Rrp5,

Mak21, Noc2 or Nop4, have multiple RNA binding domains to assist in the folding and compaction of pre-rRNA [38]. Rrp5 forms a module with Noc1 and Noc2 and coordinates cleavages at sites A_2 and A_3. The C-terminal domain of Rrp5, which is already present in the SSU processome, binds the ITS1 close to the A_2 site while its N-terminal domain binds close to the A_3 site. Interestingly, these two domains are necessary for the respective cleavages at these sites [95-97].

Although there is no structural information of the earliest stages, different reports have described the composition of the hypothetical earliest pre-60S r-particles. Thus, the so-called Urb1/Npa1 module formed by the Urb1/Npa1, Urb2/Npa2, Dbp6, Nop8, Rsa3, and Rbp95 factors seems to associate very early helping the initial compaction of the central core of the $27SA_2$ pre-rRNA and controlling the interactions of this precursor with many snoRNAs, thus apparently preventing unproductive rRNA structures [98-100]. Some of these snoRNAs, as snR190, have not a rRNA modification guiding function but a structural one similarly to that of U3 snoRNP in the SSU processome. Another remarkable characteristic that defines this very early pre-60S r-particle maturation state is the presence of the dimer formed by the methyltransferases Upa1 and Upa2 proteins that likely acts in coordination with H/ACA snoRNPs [79]. Furthermore, several RNA helicases are also present in this very early stage of pre-60S particle maturation, such as Dbp2, Dbp3, Dbp6, Dbp7, Dbp9, Prp43 or Mak5, probably assisting in the folding of early $27SA_2$ pre-rRNA and the release of all early associated snoRNPs [70,79,101].

Early nucleolar assembly of pre-60S ribosomal particles

The first detailed cryo-EM structural model for an early nucleolar pre-60S r-particle is the so-called state A. This structural snapshot indicates that the first part of LSU that is stably formed is that involving domains I, II, ITS2 and 5.8S rRNA from its solvent exposed face [92,93,102]. This particle is a scaffold that allows further folding of domain VI, and later, it permits generation of structure within the domain V of the 25S pre-rRNA **(Figure 11)**. A key event in these early steps of maturation is the association of the Nsa1 module (including Rrp1, Rpf1 and Mak16), which situates in the solvent

exposed face and assists in the folding and compaction of the early pre-60S r-particle **(Figure 12)** [102,103]. At this point, the N-terminal domain of Rpf1 extend from the solvent side to a location where later will be formed the PET. By this way, Rpf1 seems to act as a mould for initial construction of this important functional region of LSUs [92]. The Nsa1 module is released from particles relatively late (transition from nucleolar to nucleoplasmic pre-60S r-particles) assisted by the Rix7 ATPase, when some rearrangements in the particles make it accessible to the ATPase [92,103,104].

In addition to the Nsa1 module, there is a group of assembly factors (Ytm1, Erb1, Nop7, Rlp7, Cic1, Nop15, Has1) generally named A_3-factors that associates early in nucleolar pre-60S r-particles. Mutation in or deletion of any of these factors result in defective processing and accumulation of the $27SA_3$ pre-rRNA. Most of these factors bind directly or in proximity to the ITS2 region, forming a structure known as the foot of the pre-60S r-particles [105-110]. How factors binding to the ITS2 region of pre-rRNA participate in the maturation of the far away ITS1 region is still unclear [92]. One of the most peculiar A_3-factors is Erb1. This factor contains a globular C-terminal domain and a long N-terminal extension, which protrudes from the base of the foot through its back edge to its top interacting with several other factors from the foot region such as Rlp7, Nop7, Has1 or Nop16 and the r-protein eL36. Then, it continues over the immature LSU interface making contacts with factors Ebp2 and Brix1 **(Figure 12)**. Later, in the context of the transition of nucleolar to nucleoplasmic pre-60S r-particles, the N-terminal extension of Erb1 also mediates a stable association of factors such as Spb1 and Noc3 with the subunit interface. At this late nucleolar state, domain III of rRNA is conformed allowing the stable binding of the globular domain of Erb1, in coordination with its interaction partner Ytm1, to the edge between the base of the foot and the maturing subunit interface. This interaction is important to the stable assembly, at this later stage, of r-proteins eL27 and eL38. In conclusion, Erb1 crosses half of the early stable pre-60S r-particle acting as a key coordinator to assist the formation of rRNA domains I, III and IV during nucleolar maturation of pre-60S r-particles, helping the assembly of selected r-proteins and the stable association of different assembly factors [92,93,105,111-113].

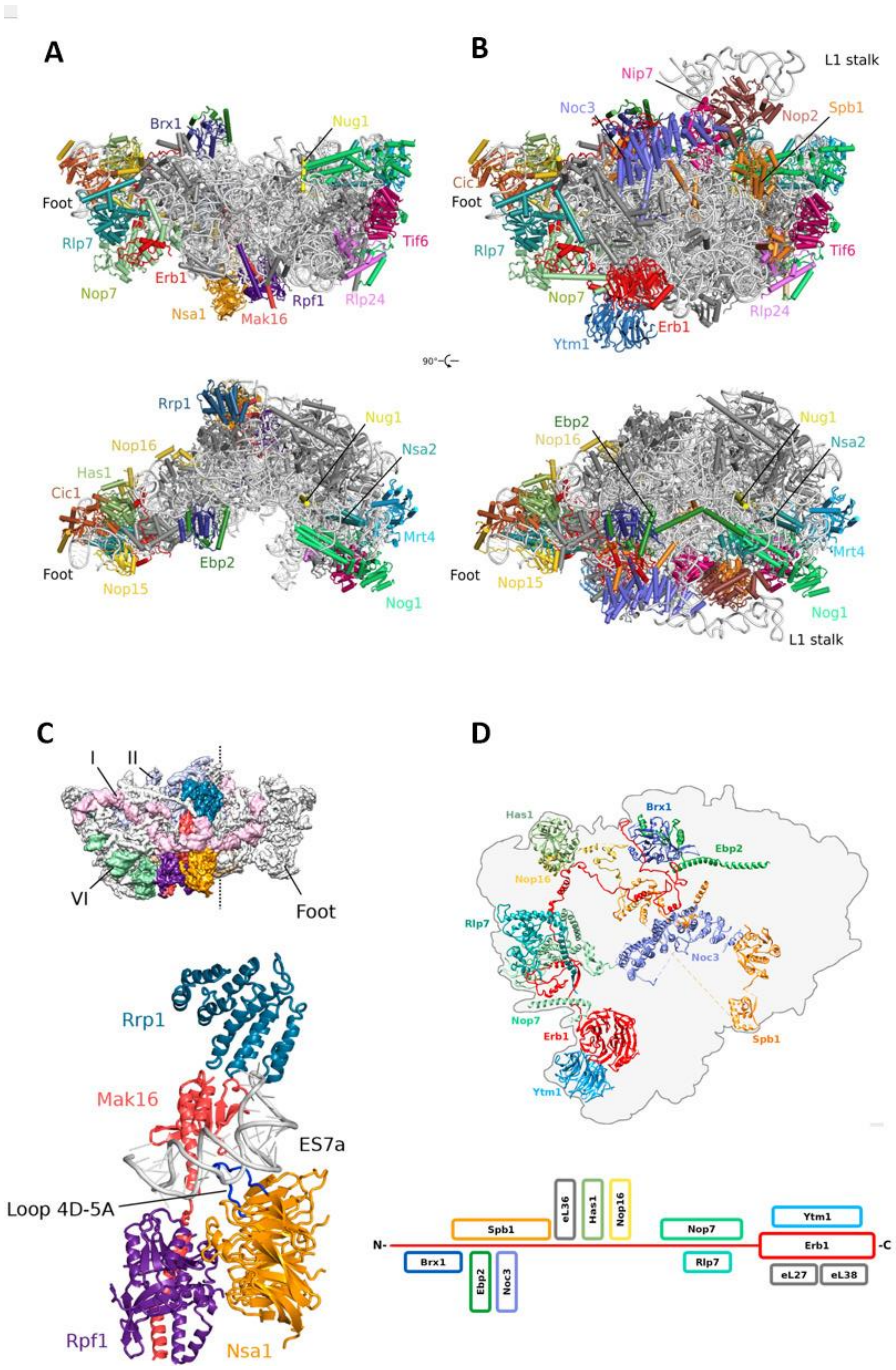

Figure 12. Cryo-EM structures of early to late nucleolar pre-60S r-particles. (**A**) Cryo-EM maps of the early nucleolar states. Front and top views of early pre-60S r-particles. The Nsa1 module is bound stabilizing the solvent exposed face and coordinating domains I and II. The foot structure is present. Only the terminal extension of Erb1 is present while its globular domain already bound to Ytm1 remains flexible. (**B**) Front and top views of later pre-60S r-particles. The Nsa1 module has already been released by the ATPase Rix7. Erb1-Ytm1 are stably incorporated to the particle and Rea1 can be recruited. (**C**) Depiction of the Nsa1 module containing Nsa1, Mak16, Rpf1 and Rrp1 bound to ES7a. The densities of 5.8S rRNA, and rRNA domains I, II, and VI of 25S rRNA are shown. The ATPase Rix7 is predicted to interact with loop 4D-5A of Nsa1. (**D**) Representation of Erb1 interaction network. Architecture of Erb1 showing its N-terminal part and its globular WD40 repeat domain. Erb1 contact numerous assembly factors and r-proteins. Adapted from [92].

Cryo-EM analysis suggests that pre-60S r-particle maturation proceeds by the association to the so-called B-factors, which are required for 27SB pre-rRNA processing **(Figure 13)**. Association of B-factors occurs in a hierarchical manner and makes the pre-60S r-particles less flexible and more stable [92,114]. Some B-factors, such as Nog1 controls maturation of PET. Others such as Dbp10, Nug1, Rsa4, Nsa2 and Nog2 bind to the maturing PTC or close to it. Whereas Nug1 and Nsa2 bind at last steps of early nucleolar assembly, Rsa4 and Nog2 are only nucleoplasmic factors. Moreover, other relevant B-factors such as Spb1, Nip7 or Nop2 associate only in later stages in the context of the transition of pre-60S r-particles from the nucleolus to the nucleoplasm. Although all these factors are necessary for the correct processing of the 27SB pre-rRNA, their exact implication in this process is still unclear [91,114-121].

Late nucleolar/early nucleoplasm transition of pre-60S ribosomal particles

Several remodelling events, assembly of selected r-proteins, and association and release of assembly factors are needed to process the 27SB rRNA at the C_2 site in ITS2. These steps take place in the context of the transition of pre-60S r-particles from the nucleolus to the nucleoplasm. Along this transition, the subunit interface and main functional centres such as PTC and PET start becoming evident as they gradually mature, being their construction necessary to initiate the removal of the ITS2 segment. Parts of domain V continue to assemble at this stage. Besides, domain III and part of the IV are also stabilised. All these rearrangements contribute to the closure of the lateral side of a still immature PET. At this point, the B-factors Spb1, Nip7, Nop2 and Noc2-Noc3 complex bind to domains V and IV of the rRNA in the subunit interface contributing to the formation of the PTC [92,122].

At this stage, Nsa1 is released by Rix7. Likely, the dissociation of Nsa1 destabilises the rest of component of the Nsa1 module as they also leave the pre-60S r-particle at this step. The exit of Rpf1, which N-terminal extension was partially occupying the site of the PET, permits the formation of the vestibule of the PET **(Figure 12)** [92,103,104]. In addition, the factor Ssf1 occupies the position that the eL31 r-protein will have at the mature LSU. Therefore, the rim around the exit of the tunnel can now be completed

with the release of Ssf1, Rrp14 and Rrp15 and the assembly of eL19, uL23 and eL31 r-proteins [93].

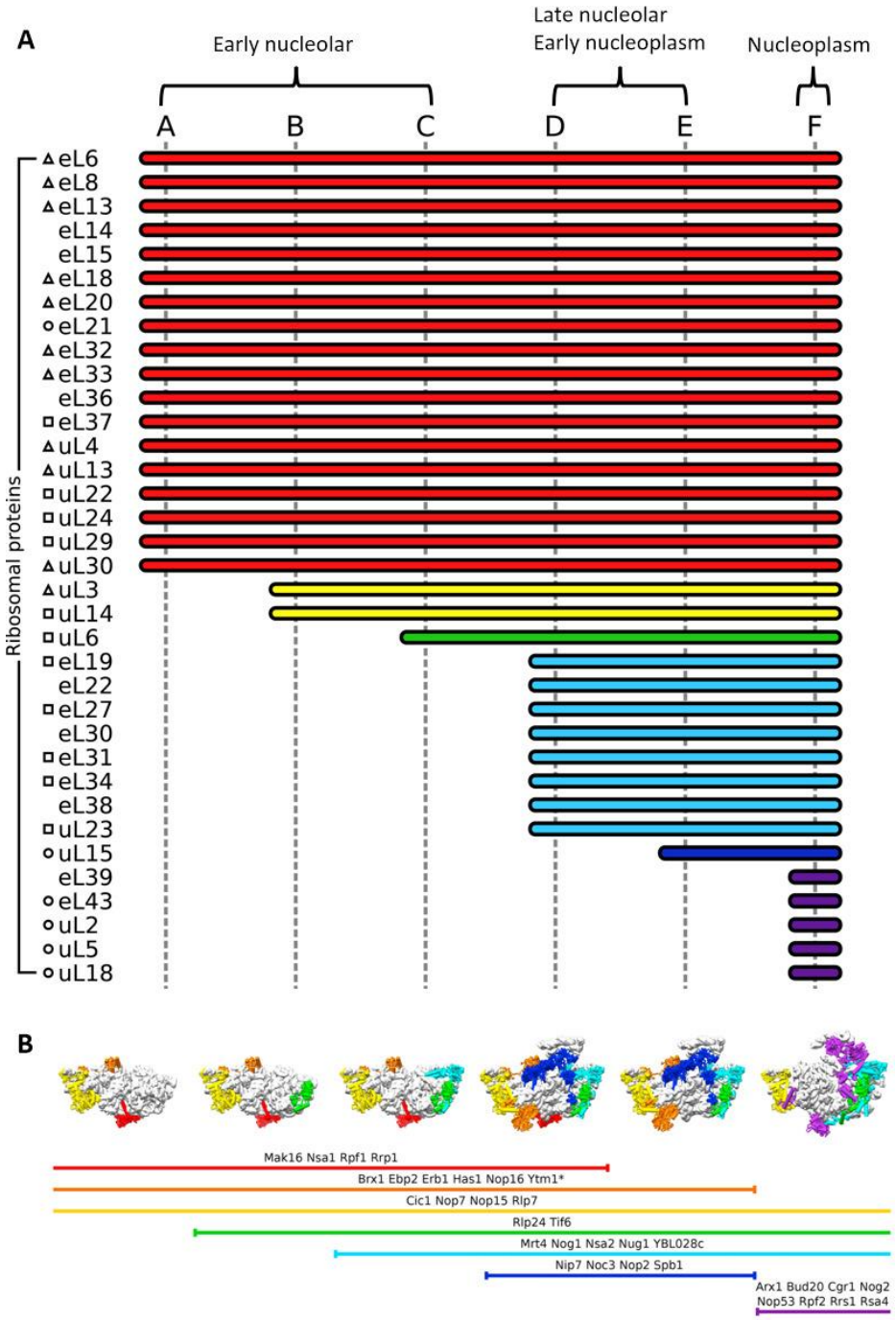

Figure 13. Composition of different nuclear pre-60S r-particles. (**A**) The r-proteins present in different states (from A to F) of pre-60S r-particles is shown. Colours refers to the stable incorporation of the r-proteins to the core particle. Triangles, squares and circles indicates known maturation phenotypes (early, middle and late) upon depletion of each r-protein. (**B**) Schematic representation of assembly factors associated with the above six states of pre-60S r-particles. Factors are clustered in colours based on the time point of stable entry and dissociation from the maturing particles. *Ytm1 was clustered with Erb1, as the two proteins form a stable complex. Adapted from [92].

At this maturation state, the pre-rRNA region that will form the future L1-stalk starts its definition by interactions with a set of factors included Ebp2, Nip7, Noc3, Nsa2 and Nop2. Furthermore, this pre-rRNA region of the future L1-stalk is displaced far from its final position and located at the top of the particle occupying the anchor site of the 5S-RNP and avoiding the formation of the CP. Although the 5S-RNP had already been attached to domain V at earlier stages, it still remains flexible **(Figure 11 and 14)** [92,121,123].

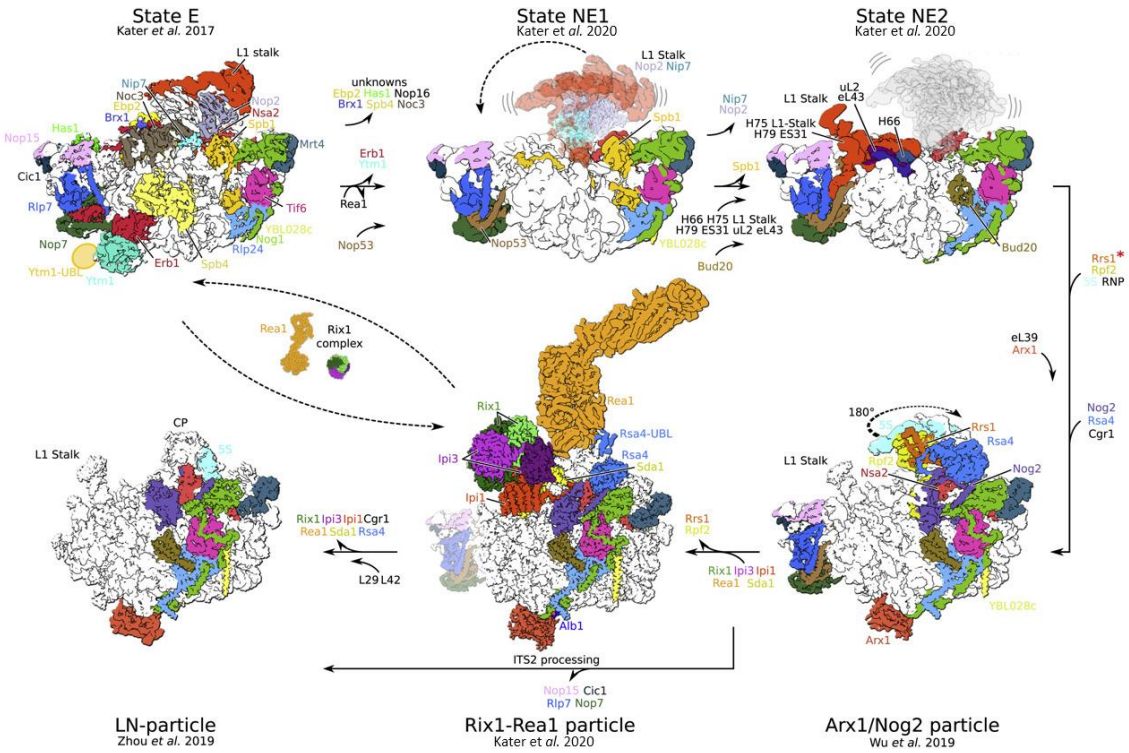

Figure 14. Rea1-dependent nuclear maturation events of pre-60S r-particles. The ATPase mediates two different reactions. First, Rea1 allows the release of Erb1-Ytm1 to permit the binding of Nop53, which eventually leads to the foot and ITS2 removal. Release of Erb1 induces the release of factors, step that is related to the stabilisation and conformation of the L1-stalk. The 5S RNP can stably bind to the core particle as part of these reactions. Second, Rea1 induces the rotation of 5S RNP within the central protuberance, its own release and that of Rsa4. Adapted from [123].

Following maturation, the large AAA ATPase Rea1 binds to Ytm1 and its ATPase activity induces the release of this factor together with Erb1, which is its interaction partner. The release of Erb1, which has allowed the earlier establishment of multitude of contacts within the pre-60S r-particles, seems to destabilise several local regions of the particles triggering novel remodelling events; these lead to the release of Has1,

Nop16, Nip7, Nop2, Noc3, Brx1 and Ebp2 and the relevant re-accommodation of the N-terminal extension of Rlp7 in an alternative position [92,93,111,112,124]. This allows the association of the Nop53 factor to ITS2 next to Nop7 at the foot. The association of Nop53 is a key event for later nucleoplasmic removal of ITS2 [92,115,125]. At this point, the release of Spb1 permits the L1-stalk to acquire a mature like conformation and to attach the particle. Concomitantly the r-proteins uL2 and eL43 associate and fix the L1-stalk **(Figure 14)** [123].

Late nucleoplasmic formation of pre-60S r-particles

As above mentioned, cryo-EM analysis has deduced that the release of Erb1 triggers an important sequence of remodelling events to the nucleoplasmic pre-60S particles. At the late nucleoplasmic states, the subunit interface progresses with the compaction of domain IV and the association of factors as Cgr1, Nog2 and Rsa4. The PET completes its maturation with the assembly of the eL39 r-protein. Interestingly, at this stage, but not before, the C-terminal extension of Nog1 totally occupy the pipe of PET and the heterodimer formed by Arx1 and its interaction partner Alb1 binds obstructing the exit of PET [92,115,123,126]. The dynamics of association of the C-terminal extension of Nog1 with the pre-60S r-particles suggests multiple functions for Nog1. First, Nog1 can act as a scaffold to form the tunnel. Second, Nog1 can probe the proper formation of the PET. Third, Nog1 can occupy the tunnel to avoid the entry of other proteins and prevents premature translation. Furthermore, as the presence of Nog1 is necessary for the cleavage at site C_2, it is probably that the appropriate formation of the PET would be a pre-requisite for ITS2 removal [127,128]. As discussed later, the pipe of PET will be occupied by other factors in cytoplasmic pre-60S r-particles **(Figure 17)** [126,129,130].

At this stage, the stably assembly of the 5S rRNP complex occurs. In yeast, 5S rRNA first assembles as a complex with the r-proteins uL5 and uL18. This 5S RNP is bound *in block* to the still flexible domain V at an early stage in the nucleolus by the anchor function of Rpf2 and Rrs1 assembly factors but remains undocked to the core pre-60S r-particle until later maturation stages [131]. Syo1 is the dedicated chaperone for uL18

that escorts the 5S rRNP to the nucleus and helps in its initial assembly too [25,132,133]. Once in the nucleoplasm and after stabilisation of the L1-stalk, the 5S RNP can stably bind to the pre-60S r-particle in the base of this stalk to constitute the main component of the CP. However, in this initial conformation, the 5S RNP presents a 180° rotated conformation in comparison to the position it adopts in the mature LSU, thus, needing rotation prior to pre-60S r-particles export to the cytoplasm **(Figure 14)**. This step is coupled to the removal of the Rix1 complex and the Rsa4 factor by the ATPase Rea1 [92,121,123].

One of the last steps in the nucleoplasmic maturation of pre-60S r-particles involves the ATPase Rea1 and the Rix1 complex, whose association to the pre-60S r-particles triggers a sequence of events that ultimately induces ITS2 removal. Rea1, in a new round of action, binds now to its second target Rsa4. Moreover, the Rea1-interacting Rix1 complex also associates at this late nucleoplasmic state to the pre-60S r-particle. The Rix1 complex situates on top of L1-stalk and the Sda1 assembly factor, next to the CP **(Figure 14)**. This positioning of Rea1-Rix1 also triggers the release of Rpf2 and Rrs1 and the concomitant rotation of the CP. After that, the ATPase activity of Rea1 induces the release of Rsa4 and the own Rea1-Rix1 machinery. Then, the assembly of uL2 and eL43 r-proteins promotes the completion and stabilization of the CP. As the CP rotation precedes ITS2 processing and the foot structure removal, it is possible that this rotation somehow induces the subsequent cleavage at C_2 site [121,123,134]. This pre-rRNA processing step is carried out by the Las1 complex, which is formed by the endonuclease Las1, the kinase Grc3, the exonuclease Rat1 and its cofactor Rai1. After CP rotation, Grc3 drives Las1 to site C_2, then Las1 cleaves at this site generating the 7S and 25.5S pre-rRNAs. After that, Grc3 phosphorylates the 5' OH of the 25.5S pre-rRNA which enables the trimming of this pre-rRNA by Rat1 **(Figure 15)** [59,135-138]. Two other 5' to 3' exonucleases, Rrp17 and Xrn1, are also capable to trim the 25.5S pre-rRNA to mature 25S rRNA [56,57].

On the other hand, once cleavage at site C_2 has occurred, Nop53 could recruit the exosome through its Mtr4 cofactor to the particle [125,139-141]. Mtr4 is an RNA helicase which forms part of the Trf4/5-Air1/2-Mtr4 polyadenylation complex (TRAMP). The polyadenylation is thought to provide a grip for Mtr4 to unwind ITS2 rRNA and

maybe for restructuration of some proteins to make the ITS2 accessible for the exosome [142-145]. The exosome acts in two steps. First, it removes all but the last 30 nucleotides of ITS2 from the 3' end of the 7S pre-rRNAs. In a second step, it degrades all but the last 8 nucleotides producing the 6S pre-rRNAs. The 6S pre-rRNAs will be finally processed in the cytoplasm to mature 5.8S rRNA. Just before or during the exosome binding, the foot is completely remodelled and only Nop7 remains stably associated **(Figure 15)** [61,146].

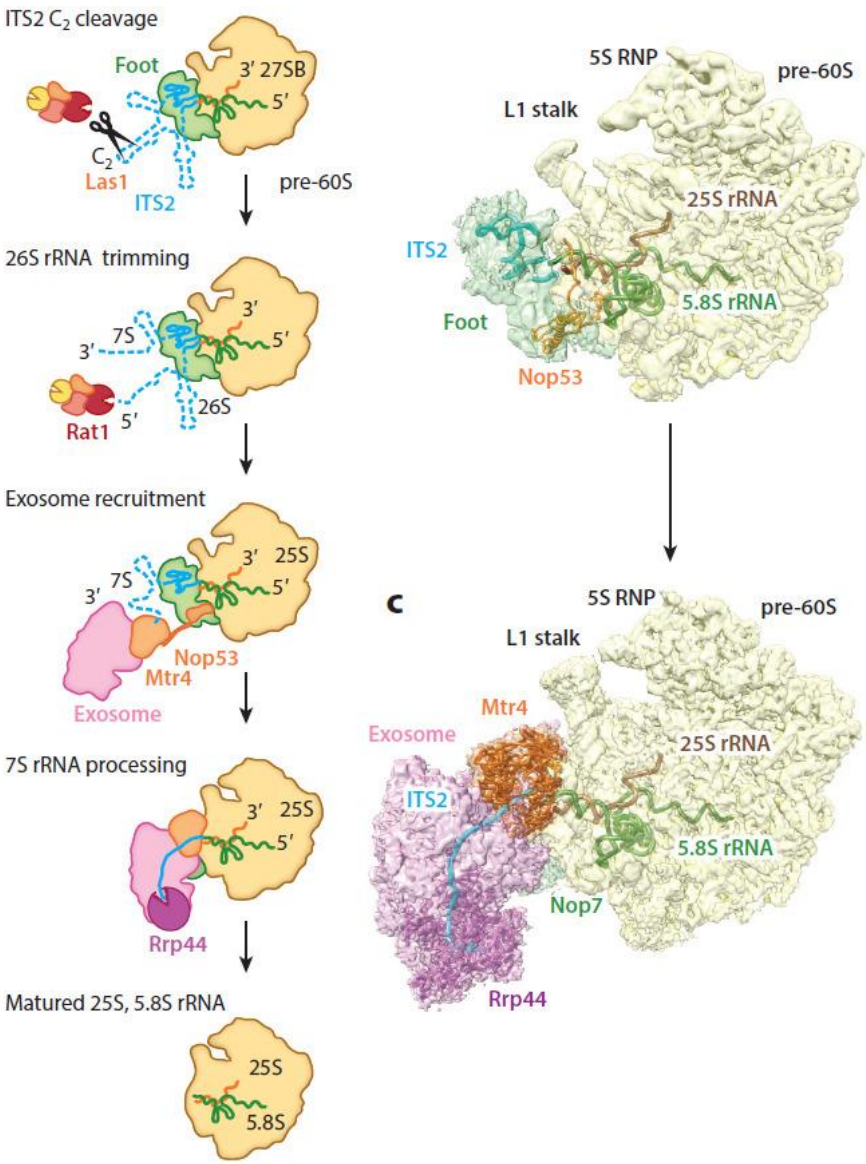

Figure 15. Removal of ITS2 from the pre-60S r-particles. The endonuclease Las1 cleaves the ITS2 at site C_2, which generates 7S and 25.5S (also 26S) pre-rRNAs from 27SB pre-rRNA. The 25.5S pre-rRNA is 5' to 3' trimmed by the exonuclease Rat1. Nop53 recruits the exosome by mean of the Mtr4 cofactor to allow 3' to 5' processing of 7S pre-rRNAs. Concomitantly to these steps, the assembly factors of the foot are released from particles. Adapted from [77].

Export of the pre-60S ribosomal particle to the cytoplasm

The nucleoplasmic pre-60S r-particle needs to get remodelled before gaining export competence. Thus, one of these steps is the release of Nog2. This GTPase act as a hub protein situated at the centre of the immature PTC interacting with several factors as Nog1, Nsa2, Rpf2, Rsa4, Bud20 or Dbp10 and with pre-rRNA from domains II and IV. The association of Nog2 with the PTC suggests a role as a controller of its maturation [126,147]. The release of Nog2 is dependent of two activities, the ATPase activity of Rea1 and the GTPase activity of the own Nog2 [148]. Nog2 deeply interacts with the Ipi1 component of the Rix1 complex and with the Nsa2 factor **(Figure 14)**. As the release of Rsa4 and the Rea1-Rix1 machinery occurs before of that of Nog2, it is likely that this step, in a direct or indirect manner, triggers the activation of the GTPase activity of Nog2 and its consequent release [123]. Curiously, the binding site of Nog2 in pre-60S r-particles overlaps with that of the export factor Nmd3, so the latter can only bind after the release of the former. By this way, Nog2 release functions as a checkpoint for acquiring export competence [130,148,149].

There are several other factors involved in the transport of the pre-60S particle to the cytoplasm, among them the Mex67-Mtr2 complex, which has some overlapping with Mrt4, the placeholder of uL10 r-protein [150], the dimer Arx1-Alb1, Rrp12, Bud20, Npl3, Ecm1 and Gle2 **(Figure 16)** [151-154]. However, Nmd3 is the main responsible for the export, whereas the rest of transport factors increases the efficiency of this process. Nmd3 is the only NES containing adaptor; the NES of Nmd3 is essential for nuclear export, which is dependent of the exportin Crm1 [151]. Arx1-Alb1, Bud20 and Ecm1 are thought to directly interact with nucleoporins to facilitate the translocation to the cytoplasm [155-158]. Npl3 interacts with nucleoporins and it is also thought to shield the particle from the hydrophobic environment by interacting with uL23 r-protein and pre-rRNA [159]. Gle2 mediates the export by interacting specifically with the nucleoporin Nup116 [160]. Mex67-Mtr2 form a dimer that directly interacts with nucleoporins and together with Rrp12 are the only adapter factors shared with pre-40S r-particles [85,161-163]. All these factors are located at different positions in the pre-60S r-particle. This abundance of export factors reflects the need of a rapid export of

pre-ribosomal particles for the high cellular demand of ribosomes [35]. In addition, it seems that most of these factors also neutralise the partial negative charge of the subunit interface of particles, as some important r-proteins in this area did not still assemble [122]. Before getting export competence, several assembly factors are released and the particle gets compacted to fit the diameter of the NPC [122,164].

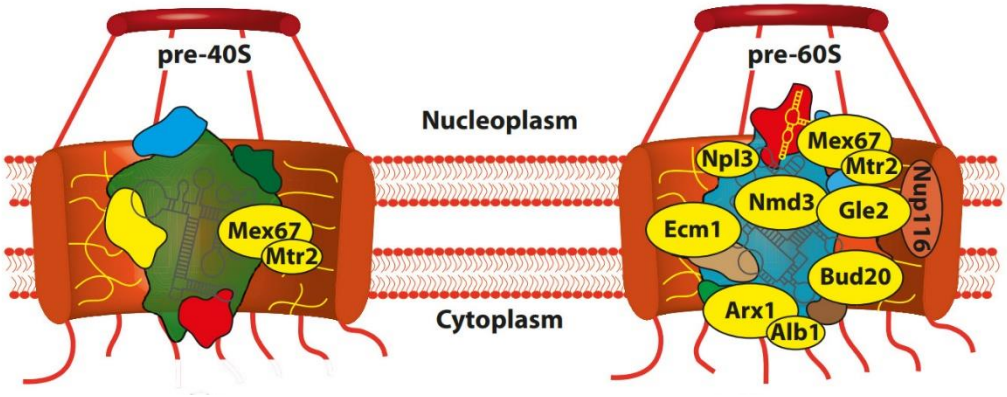

Figure 16. Representation of the export of pre-40S and pre-60S r-particles through the NPC. The cartoons show all the export factors (yellow) that have been identified as ensuring the rapid export of pre-ribosomal particles to the cytoplasm, and how these factors interact with hydrophobic repeats of some special nucleoporins from the nucleopore channel. Adapted from [151].

Cytoplasmic assembly of pre-60S ribosomal particles

In the cytoplasm, the last steps of the maturation take place. There, the last rRNA processing events occur, the construction of the functional centres is completed and proofread to ensure the functionality of the mature LSU. Nine r-proteins are incorporated in the cytoplasm, and all the remaining assembly factors are released *via* the activity of selected ATPases and GTPases, in a sequential manner **(Figure 17)** [87,165].

The cytoplasm maturation of pre-60S r-particles probably initiates with the recruitment of the ATPase Drg1, which depends on the factor Rlp24. The ATPase activity of Drg1 induces its own release and that of Rlp24. Rlp24 is a paralog of the eL24 r-protein and act as its placeholder, thus, once Rlp24 is released, the assembly of eL24 could take place [165-167]. The ATPase activity of Drg1 is also necessary for the release of the nearby Nog1, Nsa2 and Nug1 factors. As Rlp24 interacts with Nog1, it is likely that the

release of Rlp24 pulls Nog1 out of the pipe of PET [167,168]. Once eL24 is assembled, pre-60S r-particles can interact and probably recruit Rei1 [169]. Interestingly, the C-terminal extension of Rei1 penetrates deep into the PET similarly as does the C-terminal extension of Nog1. As Nog1, Rei1 probes the exit of the PET impeding its premature occupation [129]. However, Rei1 presents an additional role in the release of the dimer Arx1-Alb1. Thus, Rei1 together with Jjj1 and the ATPase Ssa1 are necessary for the release of Arx1-Alb1, which is accompanied by the own release of all these factors [169-173]. Once Rei1 leaves the cytoplasmic pre-60S r-particle, its homolog Reh1 occupies the PET. However, the exact role of this replacement is unclear [129,130,174].

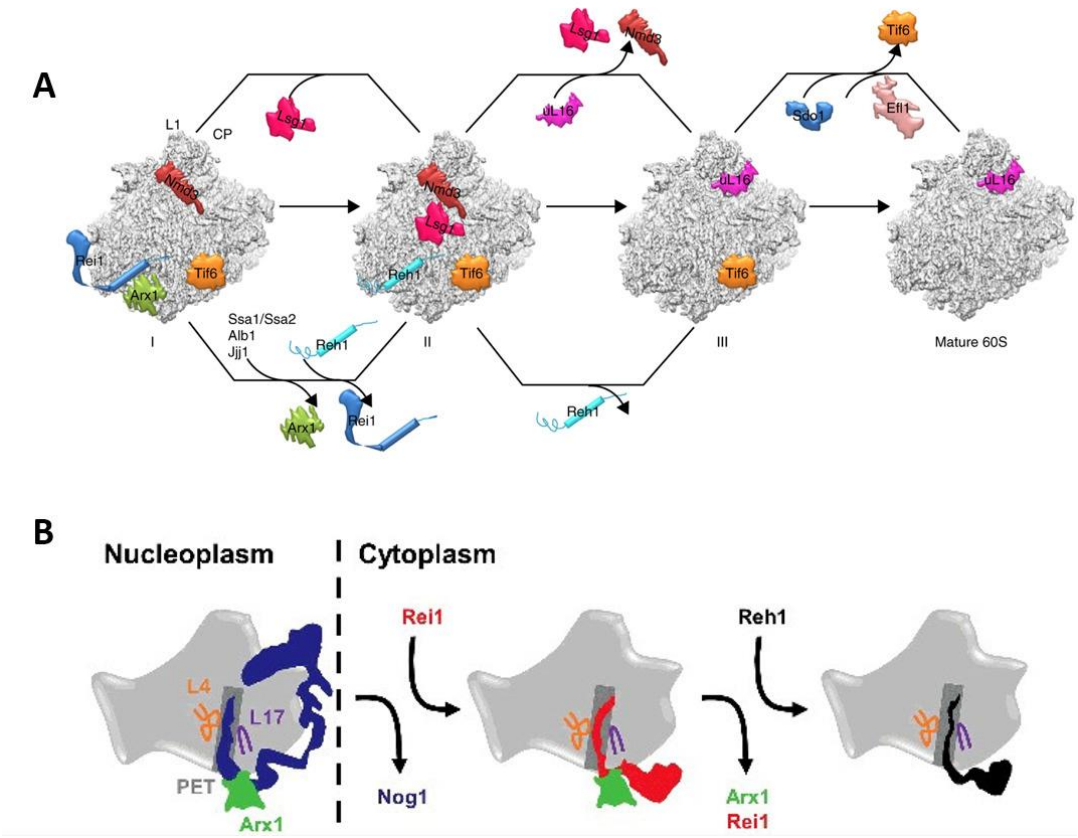

Figure 17. Final cytoplasmic steps of pre-60S r-particle maturation. (**A**) The cartoons show two parallel pathways for the maturation of the PTC-CP and the PET functional centres of pre-60S r-particles. The Drg1 activity facilitates the replacement of Nog1 by Rei1. Rei1 together with Jjj1 and Ssa proteins enables the release of the export receptor Arx1, located at the exit of PET. Lsg1 GTPase activity is responsible for the Nmd3 release. Finally, the activity of the GTPase Efl1 together with its cofactor Sdo1 induces the release of Tif6 from the subunit joining face of the particle. It is not known how Reh1 exits the particle. (**B**) Cartoon showing how the PET is proofread by the sequential association of Nog1, Rei1 and Reh1 interacting with Arx1 at the exit of the PET. Adapted from [126,130].

One of the more interesting cytoplasmic steps is the formation of the P-stalk. Apparently in the cytoplasm, the factor Yvh1 allows the dissociation of Mrt4, which is the placeholder of uL10. Although some authors have discussed that this step can occur in the nucleoplasm, it seems this exchange is a predominantly cytoplasmic event [150,175-177]. Upon the assembly of uL10 at the base of P-stalk, the two heterodimers of P1-P2 r-proteins can join the almost mature LSU and complete the formation of the P-stalk. Furthermore, the formation of the P-stalk is apparently a pre-requisite for the downstream release of Tif6 and Nmd3 [165,177].

Nmd3 and the assembly of the eL40 r-protein assist the assembly of the uL16 r-protein [178]. An internal loop of uL16 that embraces the P site of the ribosome is a central controller of the transitions between rotated and non-rotated states that occurs in the mature and elongating ribosome [179]. At this stage, the P site is occupied by Nmd3 but the abovementioned loop can now compete and contribute to displace Nmd3. This, together with the activity of the GTPase Lsg1, allows the release of Nmd3 from particles [178,180-182]. The incorporation of uL16 and the release of Nmd3 are essential for the completion of the PTC region of LSUs [178].

Before gaining final translation competence, almost mature LSUs still need to dissociate the Reh1 and Tif6 factors. In the case of Reh1, it is not known the timing and the mechanism of its release. Tif6 is an anti-association factor that prevents the joining of the pre-60S r-particles with SSUs. In this case, the internal loop of uL16 that assists the release of Nmd3 is also responsible for the recruitment of the Sdo1 factor to the P site of LSUs [178,179]. Sdo1 is the cofactor of the GTPase Efl1, which activity is responsible for the release of Tif6 [183-187]. Efl1 binds the GTPase activating centre (GAC). After Efl1 binding, Sdo1 is repositioned and stimulates the GTPase activity of Efl1, which induces a conformational change allowing the release of Tif6 by competing for its binding site in pre-60S r-particles [188]. Once Tif6 has abandoned the pre-60S ribosomal particle, it immediately recycles back to the nucleolus and the mature LSU acquires the translation competence.

OBJECTIVES

The goal of this thesis work is to progress in the knowledge of the biogenesis of the LSU of the ribosome. In particular, to understand how different r-proteins and protein assembly factors cooperate to produce a mature LSU. To achieve this aim, we have analysed loss-of-function mutations of two different r-proteins from the yeast model *S. cerevisiae* that remained uncharacterised at the beginning of this work.

As particular objectives, we have worked on the following aspects:

- The study of the functional role of the eL22 r-protein during the formation of LSUs and how its loss-of-function impacts on pre-rRNA processing and LSU maturation.

- The functional characterisation of the eL15 r-protein during the maturation process of LSUs and how its loss-of-function impacts on the association of assembly factors and the assembly of other 60S r-proteins with early pre-60S ribosomal particles.

CHAPTER 1

ROLE OF THE YEAST RIBOSOMAL PROTEIN eL22 IN RIBOSOME BIOGENESIS

INTRODUCTION

Along the ribosome biogenesis pathway, the r-proteins are assembled at different points of the process assisted by a myriad of assembly factors. Although ribosomes are quite conserved in all organisms, cytoplasmic ribosomes in eukaryotes contain several exclusive r-proteins not found in their prokaryote counterparts; in eukaryotes, the N- and C-terminal and internal extensions of r-proteins are also more common and larger than the equivalents of prokaryotes [11]. Most yeast r-proteins have been well studied and their roles in ribosome biogenesis unravelled in some extent in the yeast *S. cerevisiae*. However, there is a few examples of r-proteins that still remain uncharacterised. In this study, we aim to further progress in the still unclear role of the yeast eL22 r-protein in ribosome biogenesis. eL22 is a eukaryote-specific r-protein that is encoded by two paralogous genes in *S. cerevisiae*, *RPL22A* (YLR061W) and *RPL22B* (YEL034C-A) [189]. These genes encode proteins of 121 and 122 amino acids, respectively, that share an 84.6% identity and 94.3% similarity. Changes between the two proteins includes the following substitutions from the eL22A to eL22B proteins: I11V, A12I, F15L, A34S, E44D, V54I, T55E, T61S, V62I, T68V, T98I, K99R, T100Q, E102Q, R104K, A106V, E114D and E120D, and an insertion of an A115 in eL22B. The conformation of eL22 is mainly globular. In the mature LSU, eL22 is located in the surroundings of the exit of the PET embedded between eL31 and eL38 [7]. In yeast, eL22 seems to be assembled at middle stages of nucleolar pre-60S r-particle maturation, but experimental validation of this statement is still required [92]. During late nucleoplasmic stages of assembly, eL22 is located at its final position, stablishing contacts with the C-terminal extension of the ribosome biogenesis factor Rlp24. Moreover, eL22 interacts with the C-terminal extension of Nog1 that penetrates into the PET [115]. In the cytoplasm, once Nog1 and Rlp24 are released from pre-60S r-particles and Rei1 is associated to continuing probing that the PET is correctly formed, eL22 interacts with the globular and the distal part of the C-terminal extension of Rei1 (**Figure 1**), which is inserted into the PET and extends almost along its entire length to reach the PTC site at the other end of the tunnel [129].

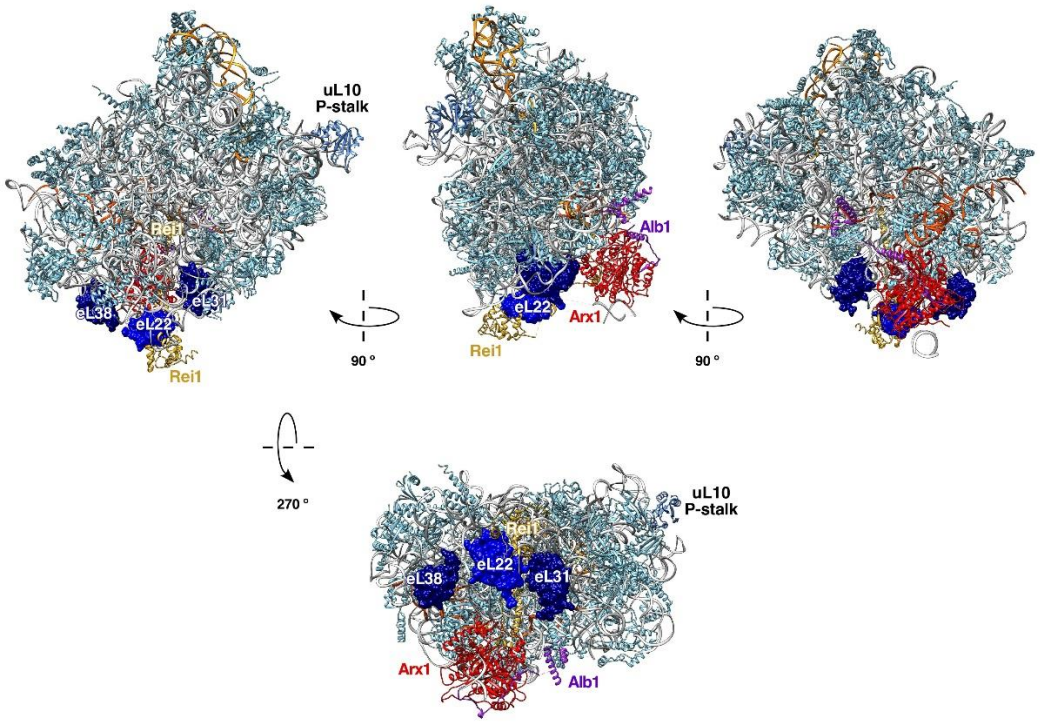

Figure 1. **Position of eL22 and its neighbourhood in the three-dimensional structure of the cryo-EM reconstruction of Rei1 and Arx1-Alb1 bound to yeast 60S r-subunits**. The r-proteins eL22 (blue), eL31 (marine blue), and eL38 (marine blue) and the assembly factors Rei1 (yellow), Arx1 (red) and Alb1 (purple) are highlighted. The rest of r-proteins are coloured in light blue, the 5.8S rRNA in coloured in orange, the 5S rRNA in pale orange and the 25S rRNA in pale grey. The representation was generated with the UCSF Chimera program, using the atomic model for the structure of the 60S-Arx1-Alb1-Rei1 complex (PDB ID: 5APO [129]). Upper particles: interface view of the 60S r-subunit (left) that is rotated around the Y-axis 90° twice to obtain the solvent-side view (right). At the bottom, result of rotated around the X-axis 270° the structure in the interface view.

Due to the key role of ribosomes in cellular physiology, deletions of most r-protein genes are detrimental to cells, causing non-viability or severe growth defects [30]. However, previous studies have shown that yeast cells lacking eL22 results in just a moderate growth defect mainly caused by the absence of the *RPL22A* gene, which represents the major contribution to the mRNA and protein levels for eL22 [30,190-194]. The differences on levels of eL22A and eL22B r-protein variants are due to an expression regulatory mechanism based on the intronic regions of their mRNAs. In this sense, the splicing of the *RPL22B* mRNA is specifically inhibited by the own eL22 protein. The unspliced mRNA is then efficiently eliminated by the Nonsense Mediated Decay (NMD) and Xrn1 dependent 5'-3' cytoplasmic degradation pathway [193,195,196]. Moreover,

the splicing efficiency of the *RPL22B* mRNA varies upon different stress conditions [195,197]. Besides, *RPL22A* mRNA is also downregulated by eL22 but to a lesser extent, allowing efficient synthesis of the eL22A r-protein [193,196].

Other studies have shown that eL22 has additional roles in general splicing and therefore in the expression of genes involved in many different cellular processes, among them ribosome biogenesis. In this sense, high levels of eL22 result in a negative feedback that downregulates ribosome biogenesis [191-194,197]. In yeast, the absence of eL22 or a decrease on its levels have been also related to an increased replicative lifespan, increased resistance to endoplasmic reticulum stress and capability of entering in meiosis [30,192,194,198]. Furthermore, some studies have also found that the absence or decreased levels of eL22 lead to aberrant polysome profiles, pointing out a possible role during ribosome maturation and/or translation [30,192].

In humans, there is a family of unrelated developmental rare diseases known as ribosomopathies that are linked to mutations in a wide range of r-proteins and assembly factors [43]. These diseases display a variety of different phenotypes with significant different clinical presentations and potential for treatment, but most cause defects during haematopoiesis and an increased susceptibility to cancer [42]. In fact, as shown in **Figure 2,** human eL22 is the second r-protein more misregulated during cancer just after uL18 [42]. The role as tumour suppressor of the uL18 r-protein together with that of its partner in the 5S RNP complex, the uL5 r-protein, has been well characterised. It has been reported that these two r-proteins bind to and inactivate the E3 ubiquitin ligase Mdm2, therefore avoiding p53 degradation. Although eL22 has also been described to participate in this inhibitory circuit by binding to both uL18 and Mdm2, its role during tumorigenesis remains unclear. Apparently, the positive selection of *RPL22* mutations provides a significant advantage to cells containing wild-type p53, as these mutations could impair the activation of p53 and therefore its signalling, thus enhancing the susceptibility to cancer [199].

In addition, eL22 have been described to participate in other cellular processes in eukaryotes, such as the invasion of the Epstein-Barr virus in human cells and the integration of certain transposon elements in *Drosophila* [200,201].

Our group is interested in understanding the contribution of specific 60S r-proteins to ribosome biogenesis. There are dispersed reports suggesting a role of eL22 during the biogenesis of LSUs. In this thesis work, we have undertaken a systematic and specific functional analysis of yeast eL22 in ribosome synthesis to demonstrate its relevance during this process.

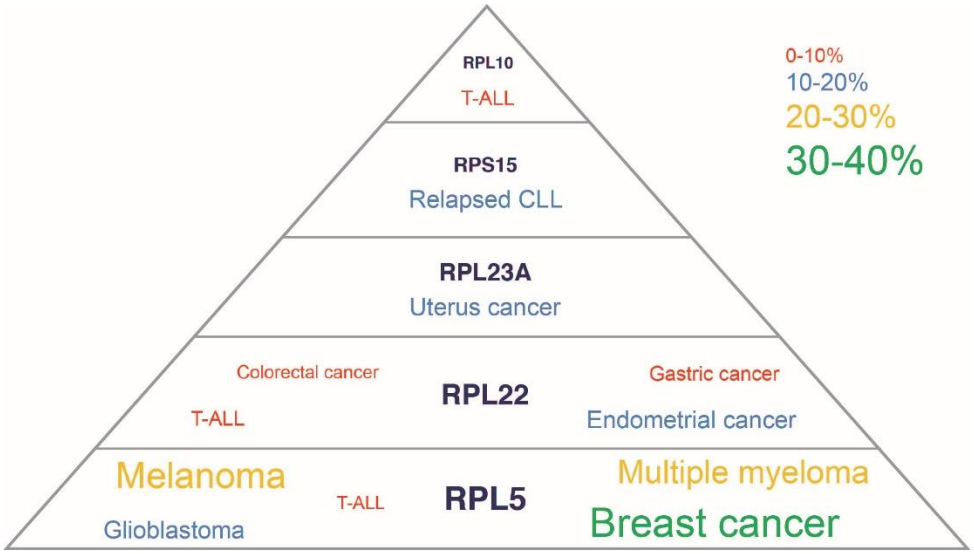

Figure 2. Main r-protein genes with recurrent somatic mutations in human cancer. The figure shows that eL22 is the second r-protein with mutations found in different cancer types. The incidence percentages of the r-protein defects in specific cancers are shown. Typography font size is proportional to the incidence of the r-protein mutations in the cancer types where they have been described. CLL stands for chronic lymphocytic leukemia, and T-AA for T-cell acute lymphoblastic leukemia. Taken from [42].

MATERIALS AND METHODS

Strains and microbiological methods

All the strains of *Saccharomyces cerevisiae* used in this thesis work are listed in **Table 1**. The strains JFY010 (*rpl22A*::kanMX4), JFY011 (*rpl22B*::kanMX4), JFY084 (*rpl38*::kanMX4), JFY449 (*rpl31A*::kanMX4), JFY535 (*alb1*::KANMX4), JFY540 (*arx1*::kanMX4) and JFY551 (*rps9B*::kanMX4) are meiotic segregants from their corresponding heterozygous diploid strains obtained from the Euroscarf collection. In order to generate double and triple deletion mutants, the corresponding strains were crossed, sporulated and tetrads were dissected. Phenotypes involving *alb1Δ* and *arx1Δ* deletions were re-checked using strains harbouring these deletions from the Fromont-Racine group. Strain JFY012 *(rpl22A*::kanMX4 *rpl22B*::kanMX4) is a haploid segregant derived from crossing JFY010 and JFY011. Strains JFY114 (*rpl22A*::kanMX4 *rpl22B*::kanMX4 *rpl38*::kanMX4), JFY497 (*rpl22A*::kanMX4 *rpl22B*::kanMX4 *rei1*::natMX4), JFY501 (*rpl22A*::kanMX4 *rpl22B*::kanMX4 *alb1*::natMX4), JFY524 (*rpl22A*::kanMX4 *rpl22B*::kanMX4 *arx1::*HPH) and JFY531 (*rpl22A*::kanMX4 *rpl22B*::kanMX4 *rpl31A*::kanMX4) are haploid segregants derived from crossing JFY012 with JFF084, LMA523, LMA525, LMA539 and JFY449, respectively. Strains JFY563 (*rpl22A*::kanMX4 *rpl22B*::kanMX4 *arx1*::kanMX4) and JFY564 (*rpl22A*::kanMX4 *rpl22B*::kanMX4 *alb1*::kanMX4) are haploid segregants derived from crossing JFY012 with JFY540 and JFY535, respectively. The correctness of all deletions was verified by PCR.

Strains were grown at the permissive temperature of 30 °C by default. The low temperature of 22 °C and the high temperature of 37 °C were used in the indicated cases. Cells were grown in rich YP(A)D medium (typically 1% yeast extract, 2% glucose, 2% peptone with a supplementation of 0.2% adenine) or in synthetic minimal SD medium (0.5% ammonium sulphate, 0.15% yeast nitrogen base, 2% glucose) supplemented with the appropriate amino acids and bases. When required, 2% glucose was substituted by 2% galactose as carbon source (SGal media). For the preparation of solid medium, 2% agar was added. When needed, cells were transformed with

appropriate vectors using the lithium acetate method [202]. Tetrads were dissected using a Singer MSM200 micromanipulator. DNA manipulation techniques were done according to established protocols [203]. Growth and handling of yeast and preparation of yeast media were done according to established procedures [204].

Plasmids and oligonucleotides

The DH5α strain of *Escherichia coli* was used for cloning and propagation of all plasmid vectors of this work. These are listed in **Table 2**. The construction of the plasmids YCplac111-RPL22A and YCplac111-RPL22A-GFP was carried out by amplification of the appropriate DNA fragments by PCR using distinct oligonucleotides. The PCR products were subsequently cloned in the appropriate vectors and verified by DNA sequencing. The oligonucleotides used in this study are listed in **Table 3**. Other plasmids have been previously reported in the studies that are appropriately indicated.

Translation accuracy assays

To quantify the efficiency of amino acid misincorporation and readthrough, the JFY012 strain (*rpl22A*::kanMX4 *rpl22B*::kanMX4) and the positive control strains YDB339 (*upf1::hisG* [PSI+]) and JFY551 (*rps9B*::kanMX4 [pRS315-*rps9B*-D94N]*)* were transformed with different dual luciferase reporter plasmids [205,206], which are also listed in the **Table 2** These plasmids allow to monitor translation fidelity *in vivo* by measuring luminescence in a luciferase assay. Cells were grown until mid-log phase in SD-Ura medium at 30 °C and luciferase activity was measured using the Dual Glo Luciferase Assay System (Promega) in a luminometer CLARIOstar 1.2 microplate reader (BMG Labtech). Misreading or readthrough rates were calculated as the percentage of firefly*/Renilla* activity of the reporter plasmid divided by the firefly*/Renilla* activity of the reference plasmid. For each strain, the experiment was done in quadruplicate replica and the results show as the mean ± the standard deviation.

Polysome profile analysis

Cell extracts for polysome analysis were obtained accordingly to previously described procedures [207]. Yeast cultures of 200 ml were grown to mid-log phase, then translation was blocked by adding 1 ml of cycloheximide (20 mg/ml) and finally cells were collected by centrifugation. Then, cells were resuspended in 500 µl of lysis buffer (10 mM Tris-HCl, pH 7.5, 100 mM NaCl, 30 mM $MgCl_2$, 100 µg/ml cycloheximide, 200 µg/ml heparin, 0.2 µl/ml DEPC) and 500 µl of glass beads (0.45 µm diameter) were added. Cells were lysed by vortexing 8 min at maximum speed. Cells extracts were clarified by centrifugation at 13,000 rpm for 10 min. Glycerol to a 10% of final concentration was added and samples were quantified and stored at -80 °C. Ten A_{260} units of cell extract were separated by centrifugation in a Beckman Coulter rotor SW41Ti at 39,000 rpm in a 7-50% sucrose gradient for 2 h and 45 min. Then, the A_{254} of the gradients was continuously recorded by an ISCO UA-6 system in order to obtain the polysome profiles. All the protocol, except the acquisition of the profiles, was conducted at 4 °C.

Visualization of proteins tagged with a fluorescent reporter by microscopy

In order to check the localisation of eL22 assembly, the JFY012 strain *(rpl22A*::kanMX4 *rpl22B*::kanMX4) was transformed with two plasmids: one expressing a yEGFP-tagged eL22A protein and another expressing the Nmd3-Δ100 protein, which dominantly inhibits the nuclear transport of LSUs [153]. Cells were grown in liquid SD-Ura-Leu medium and shifted for 24 h to SGal-Ura-Leu medium. Then, cells were stained with Hoechst and inspected by fluorescence microscopy.

In order to study the subcellular location of pre-ribosomal particles upon absence of eL22, the strains BY7471 (wild type), JFY010 (*rpl22A*::kanMX4), JFY011 (*rpl22B*::kanMX4) and JFY012 *(rpl22A*::kanMX4 *rpl22B*::kanMX4) were transformed with plasmids expressing the tagged proteins Nop1-mRFP and uL23-yEGFP or uS3-yEGFP. In this case, the different strains were grown in SD-Ura medium until mid-log phase and then washed with PBS buffer (140 mM NaCl, 8 mM Na_2HPO_4, 1.5 mM KH_2PO_4, 2.75 mM

KCl, pH 7.3); cells were visualized using an Olympus BX61 fluorescence microscopy and the acquired images were analysed with the Olympus cellSens software.

RNA extractions and steady-state RNA levels analysis

Total RNA was extracted from samples corresponding to 10 OD_{600} units of mid-log phase cultures by the acid-phenol method [208]. Cells were first collected and resuspended in 400 µl of TES buffer (10 mM Tris-HCl, pH 7.5, 10 mM EDTA, pH 8.0, 0.5% SDS). Then, 400 µl of acid phenol was added, vigorously mixed, and samples were incubated for 60 min at 65 °C with agitation. Samples were centrifuged and washed once with acid phenol, another time with chloroform and then precipitated by overnight incubation with 1 ml ethanol 96% and 40 µl 3 M sodium acetate at -20 °C, followed by 15 min of centrifugation at maximum speed in a microfuge. Finally, samples were resuspended in 100 µl of distilled water and RNA quantified by using a NanoDrop spectrophotometer (Thermo Fisher Scientific).

Equal amounts of total RNA (normally, 5 µg) were loaded and resolved by electrophoresis in 7% polyacrylamide-8 M gel (for low molecular-weight RNAs) and 1.2% agarose-6% formaldehyde gel (for high molecular-weight RNAs). After migration, RNAs were transferred to a nylon membrane (HybondN, GE Healthcare) and crosslinked as previously described [209]. For northern hybridization, specific antisense oligonucleotides **(Table 3)** were labelled with [γ-^{32}P] ATP (6000 Ci/mmol; Perkin Elmer) and used as probes to detect distinct pre-rRNAs and mature rRNAs. For primer extension analysis, equal amounts of total RNA were subjected to reverse transcription using the specific labelled oligonucleotide probe g ([γ-^{32}P] ATP) as primer. After primer extension, reverse-transcribed DNA was separated by electrophoresis in a 7% polyacrylamide-8 M gel, and the gel placed on a sheet of Whatman filter paper to dry down under vacuum. Nylon membranes or Whatman filter papers were exposed to Phosphorimager screens (Fuji, BAS-IP MS; GE Healthcare) for different times. Visualization was done using a Typhoon™ FLA-9000 imaging system (GE Healthcare). When required, signal intensities were quantified using the GelQuant.NET software.

Pulse-chase labelling of pre-rRNAs

Pulse-chase labelling experiments were done as previously described [210]. Strains BY4741 (wild type) and JFY012 (*rpl22A*::kanMX4 *rpl22B*::kanMX4) were first transformed with an empty YCplac33 plasmid in order to acquire prototrophy for uracil. Cells were grown in liquid SD-Ura medium at 30 °C until mid-log phase and then 40 $0D_{600}$ units were pulse-labelled for 2 min with 100 μCi of [5,6-^{3}H] uracil (45-50 Ci/mmol, PerkinElmer). The pulse was finished by adding a large excess of unlabelled uracil (1 mg/ml). Then, cells were chased for 0, 5, 15, 30, and 60 min. Cells were washed with cold water and frozen until RNA extraction.

Total RNA was extracted by the hot acidic phenol-chloroform procedure described above. Incorporation of labelled uracil was measured by a scintillation counter and about 3000 cpm per RNA sample was loaded and resolved by electrophoresis in a 7% polyacrylamide-8 M urea gel or a 1.2% agarose-6% formaldehyde gel. RNA was transferred to a nylon membrane (HybondN, GE Healthcare), then crosslinked to the membrane and exposed to a tritium screen (BAS-IP TR2040E; GE Healthcare) for different times. Finally, the screen was revealed using a Typhoon™ FLA-9000 imaging system (GE Healthcare).

Affinity purification of complexes containing eL22A-GFP

The strain JFY012 (*rpl22A*::kanMX4 *rpl22B*::kanMX4) was transformed with either YCplac111-L22AGFP or YCplac111-L22A. Then, yEGFP-tagged eL22 was precipitated following the established one-step GFP-Trap_A procedure (Chromotek) [211]. About 40 OD_{600} units of cells growing at mid-log phase in SD-Leu medium were collected and washed twice with cold water. Cells were resuspended in 500 μl of lysis buffer (10 mM Tris-HCl, pH 7.5, 150 mM NaCl, 0.5 mM EDTA, 1.5 mM $MgCl_2$, 1 mM DTT, 0.5% NP-40, complete Protease Inhibitor (Roche)) and 300 μg of glass beads (0.45 μm diameter) were added. Cells were lysed using a FastPrep-24 homogenizer (MP Biomedicals) and then clarified by 15 min of centrifugation at the maximum speed. About 50 μl of GFP-Trap_A beads were added to each cell extracts and incubated for 2 h at 4 °C with end-over-end tube rotation. Then, the beads were washed three times

with 1 ml of lysis buffer and collected. Finally, RNA was purified by the phenol-chloroform procedure and analysed by northern hybridization as described above. RNA was also extracted from total cell extracts and the samples included in the northern blot analysis.

Table 1. Yeast strains used in this study

Strain	Relevant genotype	Source
BY7471	*MAT***a** *his3Δ1 leu2Δ0 met15Δ0 ura3Δ0*	Euroscarf
Y22672	*MAT***a**/*MAT*α *his3Δ1/his3Δ1 leu2Δ0/leu2Δ0 met15Δ0/MET15 LYS2/lys2Δ0 ura3Δ0/ura3Δ0 RPL22A/rpl22A*::kanMX4	Euroscarf
Y25844	*MAT***a**/*MAT*α *his3Δ1/his3Δ1 leu2Δ0/leu2Δ0 met15Δ0/MET15 LYS2/lys2Δ0 ura3Δ0/ura3Δ0 RPL22B/rpl22B*::kanMX4	Euroscarf
Y23329	*MAT***a**/*MAT*α *his3Δ1/his3Δ1 leu2Δ0/leu2Δ0 met15Δ0/MET15 LYS2/lys2Δ0 ura3Δ0/ura3Δ0 RPS9B/rps9B*::kanMX4	Euroscarf
JFY010	*MAT*α *his3Δ1 leu2Δ0 met15Δ0 ura3Δ0 rpl22A*::kanMX4	This work
JFY011	*MAT***a** *his3Δ1 leu2Δ0 met15Δ0 ura3Δ0 rpl22B*::kanMX4	This work
JFY012	*MAT*α *his3Δ1 leu2Δ0 met15Δ0 ura3Δ0 rpl22A::*kanMX4 *rpl22B*::kanMX4	This work
YDB339	*MAT***a** *ura2–52 his3Δ200 trp1-Δ901 ade2-101 leu2-3,112 pep4::LEU2 ste6::HIS3 upf1::hisG [PSI+]*	[206]
JFY551	*MAT***a** *his3Δ1 leu2Δ0 met15Δ0 ura3Δ0 rps9B*::kanMX4	This work
LMA523	*MAT***a** *his3Δ1 leu2Δ0 ura3Δ0 rei1*::natMX4	[169]
LMA525	*MAT***a** *his3Δ1 leu2Δ0 ura3Δ0 alb1*::natMX4	[169]
LMA539	*MAT***a** *his3Δ1 leu2Δ0 ura3Δ0 arx1*::HPH	[169]
Y25234	*MAT***a**/*MAT*α *his3Δ1/his3Δ1 leu2Δ0/leu2Δ0 met15Δ0/MET15 LYS2/lys2Δ0 ura3Δ0/ura3Δ0 RPL38/rpl38*::kanMX3	Euroscarf
Y23772	*MAT***a**/*MAT*α *his3Δ1/his3Δ1 leu2Δ0/leu2Δ0 met15Δ0/MET15 LYS2/lys2Δ0 ura3Δ0/ura3Δ0 RPL31A/rpl31A*::kanMX4	Euroscarf
Y21303	*MAT***a**/*MAT*α *his3Δ1/his3Δ1 leu2Δ0/leu2Δ0 met15Δ0/MET15 LYS2/lys2Δ0 ura3Δ0/ura3Δ0 ALB1/alb1*::kanMX4	Euroscarf
Y24036	*MAT***a**/*MAT*α *his3Δ1/his3Δ1 leu2Δ0/leu2Δ0 met15Δ0/MET15 LYS2/lys2Δ0 ura3Δ0/ura3Δ0 ARX1/arx1*::kanMX4	Euroscarf
JFF084	*MAT***a** *his3Δ1 leu2Δ0 ura3Δ0 rpl38*::kanMX4	This work
JFY449	*MAT***a** *his3Δ1 leu2Δ0 ura3Δ0 rpl31A*::kanMX4	This work
JFY535	*MAT***a** *his3Δ1 leu2Δ0 ura3Δ0 alb1*::kanMX4	This work
JFY540	*MAT***a** *his3Δ1 leu2Δ0 ura3Δ0 arx1*::kanMX4	This work
JFY497	*MAT***a** *his3Δ1 leu2Δ0 met15Δ0 ura3Δ0 rpl22A*::kanMX4 *rpl22B*::kanMX4 *rei1*::natMX4	This work
JFY501	*MAT***a** *his3Δ1 leu2Δ0 met15Δ0 ura3Δ0 rpl22A*::kanMX4 *rpl22B*::kanMX4 *alb1*::natMX4	This work
JFY524	*MAT*α *his3Δ1 leu2Δ0 met15Δ0 ura3Δ0 rpl22A*::kanMX4 *rpl22B*::kanMX4 *arx1*::HPH	This work
JFY531	*MAT***a** *his3Δ1 leu2Δ0 met15Δ0 ura3Δ0 rpl22A*::kanMX4 *rpl22B*::kanMX4 *rpl31A*::kanMX4	This work
JFY564	*MAT***a** *his3Δ1 leu2Δ0 met15Δ0 ura3Δ0 rpl22A*::kanMX4 *rpl22B*::kanMX4 *alb1*::kanMX4	This work
JFY563	*MAT***a** *his3Δ1 leu2Δ0 met15Δ0 ura3Δ0 rpl22A*::kanMX4 *rpl22B*::kanMX4 *arx1*::kanMX4	This work
JFY114	*MAT***a** *his3Δ1 leu2Δ0 met15Δ0 ura3Δ0 rpl22A*::kanMX4 *rpl22B*::kanMX4 *rpl38*::kanMX4	This work

Table 2. Plasmids used in this study

Name	Relevant information	Source
YCplac33	*CEN, URA3*	[212]
YCplac111	*CEN, LEU2*	[212]
YCplac111-RPL22A	*RPL22A, CEN, LEU2*	This study
YCplac111-L22AGFP	*RPL22A-yEGFP, CEN, LEU2*	This study
pRS316-RPL25-eGFP NOP1-mRFP	*RPL25-yEGFP, mRFP-NOP1, CEN, URA3*	[213]
pRS316-RPS3-eGFP NOP1-mRFP	*RPS3-yEGFP, NOP1-mRFP, CEN, URA3*	[213]
YEplac195-lucCAAA (pDB688)	*Renilla* and firefly control construction 2µ, *URA3*	[205]
YEplac195-lucCAAA H245R CGC (pDB868)	*Renilla* and firefly H245R construction 2µ, *URA3*	[205]
YEplac195-lucCGAC (pDB690)	*Renilla* and firefly CGA control codon construction, 2µ, *URA3*	[206]
YEplac195-lucUGAC (pDB691)	*Renilla* and firefly UGA stop codon construction, 2µ, *URA3*	[206]
YEplac195-lucUAGC (pDB720)	*Renilla* and firefly UAG stop codon construction, 2µ, *URA3*	[206]
YEplac195-lucCAGC (pDB721)	*Renilla* and firefly CAG control codon construction, 2µ, *URA3*	[206]
YEplac195-lucCAAC (pDB722)	*Renilla* and firefly CAA control codon construction, 2µ, *URA3*	[206]
YEplac195-lucUAAC (pDB723)	*Renilla* and firefly UAA stop codon construction, 2µ, *URA3*	[206]
pRS315-*rps9B*-D94N (pDB957)	*rps9B*-[D94N], *CEN, LEU2*	[205]
pRS316-GAL-*NMD3Δ100*	*GAL::NMD3Δ100, CEN, URA3*	[214]

Table 3. Oligonucleotides used in this study

Name	5'-3' sequence	Use
L22A UP	CTGCAGCCATTGACCTTATGTTCG	Cloning
L22A DOWN	CTGCAGGAGTTATTAGGTCGAGGC	Cloning
L22A GFP UP	GAATTCTGGGTTTGAAATCA	Cloning
L22A GFP DOWN	TCTAGATTCTTCGTCTTCTTCTTCG	Cloning
L22A COMP UP	CAACCCAAAGACTTTGGAAT	PCR verification
L22A COMP DOWN	ACCATATAGCCATTTCGACT	PCR verification
L22B COMP UP	CCGTATCGTGCACAGATTTA	PCR verification
L22B COMP DOWN	AGGGCCAAATCTATGTACTG	PCR verification
L22A SEC1	GAGATTAACAACTTTACCTG	Sequencing verification
L22A SEC2	GATATAGACTTCCAGAAAGC	Sequencing verification
L22A SEC3	CTCTACCAAGACCAACGAAT	Sequencing verification
REI1 COMP UP	TGTCCTATCAAACATTCTGG	PCR verification
REI1 COMP DOWN	AGGCTTAAAGTTGGCTCAAG	PCR verification
ARX1 COMP UP	TCTGTCAGTTTTAGAATCTG	PCR verification
ARX1 COMP DOWN	TTTGTGGAAGAACCTGCTAA	PCR verification
ALB1 COMP UP	TCTACTTTTTCGTCTTGTGC	PCR verification
ALB1 COMP DOWN	ACCAATTTACGTTCCACTAC	PCR verification
RPL31A COMP UP	GTCTGAGTAACTTGTGGAGTC	PCR verification
RPL31A COMP DOWN	GCGTACATCCTAGCCTAAC	PCR verification
RPL38 COMP UP	GAATTCGCTCCCAGCAGATCCAAG	PCR verification
RPL38 COMP DOWN	GGATCCGATGAATTTTTGAATGAGGCTCC	PCR verification
Probe b (18S)	CATGGCTTAATCTTTGAGAC	18S rRNA hybridization
Probe c (3-D/A_2)	GACTCTCCATCTCTTGTCTTCTTG	Pre-rRNA hybridization
Probe d (A_2/A_3)	TGTTACCTCTGGGCCC	Pre-rRNA hybridization
Probe e (5.8S)	TTTCGCTGCGTTCTTCATC	5.8S rRNA hybridization
Probe f (E/C_2)	GGCCAGCAATTTCAAGTTA	Pre-rRNA hybridization
Probe g (C_1/C_2)	GAACATTGTTCGCCTAGA	Pre-rRNA hybridization and primer extension
Probe h (25S)	CTCCGCTTATTGATATGC	25S rRNA hybridization
Probe 5S	GGTCACCCACTACACTACTCGG	5S rRNA hybridization

RESULTS

Loss of eL22 results in a mild growth defect that is exacerbated at low temperatures

To investigate the role of eL22 in ribosome biogenesis, we first studied the phenotypic consequences on growth of deleting either the *RPL22A* (thereafter, *rpl22AΔ* strain) or *RPL22B* (thereafter, *rpl22BΔ* strain) genes and of deleting simultaneously both genes (thereafter, *rpl22Δ* or *rpl22* null strain). The growth of these strains and that of an isogenic wild-type control were tested by serial dilutions onto YP(A)D plates at different temperatures. Although deletion of most r-protein genes causes lethality or a severe growth defect (e.g.[30]), our analysis found that cells lacking eL22 displayed just a moderate slow growth when grown at the permissive temperature of 30 °C **(Figure 3)**. This phenotype was practically suppressed when the incubation temperature was 37 °C. However, at lower temperatures (22 °C), the absence of eL22 led to a severe growth defect. As also observed in **Figure 3**, the responsible for this growth defect was the deletion of the *RPL22A* rather than that of the *RLP22B* gene, as the *rpl22* null strain grew similarly as the *rpl22AΔ* single mutant. Moreover, the *rpl22BΔ* single mutant grew identically to the isogenic wild-type strain at the different temperatures tested. These results are in agreement with previously published data and indicate that eL22 is required for optimal growth, specially at low temperatures [30,190,192].

Loss of eL22 does not affect translation fidelity

As eL22 is not essential for growth, at least under standard laboratory conditions, ribosomes lacking eL22 are assembled and engaged into translation. It has been previously shown that the absence of or mutation in specific r-proteins can lead to a reduction in translation fidelity [215-217]. Thus, we wondered whether part of the growth defects led by the absence of eL22 could be attributed to a decrease in the translation accuracy of ribosomes lacking eL22. To investigate this, we used a set of reporter plasmids based on the dual *Renilla/*firefly luciferase system [205,206]. These constructs contain an upstream *Renilla* luciferase gene followed by a firefly luciferase gene under the control of the *PGK* promoter with both ORFs being separated by an in-

frame linker sequence. In the control plasmid, the two luciferase reports are synthesised as a single bi-functional polypeptide chain, but in the readthrough reporters, a single in-frame stop codon within the linker sequence impedes the translation of the distal firefly gene [206].

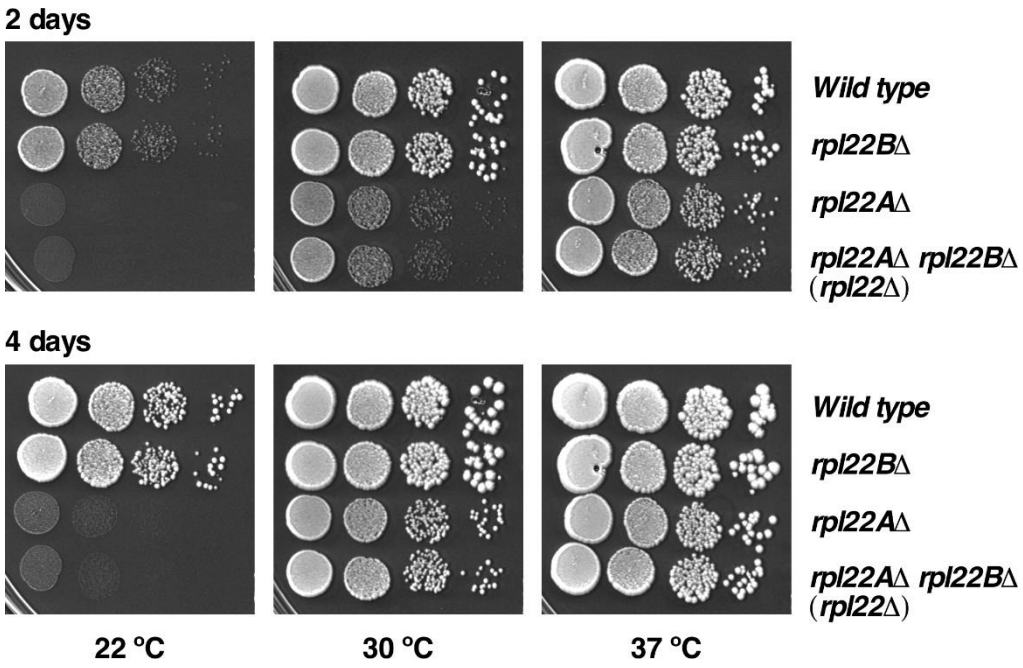

Figure 3. Deletion of *RPL22* genes results in a cold-sensitive phenotype. Growth comparison of wild type, single *rpl22ΔA* and *rpl22ΔB* deletions and double *rpl22ΔA rpl22ΔB* (hereafter *rpl22Δ*) deletion strains. Cells were grown at 30 °C in YP(A)D media until mid-log phase, diluted to an OD_{600} of 0.05 and then 10-fold serial dilutions were spotted onto plates of YP(A)D media. Plates were incubated at 22, 30 and 37 °C for 2 (upper panels) and 4 days (bottom panels).

We also used reporters to evaluate misreading; in this case, the control plasmid codes a functional firefly luciferase (CAC codon coding for a His residue at position 245) while the misreading reports contain mutated non-luminescent versions of firefly luciferase which need that ribosomes commit a specific error to generate luminescence that can be then quantified. In our case, we made use of a mutant variant containing the CGG codon coding for an Arg residue at position 245 of the firefly luciferase protein, which leads only to residual luciferase activity; any increase in this activity must result from a misreading event that allows misincorporation of, normally, a His residue at the mutated CGC codon [205]. We performed cell extracts of isogenic wild-type and eL22-

lacking strains grown at 30 °C and the firefly/*Renilla* ratio obtained for each plasmid. As shown in **Figure 4**, our results do not evidence any significant difference either on readthrough or misincorporation during translation of eL22-lacking ribosomes, in contrast to the positive control strains used to evaluate these mistranslation events. We conclude that ribosomes lacking eL22 are apparently not more error-prone than wild-type ones, and therefore that eL22 is likely not involved in the fidelity of translation elongation.

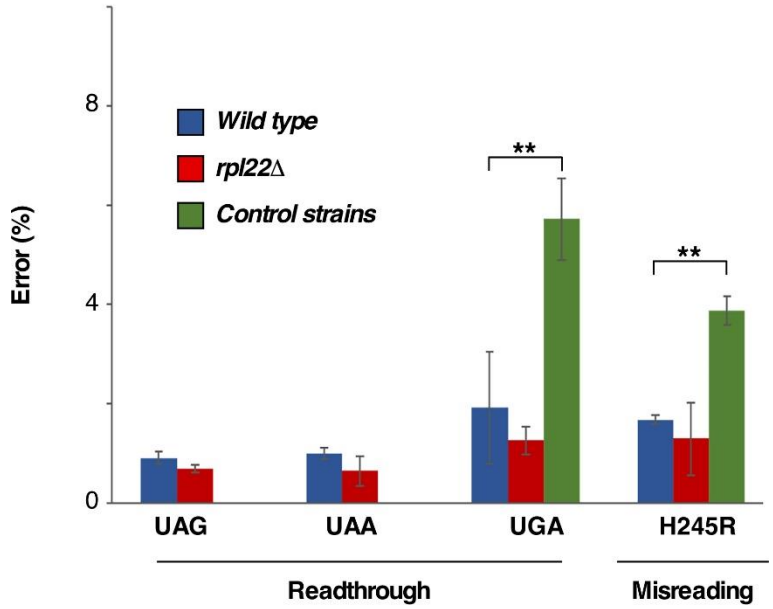

Figure 4. Translational readthrough and misreading in the *rpl22* null strain. Measurement of the readthrough and misincorporation frequencies events during translation in a yeast strain lacking eL22. Wild-type and *rpl22*Δ cells were transformed with different couples of plasmids to measure UAG readthrough (pDB720 or pDB721), UAA readthrough (pDB722 or pDB723) and UGA readthrough (pDB690 or pDB691) or Arg245(GGC) to His245 (CAG) misreading (pDB688 and pDB868). A *upf1Δ* strain was used as a positive control for the UGA readthrough error [206] and a *rps9B*[D94N] strain was used as positive control for the misincorporation error [205]. Transformants were cultivated in liquid SD-Ura media until mid-log phase at 30 °C and then *Renilla* and firefly luciferase activity was measured. The data were expressed as the mean ± the standard deviation of four biological replicates. The percentage of error was calculated as the firefly/*Renilla* luciferase activity ratio of the nonsense or non-luminescent construct divided by the firefly/*Renilla* luciferase activity ratio of the sense or luminescent construct multiplied by 100. Significance levels were calculated by Student's t-test (*, $p < 0.05$).

eL22 associates with pre-60S r-particles during middle-nucleolar stages of assembly

Assembly of most r-proteins occurs in the nucle(ol)us, although a few LSU r-proteins appear to stably load only with cytoplasmic pre-60S r-particles. In the nucle(ol)us, r-proteins can associate to pre-ribosomal intermediates at different stages, from early to late ones [91,218]. The exact timing of eL22 assembly was initially unknown. eL22 has been found among the r-proteins present in nucleoplasmic pre-60S r-particles analysed by cryo-EM methods [134]. However, the comparative compositional analysis of various affinity purified particles spanning early to late nuclear pre-60S r-particles did result inconclusive in the case of eL22 [91]. To further study the timing of assembly of eL22, we expressed an eL22A protein tagged at its C-terminal end with a yeast enhanced GFP (yEGFP) molecule from its own promoter on a *CEN* plasmid. This eL22-yEGFP protein was fully functional as its expression restored the growth defects depicted by the *rpl22* null strain at 30 °C. Moreover, the eL22-yEGFP protein also complemented the LSU formation defect of the *rpl22* null strain (see next section and **Figure 5**).

We monitored the localisation of the eL22-yEGFP construct upon expression of the Nmd3-Δ100 dominant negative variant protein under the control of an inducible *GAL* promoter. Nmd3 is an essential factor required for the nucleo-cytoplasmic export of pre-60S r-particles [153,219]; the dominant-negative *NMD3-Δ100* allele produces a truncated protein that lacks the nuclear export signal (NES) of the factor, resulting in the trap of pre-60S r-particles in the nucle(ol)us [153]. As a result, we observed that eL22-yEGFP accumulated in the nucleus under inducible conditions of the *NMD3-Δ100* expression but, as expected for a r-protein, it was found in the cytoplasm under non-inducible conditions of the *NMD3-Δ100* allele **(Figure 6)**. These results confirmed that eL22 is assembled in the nucleus, as strongly suggested by the previous structural analysis studies [92,134].

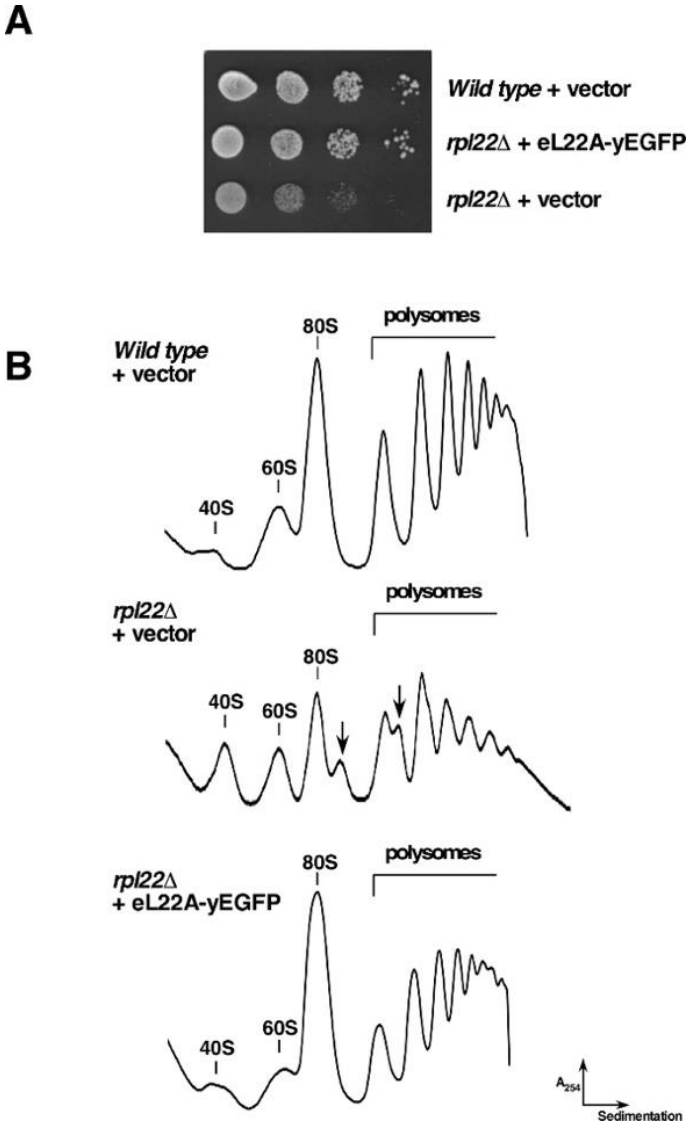

Figure 5. Functional analysis of the eL22A-yEGFP construct. (**A**) Growth comparison of the isogenic wild type and *rpl22Δ* strains transformed with an empty YCplac111 centromeric plasmid and the *rpl22Δ* strain transformed with a YCplac111 plasmid harbouring a RPL22A-yEGFP allele that expressed GFP-tagged eL22A from its own promoter. Cells were grown in SD-Leu at 30 °C until mid-log phase, diluted to an OD_{600} of 0.05 and then 10-fold series of dilutions were spotted on SD-Leu plates. Plates were incubated for two days at 30 °C. **(B)** The above strains were grown in SD-Leu media until mid-log phase at 30 °C. Then, whole cell extracts were prepared, and 10 A_{260} units of each extract were resolved in 7-50% sucrose gradients. The A_{254} was continuously measured. Peaks corresponding to free SSUs (40S) and LSUs (60S), vacant ribosomes/monosomes (80S) and polysomes are indicated. Half-mer polysomes are labelled with arrows.

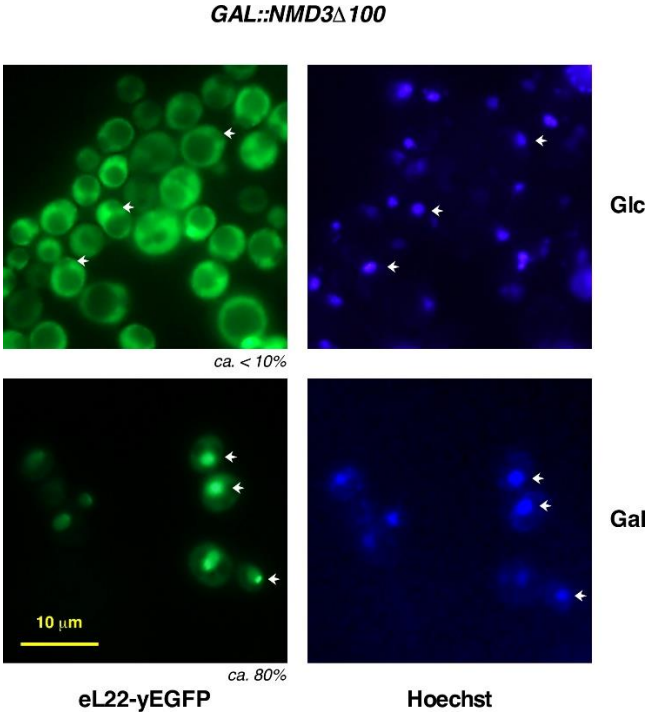

Figure 6. Nucle(ol)ar assembly of eL22. Localisation of GFP-tagged eL22 upon induction of the dominant-negative *NMD3-Δ100* allele, which expresses a truncated Nmd3-Δ100 protein lacking the nuclear export signal (NES) from a *GAL* promoter. Cells of the *rpl22* null strain expressing eL22-yEGFP from a plasmid were transformed with the pRS316-GAL-NMD3Δ100 plasmid. Transformants were grown in liquid SD-Ura-Leu medium (Glc) at 30 °C until mid-log phase and shifted for 24 h to SGal-Ura-Leu (Gal) to induce the expression of the Nmd3-Δ100 protein. Then, cells were stained with Hoechst and inspected by fluorescence microscopy. Arrows point to nuclei of representative cells. Approximately 200 cells were examined per experiment; the percentage of cells showing nucle(ol)ar accumulation of eL22-yEGFP is depicted. Scale bar, 10 µm.

Next, we affinity purified particles containing eL22-yEGFP using GFP-Trap beads and determined which pre-rRNAs co-purified with them by northern blot hybridization. As shown in **Figure 7**, eL22-yEGFP was able to co-purify with 27SB pre-rRNAs and subsequent pre-rRNA intermediates as 7S pre-rRNAs; as expected for a r-protein, there was also substantial co-purification of the mature rRNAs. However, we could not detect the $27SA_2$ pre-rRNA, which is the main intermediate of earliest pre-60S r-particles. Thus, this result strongly suggests that eL22 stably associates with early to middle nucleolar pre-60S r-particles but not at very earlier steps, as again suggested by the previous structural analysis studies [92].

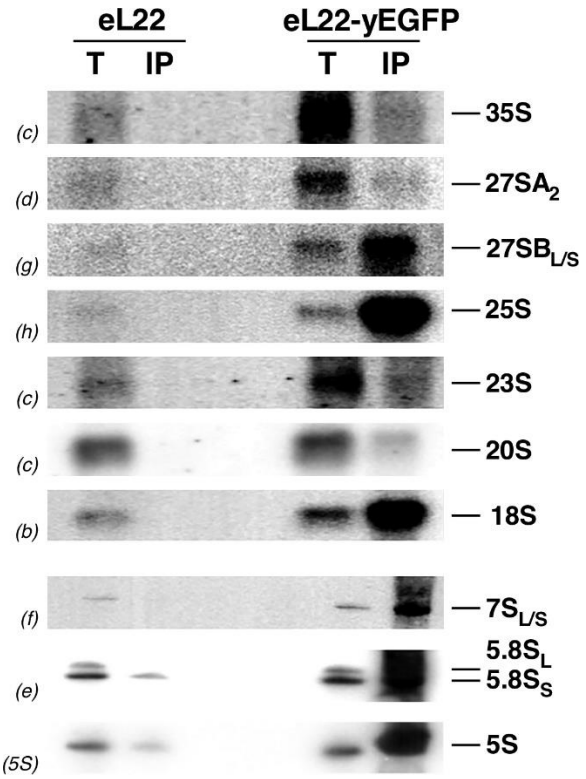

Figure 7. eL22-yEGFP stably assembles with pre-60S particles containing 27SB pre-rRNAs. Cells from the *rpl22* null strain expressing an untagged eL22 or a yEGFP-tagged eL22 protein from a plasmid were grown in SD-Leu media at 30 °C until mid-log phase. Whole cell extracts were performed and ribosomal particles affinity purified using the GFP-Trap immunoprecipitation method. Total RNA was extracted from whole cell extracts (T) and immunoprecipitates (IP) and analysed by northern blotting. Probes used to detect the different pre- and mature rRNAs are indicated between parentheses.

Loss of eL22 results in a shortage of 60S r-subunits

To investigate whether or not the absence of eL22 affects the production of mature LSUs, we analysed the polysome profiles from the *rpl22AΔ* and *rpl22BΔ* single mutants and the *rpl22* null strain at 30 °C. As shown in **Figure 8**, both *rpl22AΔ* and *rpl22Δ* mutants displayed aberrant polysome profiles compared to those of an isogenic wild-type strain, evidenced by the clear decreased levels of free LSUs *versus* free SSUs and the presence of half-mer polysomes. These profiles are a common feature of mutants specifically impaired in the biogenesis of LSUs. However, as expected, *rpl22BΔ* cells presented a normal profile similar to that obtained for the isogenic wild-type strain.

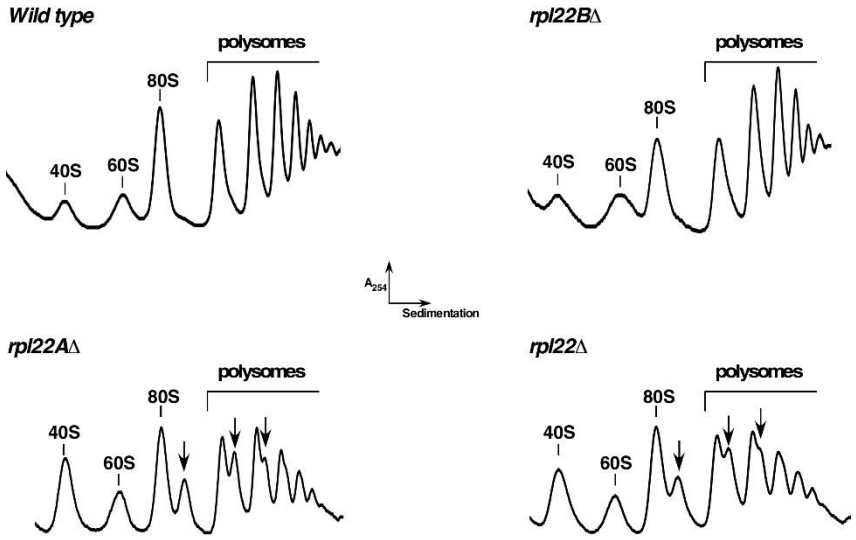

Figure 8. Absence of eL22 results in a deficit in 60S r-subunits. Polysome profiles analysis of the wild-type and *rpl22* null strains. Cells were grown in liquid YP(A)D media at 30 °C until mid-log phase, whole cell extracts were obtained and 10 A_{260} units of each extract were resolved in 7-50% sucrose gradients. The A_{254} was continuously measured. Peaks corresponding to free SSUs (40S) and LSUs (60S), vacant ribosomes/monosomes (80S) and polysomes are indicated. Half-mer polysomes are labelled with arrows.

We also analysed how the absence of eL22 affected the production of mature LSUs at 22 and 37 °C. As shown in **Figure 9**, the extent of the LSU defect did not aggravate when *rpl22* null cells were grown at 22 °C (**Figure 9A**) but was almost completely eliminated when cells lacking eL22 were grown at 37 °C (**Figure 9B**)**.** Thus, we conclude that eL22 plays an important role for the production of LSUs; we hypothesize that eL22 must exert its function through the proper folding of pre-rRNA. At low temperatures, pre-rRNA may be trapped in an unproductive conformation in the absence of eL22, circumstance that might be bypassed at high temperatures, thus allowing more intermediate pre-60S r-particles to mature and impacting growth to a lesser extent.

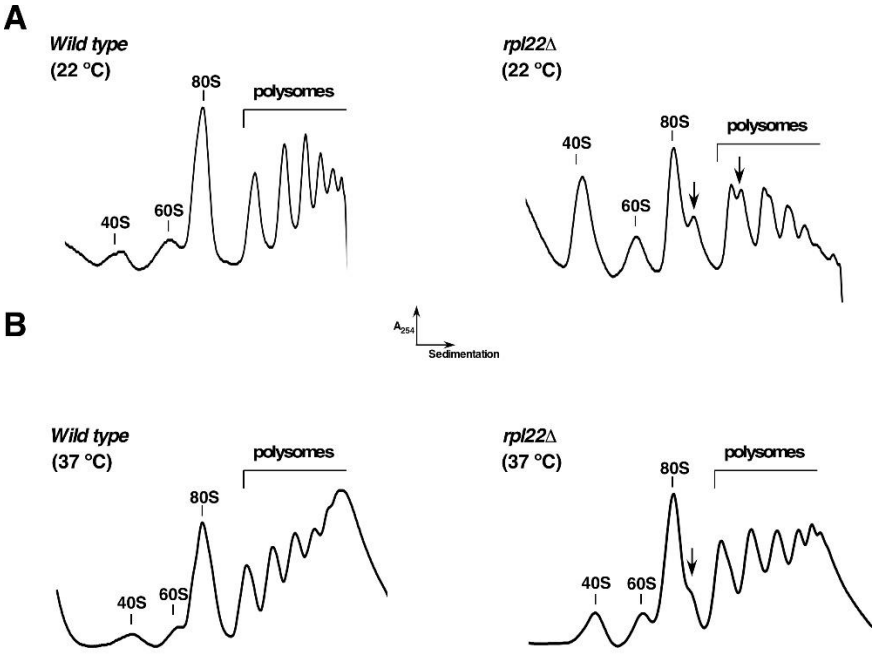

Figure 9. The 60S r-subunit shortage led by absence of eL22 is less severe at high temperatures. Polysome profiles analysis of the wild-type and *rpl22* null strains. Cells were grown in liquid YP(A)D media until mid-log phase either at 22 °C (**A**) or 37 °C (**B**). Whole cell extracts were obtained and 10 A_{260} units of each extract were resolved in 7-50% sucrose gradients. The A_{254} was continuously measured. Peaks corresponding to free SSUs (40S) and LSUs (60S), vacant ribosomes/monosomes (80S) and polysomes are indicated. Half-mer polysomes are labelled with arrows.

The absence of eL22 leads to a mild defect on the nuclear export of pre-60S r-particles

To further evaluate the consequences of the absence of eL22 on LSU maturation, we determined whether the *rpl22Δ* mutant strain was impaired in nuclear export of pre-60S r-particles. To do so, we analysed the localization of uL23-yEGFP, which was used as an LSU reporter in the *rpl22* null and the isogenic wild-type strains grown at 30 °C and 22 °C. As shown in **Figure 10**, when cells were grown at 22 °C the steady-state levels of uL23-yEGFP were cytoplasmic in the wild-type strain, as expected for a r-protein. In addition, an apparent similar localization was found in the *rpl22BΔ* strain (**data not shown**). However, we observed a mild nuclear retention of the fluorescent signal of the uL23-yEGFP reporter on some cells (ca. 30%) of the *rpl22AΔ* (**data not shown**) and *rpl22* null strain (**Figure 10**). The comparison with the localization of the mRFP-Nop1 nucleolar reporter led us to conclude that this retention was mostly nucleolar. This retention phenotype was specific for the LSU reporter since when we analysed the localisation of

uS3-yEGFP, which was used as a SSU reporter, it localised in the cytoplasm in both wild-type and *rpl22* null cells. Very faint differences in the localisation of either uL23-yEGFP was observed at 30 °C when wild-type and *rpl22* null cells were compared (**data not shown**).

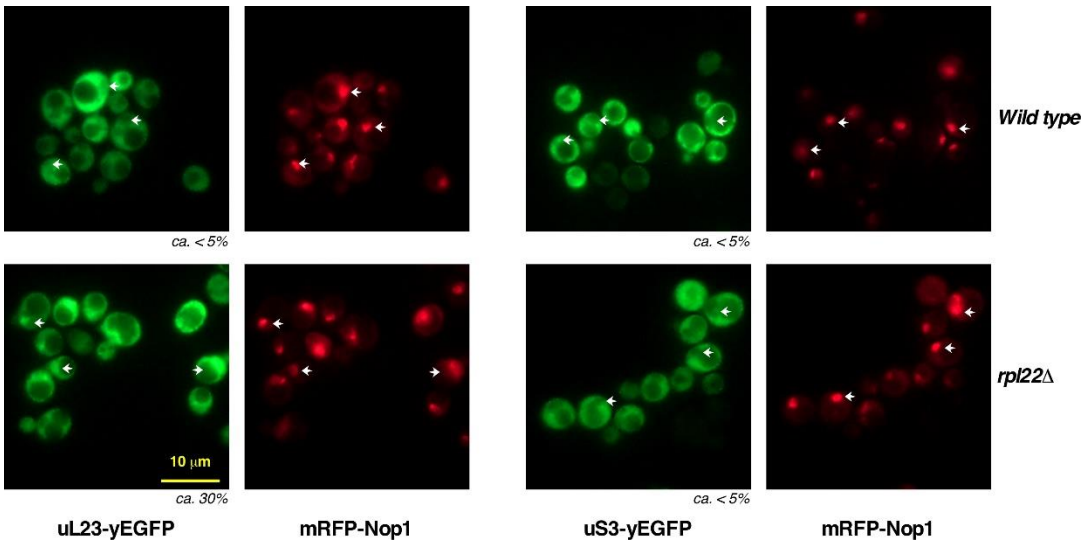

Figure 10. eL22 is required for an efficient nuclear-cytoplasmic export of pre-60S r-particles. Isogenic wild-type and *rpl22* null cells were transformed with plasmids that co-expressed mRFP-Nop1 and either uL23-yEGFP or uS3-yEGFP from their cognate promoters. uL23 r-protein was used as a reporter for pre- and mature 60S r-particles while uS3 r-protein was used as a report for pre- and mature 40S r-particles. Selected transformants were grown in liquid SD-Leu medium at 30 °C until mid-log phase, and then shifted to 22 °C for 3 h. The subcellular localisation of the GFP-tagged r-proteins and the mRFP-Nop1 nucleolar marker was analysed by fluorescence microscopy. Selected nucleoli are pointed by arrows. Approximately 200 cells were examined per experiment; the percentage of cells showing nucle(ol)ar accumulation of either uL23-yEGFP or uS3-yEGFP is depicted. Scale bar, 10 μm.

It is strongly unlikely to expect that eL22 would have a direct role in the nucleo-cytoplasmic export of pre-60S r-particles, therefore, we assume that this defect must arise from the activation of a sort of nuclear quality control mechanism that prevents exit of abnormal pre-60S r-particles from the nucle(ol)us to the cytoplasm due to the absence of the correct assembly of eL22. A similar conclusion has previously been reported upon the deletion, depletion or mutation in other r-protein genes (see Discussion).

eL22 is required for normal 27SB pre-rRNA processing

To determine whether the LSU maturation defects observed in the absence of eL22 could be attributed to an impairment of a specific step of the pre-rRNA processing pathway, we assessed the steady-state levels of pre- and mature rRNAs from the single and double *rpl22* mutants by northern blot hybridization and primer extension analyses. To do this, we first extracted and analysed RNA from wild-type cells, *rpl22AΔ* and *rpl22BΔ* single mutants and the *rpl22* null strain grown in YP(A)D at 30 °C. Consistent with the polysome profile data, no apparent defects were observed in the *rpl22BΔ* single mutant compared to the isogenic wild-type strain (**Figure 11**). In contrast, the *rpl22AΔ* single mutant and the *rpl22* null strain showed mild defects in pre-rRNA processing, which were similar in both cases. In these mutants, a significant accumulation of 27SB pre-rRNA was observed and the amount of mature 25S rRNA mildly decreased (**Figure 11A**). However, the accumulation of 27SB pre-rRNAs was not accompanied by apparent alterations in the steady-state levels of 7S pre-rRNAs and of mature 5.8S and 5S rRNAs (**Figure 11B**). Primer extension confirmed that the levels of both $27SB_L$ and $27SB_S$ pre-rRNAs increased, while levels of $27SA_2$ and $27SA_3$ pre-rRNAs remained practically unaltered (**Figure 11C**).

In the *rpl22AΔ* and *rpl22* null strains, we also observed a slight accumulation of both 35S and 23S pre-rRNAs **(Figure 11A)** that, as discussed later, could be the reflect of an increment of post- in detriment of co-transcriptional pre-rRNA processing and the consequent increase in premature cleavage at site A_3 [55]. Alternatively, as mentioned in other studies (see Discussion), these accumulations could be the indirect effect of limiting relevant assembly factors required for early processing of 35S pre-rRNA that cannot properly recycle from abnormal pre-60S r-particles as the consequence of the lack of assembly of the eL22 r-protein.

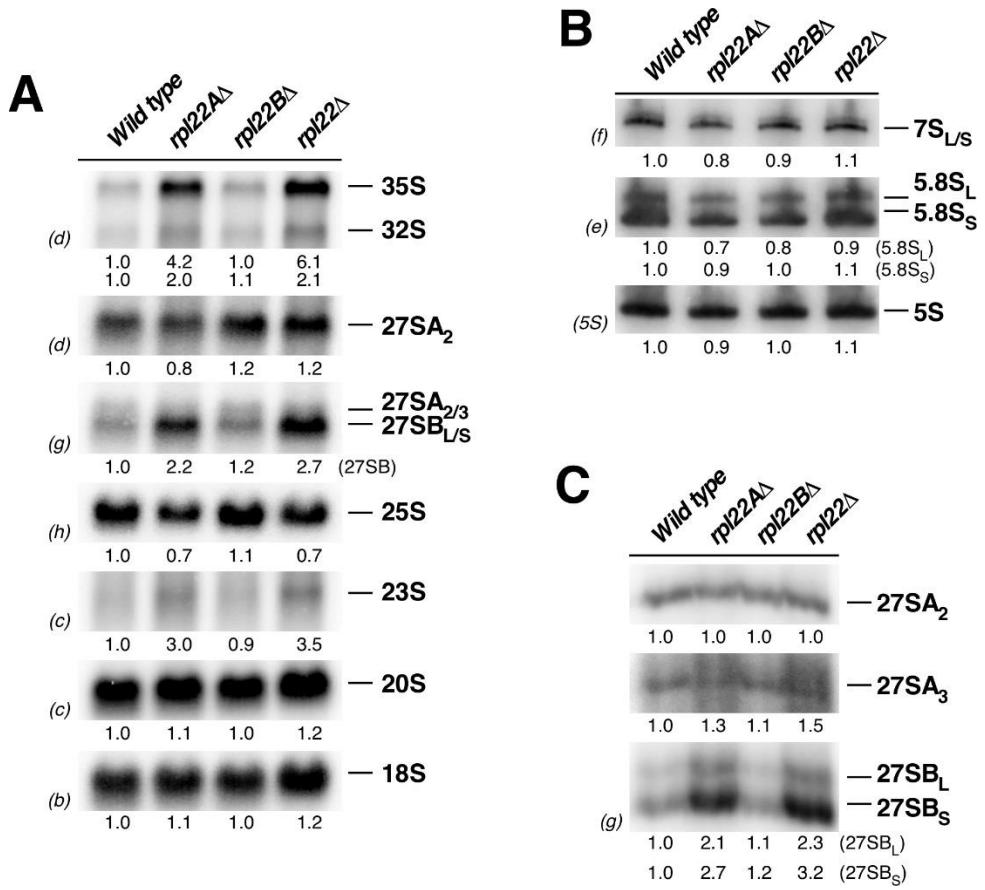

Figure 11. Absence of eL22 affects 27SB pre-rRNA processing. The indicated isogenic strains were grown in liquid YP(A)D media at 30 °C until mid-log phase. Total RNA was extracted and equal amounts (5 µg) were subjected to northern blotting or primer extension analysis. (**A**) Northern blot analysis of high-molecular-mass pre- and mature rRNAs. (**B**) Northern blot analysis of low-molecular-mass pre- and mature rRNAs. (**C**) Primer extension analysis using the probe g as primer. Signal intensities of the different RNAs were measured by phosphorimager scanning (indicated below each panel) and normalised to the signals obtained for the wild-type samples, arbitrarily set to 1.0. The probes used for hybridizations and that for primer extension analysis are indicated between parentheses and described in the Materials and Methods section.

As mature rRNAs are rather stable, to ascertain the contribution of eL22 to the dynamic conversion of pre-rRNAs to mature rRNAs, we also studied the kinetics of rRNA formation by [5,6-^{3}H] uracil pulse-chase analysis. This experiment was done with the *rpl22* null strain and its isogenic wild-type counterpart grown at 30 °C. As a result, both strains displayed very similar kinetics of rRNA synthesis, but *rpl22* null cells presented a very mild delay in the conversion of 27SB pre-rRNAs to mature 25S rRNA and a slight delay in that of 7S pre-rRNAs to mature 5.8S rRNAs **(Figure 12)**. However, these delays have only slight consequences in the efficiency of production of the corresponding mature rRNAs. No apparent impairment in either the processing of 20S pre-rRNA to

mature 18S rRNA or the synthesis of 5S rRNA was detected. Altogether, these results indicate that eL22 is not required for the maturation of rRNA. Instead, the absence of eL22 induces only a very minor defect on the specific branch of the pre-rRNA processing pathway that reduce the efficiency of the conversion of 27SB pre-rRNAs to mature 25S and 5.8S rRNAs.

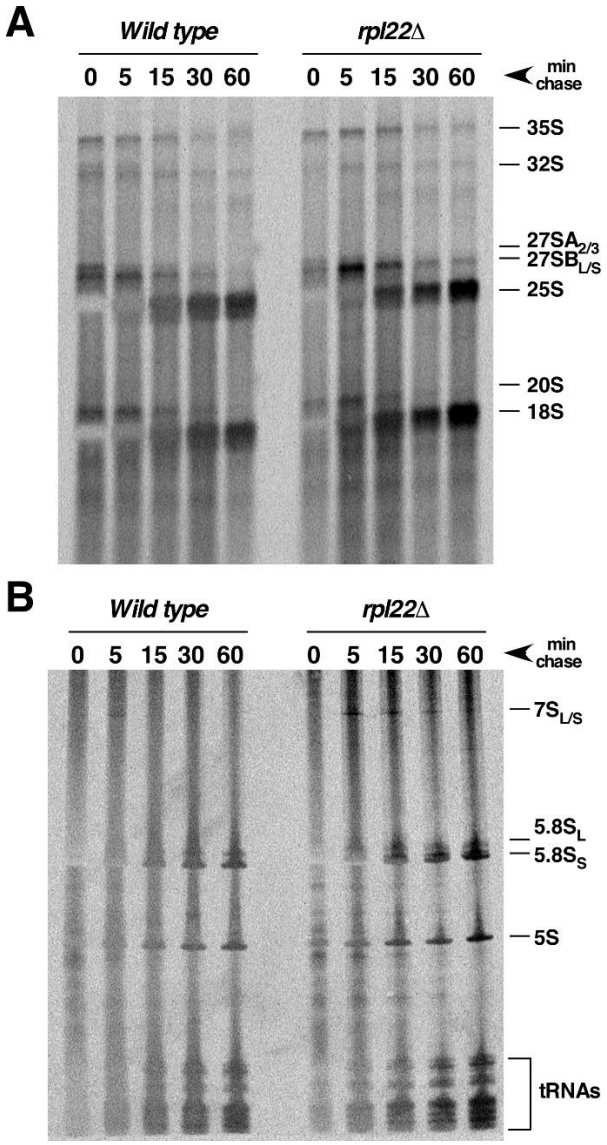

Figure 12. Absence of eL22 leads to delayed processing of 27S pre-rRNAs. Wild-type and *rpl22Δ* cells were transformed with an empty YCplac33 (*CEN URA3*) plasmid and then grown in liquid SD-Ura at 30 °C until mid-log phase. Cells were pulse-labelled for 2 min with [5,6-^{3}H] uracil, washed and chased for 5 to 60 minutes with a large excess of unlabelled uracil. Total RNA was extracted and about 3000 cpm per sample were loaded and separated on (**A**) a 1.2% agarose-6% formaldehyde gel or **(B)** a 7% polyacrylamide-8 M urea gel. RNA was transferred to nylon membranes, exposed to a ^{3}H-sensitive phosphor screen and analysed by phosphorimager scanning. The position of the different pre- and mature rRNAs is indicated.

eL22 functionally interacts with its neighbouring eL38 and eL31 r-proteins

As previously mentioned, in the cytoplasm, after the release of Nog1 and Rlp24 and the association of Rei1, eL22 is located at its final position in pre-60S r-particles (see **Figure 1**). In this spatial context, eL22 interacts with the globular domain and the initial C-terminal part of Rei1, which projects towards the PET. The two closest r-proteins that flank eL22 and the Rei1 extension on the left and right surface of the pre-60S r-particle are eL31 and eL38, respectively. Strikingly, these two r-proteins share several features with eL22. Thus, as eL22, eL31 and eL38 are non-essential eukaryote-specific r-proteins. All three are globular proteins lacking prominent N- or C-terminal extensions. Finally, they are apparently assembled in intermediate steps of LSU maturation [30,92,189]. Hence, we wondered whether eL31 and/or eL38 r-proteins were functionally related to eL22. In yeast, it has been previously reported that the absence of eL31 causes a severe growth defect whereas that of eL38 does not induce any perceptible growth impairment. Moreover, while eL38 is encoded by a single *RPL38* gene, eL31 is encoded by two paralogous genes, being *RPL31A* the one having the major contribution to growth [30,220].

To check for functional relationships between these r-proteins, we evaluated whether the growth defect caused by the absence of eL22 could be enhanced by the absence of eL31A or eL38. As shown in **Figure 13**, the introduction of the *rpl31AΔ* deletion into the *rpl22* null strain caused a very slight enhancement of the growth defect of the latter strain, while that of *rpl38Δ* led to a clear synthetic enhancement, specially at low temperatures (22 °C). The defects observed in cells lacking both eL22 and eL38 were more evident when cells were treated with sublethal concentration of specific translation antibiotics (**Figure 14**). Further studies are required to understand the functional relevance of these interactions, that unfortunately could not be done in this thesis work due to time restrictions.

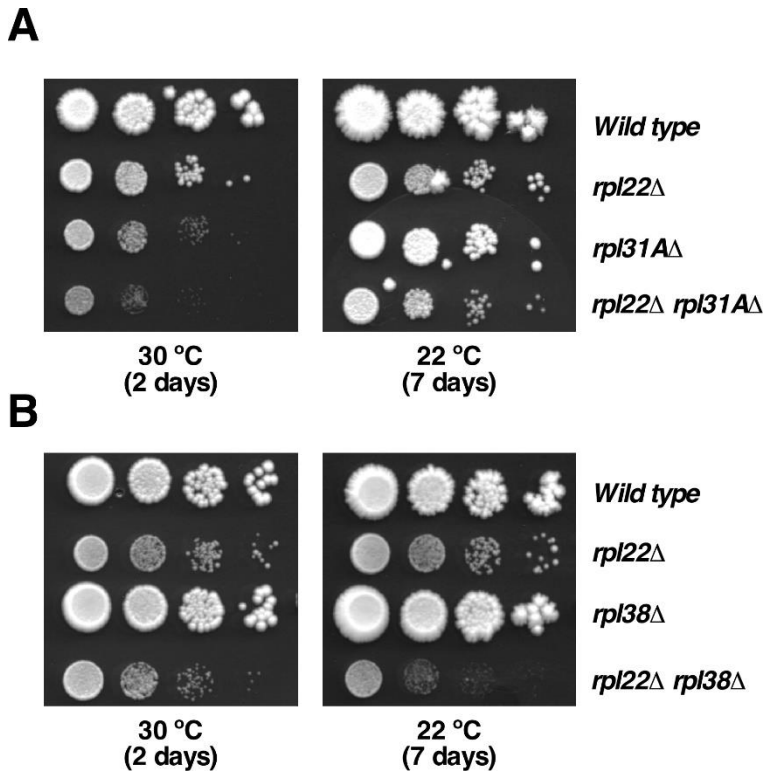

Figure 13. eL22 is functionally linked to eL31 and eL38. Growth assay of strains lacking eL22 and eL31A or eL38 r-proteins. Wild-type, single or triple deletion strains were grown in YP(A)D media at 30 °C until mid-log phase, diluted to an OD_{600} of 0.05 and then 10-fold series of dilutions were spotted on YP(A)D plates. Plates were incubated at 30 and 22 °C for the indicated times. (**A**) Analysis of cells deleted for *RPL22* and *RPL31A* genes. (**B**) Analysis of cells deleted for *RPL22* and *RPL38* genes. Note that deletion of either *RPL31A* or *RPL38* exacerbates the slow-growth phenotype of *rpl22* null cells, specially at 22 °C.

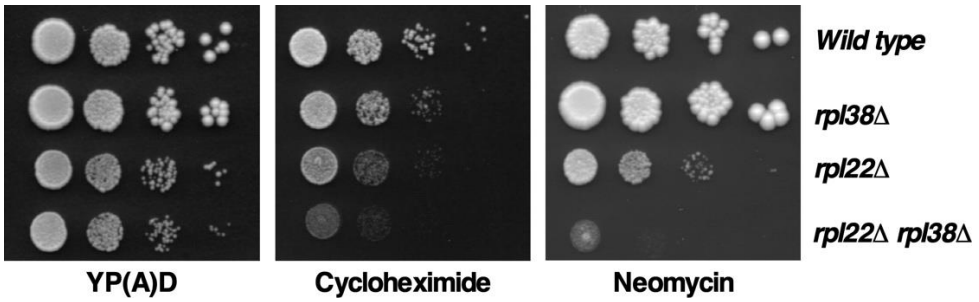

Figure 14. Drugs impairing translation enhance the growth defect of the *rpl22* null strain combined with the *RPL38* deletion. Wild-type, *rpl22Δ, rpl38Δ* and *rpl22Δ rpl38Δ* strains were grown in YP(A)D media at 30 °C until mid-log phase, diluted to an OD_{600} of 0.05 and then 10-fold series of dilutions were spotted on YP(A)D plates lacking or containing a sublethal concentrations of cycloheximide (0.075 µg/ml) or neomycin (5 mg/ml). Plates were incubated at 30 °C for 3 days.

Loss of Rei1 mildly enhances the growth defect of *rpl22* null cells

As previously mentioned, after Nog1 and Rlp24 release, Rei1 is wedged between eL22 and rRNA in cytoplasmic pre-60S r-particles (**Figure 1**). Similarly to the absence of eL22, the loss of Rei1 induces a moderate slow growth phenotype that is exacerbated at low temperatures, but suppressed at high ones [169-171,221]. To investigate whether the absence of eL22 impacts on the role of Rei1 during cytoplasmic maturation of pre-60S r-particles, we introduced the *rei1Δ* deletion into the *rpl22* null strain and studied whether this combination synergistically affects growth at either 30 or 22 °C. As shown in **Figure 15**, a very weak enhancement of the growth defect of the *rpl22* null strain was obtained upon the deletion of the *REI1* gene, specially at low temperatures.

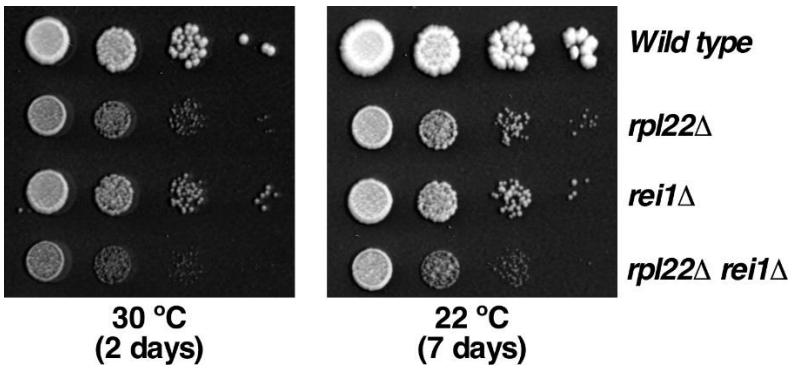

Figure 15. eL22 and Rei1 are functionally linked. Growth analysis of the deletion of *REI1* in a wild-type and a *rpl22* null strains. The indicated strains were grown in YP(A)D media at 30 °C until mid-log phase, diluted to an OD_{600} of 0.05 and then 10-fold series of dilutions were spotted on YP(A)D plates. Plates were incubated at 30 and 22 °C for the indicated times. Note that deletion of *REI1* exacerbates the slow-growth phenotype of *rpl22* null cells, specially at 22 °C.

Loss of Arx1 and Alb1 unequally suppresses the growth defects of *rpl22* null cells

Rei1 has been shown to work together with Jjj1 during the release of the assembly factors Arx1 and Alb1 from cytoplasmic pre-60S r-particles. Thus, in the absence of either Rei1 or Jjj1, the heterodimer Arx1-Alb1 that binds in the exit of PET is not efficiently release from these particles and accumulates in the cytoplasm [169-172,221]. Interestingly, the deletion of either *ARX1* or *ALB1* genes rescues the slow growth phenotype of either the *rei1Δ* or the *jjj1Δ* mutant, suggesting that the

inappropriate recycling of Arx1-Alb1, and therefore, the accumulation of cytoplasmic pre-60S r-particles bound to these factors is the cause of the defects of the *rei1Δ* or *jjj1Δ* deletion. To test whether eL22 participates in this functional circuit, we introduced the *arx1Δ* or the *alb1Δ* deletion into the *rpl22* null strain and analysed the growth of the triple mutant at either 30 or 22 °C. As shown in **Figure 16**, deletion of either gene significantly suppressed the growth defect of the *rpl22Δ* null strain, being the effect more evident upon deletion of the *ALB1* gene and at low temperatures. These results open us the possibility to investigate further the role of eL22 during cytoplasmic steps of LSU maturation that unfortunately could not be initiated in this work due to time restrictions.

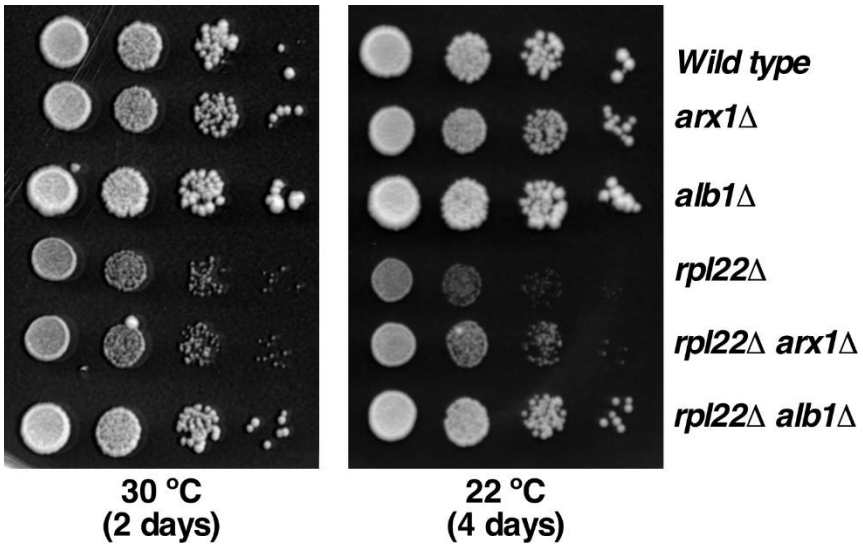

Figure 16. Deletion of either *ARX1* or *ALB1* partially rescues the slow-growth phenotype of the *rpl22* null strain. Wild-type, *arx1Δ*, *alb1Δ*, *rpl22Δ* and triple deletion *arx1Δ rpl22Δ* and *alb1Δ rpl22Δ* strains were grown in YP(A)D media at 30 °C until mid-log phase, diluted to an OD_{600} of 0.05 and then 10-fold series of dilutions were spotted on YP(A)D plates. Plates were incubated at 30 and 22 °C for the indicated times.

DISCUSSION

In eukaryotes, the biogenesis of cytoplasmic ribosomes is a very complex and highly coordinated process that implies all the r-proteins (79 in yeast), several hundreds of protein assembly factors (more than 250 in yeast) and snoRNAs (about 75 in yeast). Through the last years, the details of how this process occurs have been extensively studied in the yeast *S. cerevisiae*. Although the role of most r-proteins in ribosome biogenesis has been well studied, there are still a few of them that require characterization. In this thesis work, we have undertaken the functional analysis of one of these uncharacterised r-proteins, eL22, in the biogenesis and function of ribosomes. During the progression of this work, some functional features of eL22 have been already analysed by other groups, specially at the level of its gene expression and the role of splicing of the single introns of the paralogues *RPL22A* and *RPL22B* genes on the eL22 abundance (see later); these studies were done without a clear perspective in the understanding of the contribution of eL22 during the ribosome maturation process.

By mean of a variety of different experiments, we could note that is indeed the *RPL22A* gene the only responsible for the multiple phenotypes associated to the absence of eL22, whereas the absence of the *RPL22B* paralog seems to produce absolutely no effect in any of the features we have analysed. These results are consistent with previous published works [30,192]. Thus, it has been reported that, in standard conditions, the expression of *RPL22A* is responsible for approximately the 90% of the eL22 protein [191,197]. Furthermore, recently, different groups have revealed an extra-ribosomal role of eL22 in the feedback control of the expression of both paralogs [193,196]. As most r-proteins genes in yeast, *RPL22A* and *RPL22B* harbour one intron in their sequences. It has been demonstrated that eL22 binds to the intronic region of their own mRNAs, thus, impairing their proper maturation and resulting in their degradation. However, the affinity of the eL22 protein is much stronger for the intronic region of the *RPL22B* mRNA, while the binding to the *RPL22A* one is rather limited. This satisfactorily explains the abundance of eL22A *versus* eL22B in yeast cells. Moreover, upon deletion of *RPL22A*, levels of the *RPL22B* mRNA barely increase, thus, the phenotypes present in the *rpl22AΔ* strain are practically identical to those of the *rpl22* null strain. In turn, upon

deletion of *RPL22B*, levels of the *RPL22A* mRNA are few affected by the feedback regulation, explaining the fact that the phenotypes present in the *rpl22BΔ* strain are practically identical to those of its wild-type counterpart [193]. Interestingly, this mechanism of autoregulation seems to be conserved in higher eukaryotes, where RPL22 inhibits the expression of its paralog RPL22L1 by binding to its mRNA [222]. Further studies have been done on the autoregulation mechanism of the yeast eL22 expression. Indeed, as eL22A and eL22B are proteins with almost 90% of identity, it has been shown that the key differentiator element in the negative feedback of eL22 expression is present in the respective intronic regions of the *RPL22* mRNAs [193,196]. It is also worthy to mention that other studies have found additional extra-ribosomal roles for eL22 in the regulation of a high variety of mRNAs from factors involved in different processes as meiotic induction, one-carbon metabolic pathways or stress response; mechanistically, this regulation is again differentially dependent of the different paralogs of eL22, both in yeast and higher eukaryotes [192-194].

In our work, we have shown that the absence of eL22 led to a mild slow growth that is, however, particularly severe at low temperatures. This result is consistent with previous studies that showed cell cycle arrest at 19 °C and cell death at 4 °C linked to the absence of eL22 [192]. We assume that these growth defects are related to the role of eL22 as a component part of the ribosome; however, as eL22 has been shown to be an important regulator for global gene expression, we cannot initially exclude the possibility that these defects are due to the impact in the extra-ribosomal regulatory function of eL22 rather than in the role that it could have in ribosome biogenesis and function. Indeed, our results show that eL22-lacking ribosomes do not significantly affect translation accuracy; moreover, as we explain below, analysis of ribosome biogenesis by polysome profile, pulse-chase, northern blot and primer extension, and fluorescence microscopy indicates that only a modest deficit of LSU is induced in the absence of eL22. Clearly, only further genetic experiments could provide a definitive answer to this issue by the generation of specific dissociative mutants that could affect one function (e.g. ribosome biogenesis) without affecting the other (i.e. regulation of gene expression) or *vice versa*.

In this work, we have addressed the timing of eL22 assembly in pre-60S r-particles by using different complementary approaches, since previous studies on this regard were not completely conclusive. We first demonstrated using a GFP-tagged version of eL22 that eL22 assembles in the nucle(ol)us, as initially expected [91]. Second, we demonstrated using the GFP-trap procedure that eL22 stably assembles within nucle(ol)ar pre-60S r-particles that contain 27SB pre-rRNAs and subsequent pre-rRNAs but not earlier $27SA_2$ pre-rRNA. In agreement with these data, eL22 has been found in early pre-60S r-particles, such as those obtained upon split-tag affinity purification of Nsa1-TAP and Flag-Ytm1 and classified as state D particles by cryo-EM analysis [92].

With respect to the role of eL22 in ribosome biogenesis, we have observed a clear and specific reduction in the amount of mature LSUs by analysing polysome profiles, similarly as previously shown [192]. Therefore, eL22 is necessary for the optimal production of the LSUs. However, since eL22 is not essential under laboratory conditions, this need is not strict, specially at high temperatures where polysome profiles returned to an almost wild-type situation. At low temperatures, however, the defects might be stronger, circumstance that has been detected for several other r-protein gene mutants (i.e. [223,224]). Thus, we have observed that cells lacking eL22 display a suboptimum export of LSUs from the nucleus, specially at low temperatures, in consonance with a stronger LSU assembly failure at 22 °C than at 30 °C. By northern blot analysis, our results showed a mild delay in the processing of 27SB and 7S pre-rRNAs in cells lacking eL22. These processing defects denote that both the Las1 and the exosome complexes are unable of efficiently remove the ITS2 from their pre-rRNA substrates. As eL22 is located far away from the foot structure where the ITS2 is situated, we speculate that this phenotype should be due to an indirect reason such as the inefficient interaction and/or function of a single or a set of ribosome biogenesis factors required for these steps; for instance, Nog1 is a perfect candidate for this scenario as it has been shown to interact with eL22 in middle pre-60S r-particles [115] and it has been reported that it is required for 27SB pre-rRNA processing [225].

In the final part of this chapter, we have performed some genetic interaction analysis. Thus, we first studied the relationship between eL22 and the r-proteins eL38 and eL31, as eL22 is sandwiched between these two proteins on mature LSUs. Our

results show a very weak enhancement of the slow-growth phenotype of the *rpl22* null strain by deleting the *RPL31A* gene whereas, in contrast, a mild enhancement by deleting the *RPL38* one, specially at low temperatures and after exposition to sublethal concentrations of selected antibiotics that impair translation. The significance of these interactions requires further experiments, but it seems reasonable to speculate that if eL22 is important for proper folding of its surrounded rRNA area, pre-ribosomal particles lacking simultaneously eL22 and other r-proteins as eL38 situated in the same region may lead to a more severe conformation defect than that occurring when eL22 is missing alone.

Second, we have analysed the relationship between eL22 and a set of ribosome assembly factors that contact with or map close to it in cytoplasmic pre-60S r-particles, such as Rei1 and Arx1, respectively [173]. Recently, a complex of the yeast LSU with Rei1 and the Arx1-Alb1 heterodimer has been reconstituted and its structure studied at near-atomic resolution by cryo-EM analysis [129]. This structure revealed that Rei1 binds near the exit of the PET contacting Arx1 and eL22. During cytoplasmic maturation of LSUs, association of Rei1 occurs concomitantly to the assembly of eL24 r-protein after the release of the assembly factor Rlp24 by the Drg1 ATPase [167] and that of the assembly factor Nog1 [165]. As Nog1, Rei1 inserts its C-terminal tail into the PET [126,129]. Interestingly, loss-of-function of Rei1 impairs release and nuclear recycling of Arx1 and blocks subsequent maturation of cytoplasmic pre-60S r-particles [129,169-172]. Our results show that eL22 and Rei1 functionally interacts as demonstrated by the fact that the introduction of the *REI1* deletion into the *rpl22* null strain leads to an enhancement of its slow-growth phenotype, specially at low temperatures. This result suggests that eL22 modulates the association and/or function of Rei1 during cytoplasmic maturation of pre-60S r-particles, although clearly further experiments are necessary to validate this possibility. Supporting this model, we have also found that, as previously shown for the link between Rei1 or Jjj1 and Arx1-Alb1, where the absence of either Arx1 or Alb1 is able to suppress the growth defect of the *rei1Δ* or *jjj1Δ* strains [129,169-172], the deletion of *ARX1* or *ALB1* genes in the *rpl22* null strain, especially that of *ALB1*, significantly suppresses the growth defect of the latter strain at either 30 or 22 °C. These results are at least curious as Arx1 and Alb1 are thought to work together and redundantly as an

heterodimer, being Alb1 the modulator of Arx1, and Arx1 an export adaptor factor for LSUs that also play a role during the functional check of the PET [155,157,165]. From the functional link between Rei1 or Jjj1 and Arx1 it has been concluded that the trap of Arx1 in cytoplasmic pre-60S r-particles is the main reason of the growth defects observed in the *rei1Δ* or *jjj1Δ* cells. This trap prevents Arx1-Alb1 recycling to the nucleus and avoids progression of cytoplasmic pre-60S r-particle maturation, which includes the release of Tif6. This suggest that the recycling of these proteins is functionally connected [129,165,169-172]. Giving the location of eL22 in LSUs and its physical interaction with Rei1, we speculate that the above functional interactions between eL22, Rei1, Arx1 and Alb1 are also linked to all these cytoplasmic releasing events. Further experiments are clearly required to establish whether this hypothesis is correct.

CHAPTER 2

EARLY ROLE OF RIBOSOMAL PROTEIN eL15 DURING THE ASSEMBLY OF 60S RIBOSOMAL SUBUNITS IN *Saccharomyces cerevisiae*

INTRODUCTION

As previously mentioned in the main introduction section, r-proteins are assembled in an ordered and hierarchical manner. Eukaryotic ribosomes have several specific r-proteins, among them, eL15. In this thesis work, we have further investigated the functional relevance of the poorly characterised yeast eL15 r-protein in the biogenesis of LSUs.

eL15 is one of the r-proteins which are specific from eukaryotes. In *S. cerevisiae*, it is encoded by two paralogous genes, *RPL15A* (YLR029C) and *RPL15B* (YMR121C), which, in contrast to most yeast r-protein genes, lack of introns [189]. Moreover, it has previously been reported that the *RPL15A* gene is essential whereas the *RPL15B* is dispensable. Both genes encode functional eL15 proteins but *RPL15B* is not expressed, at least at normal growth laboratory conditions [226]. The coding regions of these two genes are nearly identical, differing in few nucleotides which results in two amino acid changes between eL15A (glutamine in position 11 and aspartic acid in position 153) and eL15B (glutamic acid in position 11 and asparagine in position 153).

The compositional analysis of different pre-ribosomal particles and the solved structures of different pre-60S intermediates by cryo-EM (i.e. [91,92]) have suggested that eL15 is assembled during early nucleolar steps of biogenesis in the surrounding area of the foot structure, interacting with the r-proteins eL8 and eL36, which are also eukaryote-specific proteins **(Figure 1)**.

In humans, the misregulation of the genes encoding eL15 has been associated with several kind of cancers [227-233]. For example, overexpression of human eL15 has been shown to promote cell proliferation in gastric and colon cancers and it has been suggested to be a potential target for anticancer therapy [227,231]. In contrast, the levels of eL15 are dramatically decreased in some sorts of pancreatic adenocarcinomas associated with the invasiveness of tumoral cells [233]. Furthermore, mutations in the human *RPL15* gene have been described as the molecular cause for some cases of the ribosomopathy named Diamond-Blackfan anemia. These mutations resulted in an

impairment on the biogenesis of LSUs and delayed ITS1 processing, which are suggestive of a very early assembly of eL15 also in human ribosomes [234].

Our group is interested in understanding the contribution of specific r-proteins from either the LSU or SSU to ribosome biogenesis. Specifically, at the beginning of this thesis work, the role of eL15 r-protein in pre-rRNA processing and ribosome biogenesis remained undefined, despite its essentiality for yeast cell growth. Herewith, we have undertaken a systematic and specific functional analysis of yeast eL15 in ribosome synthesis to reveal its important role during this process as well as its *in vivo* assembly. Among other features, we have investigated the interdependence of the incorporation of eL15 and its neighbour eL36 and eL8 r-proteins into pre-60S r-particles.

MATERIALS AND METHODS

Strains and microbiological methods

All *Saccharomyces cerevisiae* strains used in this work are listed in **Table 1**. Most of them are derived from BY4743 (*MAT***a**/α *his3Δ1/his3Δ1 leu2Δ0/leu2Δ0 met15Δ0/MET15 LYS2/lys2Δ0 ura3Δ0/ura3Δ0*) [235]. The JFY144 (*rpl15A::*kanMX4) and JFY149 (*rpl15B*::kanMX4) strains are meiotic segregants of the heterozygous diploid strains Y21584 and Y26562, respectively (Euroscarf). The JFY144 and JFY149 strains were crossed and the obtained diploid sporulated; then, tetrads were dissected and tetratypes were selected. Due to the essential nature of eL15, the diploid strains were transformed with the YCplac33-RPL15A plasmid (*CEN URA3 RPL15A*) prior to meiosis induction. The JFY168 strain (*rpl15A::*kanMX4 *rpl15B*::kanMX4 [YCplac33-RPL15A]) is a spore clone used in further experiments. This double mutant was transformed with the YCplac111-GAL-RPL15A plasmid (*CEN LEU2 GAL::RPL15A*) to generate the JFY355 strain (*rpl15A::*kanMX4 *rpl15B*::kanMX4 [YCplac111-GAL-RPL15A]) by counter-selection of the YCplac33-RPL15A plasmid on 5-FOA-containing SGal plates. The presence of the different deletion cassettes in the strains of this study was verified by PCR of the corresponding loci. A similar strategy was performed to obtain the JFY519 strain (*rpl36A*::kanMX4 *rpl36B*::kanMX4 [pAS25-RPL36B]). The strains JFY156 (*rpl36A*::kanMX4) and JFY178 (*rpl36B*::kanMX4) are meiotic segregants of the heterozygous diploids Y20779 and Y27724, respectively (Euroscarf). Then, they were crossed, sporulated and spore clones with the appropriate markers selected. In this case, prior to meiosis, the diploids were transformed with the pAS25-RPL36B (*CEN URA3 GAL::RPL36B*), which expresses eL36B from a *GAL* promoter. Spore clones were selected on YP(A)Gal plates. The JFY440 strain (*rpl15AΔ::*kanMX4 *rpl15BΔ*::kanMX4 *noc2*::*NOC2*-TAP-*URA3* [YCplac111-GAL-RPL15A]) and the JFY559 strain (*rpl36A*::kanMX4 *rpl36B*::kanMX4 *noc2*::*NOC2*-TAP-*URA3* [pAS25-RPL36B]) are meiotic segregants derived from the diploid resulting of crossing JFY355 and JFY519 with the TY1879 strain (*noc2*::*NOC2*-TAP-*URA3*).

Strains were grown at 30 °C in rich YP(A)D or YP(A)Gal medium (1% yeast extract, 2% peptone; 2% glucose or galactose as carbon source, respectively) supplemented with 0.2% adenine, or in synthetic minimal medium (SD or SGal; 0.5% ammonium sulphate, 0.15% yeast nitrogen base; 2% glucose or galactose as carbon source, respectively) supplied with the appropriate amino acids and bases. To prepare solid media, 2% agar was added to the media before sterilisation. The yeast media were prepared according to a yeast guideline book [204]. Growth and handling of yeast were carried out following standard established protocols [204]. Yeast transformation was performed following the lithium acetate method [202]. Tetrad dissections were conducted using a Singer MSM200 micromanipulator.

Plasmids

Plasmid cloning and propagation were carried out using the *Escherichia coli* DH5α strain. **Table 2** contains the list of all the plasmids employed in this chapter. In order to construct the plasmids YCplac33-RPL15A, YCplac111-GAL-RPL15A, YCplac111-HA-RPL36B and pAS25-RPL36B, the appropriate DNA fragments were generated by PCR amplification using the pertinent oligonucleotides and yeast genomic DNA as template. PCR products were subjected to DNA restriction and cloned into the corresponding vectors. Sequencing was used for the verification of the correctness of the constructions. Other plasmids have been reported in previous works as referenced in **Table 2** and were generous gifts of the authors of those publications. The sequence and description of each oligonucleotide used in this work are shown in **Table 3**. DNA manipulation techniques were performed using established protocols [203].

Protein extraction, SDS-PAGE and western blot analysis

Total yeast protein extracts were prepared and analysed by denaturing electrophoresis (SDS-PAGE) and western blotting according to standard procedures [203]. The following primary antibodies were used: mouse-monoclonal anti-Pgk1 (22C5D8; Invitrogen), rabbit polyclonal anti-eL15 (ab130992; Abcam) and rabbit

polyclonal anti-eS26 ([236]; a gift from V.G. Panse). As secondary antibodies, goat anti-mouse or anti-rabbit horseradish peroxidase-conjugated (Bio-Rad) were used. Immune complexes were revealed with an enhanced chemiluminescence detection kit (Super-Signal West Pico, Pierce).

Polysome profile analysis

Cell extracts for polysome analysis were performed as described previously [207]. When required, cells were grown in YP(A)Gal liquid medium until mid-log phase and then shifted to YP(A)D medium for 3 h in order to deplete either the eL15 or the eL36 r-proteins. After this, all steps of this procedure were performed at 4 °C. About 200 ml of cells at an optical density at 600 nm (OD_{600}) of 0.6-0.8 were processed per sample; translation was stalled by addition of 1 ml of cycloheximide (20 mg/ml) followed by an incubation of 10 min. Then, cells were collected by centrifugation and resuspended in 500 µl of lysis buffer (10 mM Tris-HCl, pH 7.5, 100 mM NaCl, 30 mM $MgCl_2$, 100 µg/ml cycloheximide, 200 µg/ml heparin, 0.2 µl/ml DEPC). Then, 500 µl of glass beads (0.45 µm diameter) were added and cells were lysed by strong vortex agitation during 8 min at 4 °C. Centrifugation at 13,000 rpm for 10 min was used to clarify the cell extracts. To the supernatants, glycerol at 10% of final concentration was added; the concentration of RNA in the samples were measured using a Nanodrop™ spectrophotometer (Thermo Fisher Scientific) and samples kept at -80 °C until used. Ten A_{260} of cell extract were separated in a 7-50% sucrose gradient by centrifugation at 39,000 rpm during 2 h 45 min in a Beckman Coulter rotor SW41Ti. The acquisition of polysome profiles was carried out through the continuously measurement of the A_{254} by an ISCO UA-6 fractionator system.

RNA extractions and analysis of steady-state RNA levels

The hot-acidic phenol chloroform method was used to extract total RNA from 10 OD_{600} units of cells grown to mid-log phase [208]. The JFY355 strain (*GAL::RPL15*) was grown until mid-log phase in SGal-Leu medium and then eL15 was depleted by shifting the cells for 3 h to SD-Leu medium; cells were collected by centrifugation and resuspended in 400 µl of TES buffer (10 mM Tris-HCl, pH 7.5, 10 mM EDTA, pH 8.0, 0.5%

SDS). After adding 400 µl of acid phenol, samples were shaken at 65 °C for 5 min and the aqueous fraction separated by centrifugation and recovered. RNA was purified by washing samples with equal volumes of acid phenol and then of chloroform. RNA was then precipitated by incubation overnight at -20 °C with 1 ml of 96% ethanol and 40 µl of 3 M sodium acetate. Finally, samples were centrifugated for 15 min, resuspended in 100 µl of distilled water and the concentration of RNA quantified using a Nanodrop™ as above.

About 5 µg of total RNA of each sample were resolved by electrophoresis in a 1.2% agarose-6% formaldehyde gel or a 7% polyacrylamide-8 M gel, depending on the size of the RNA of interest to analyse. Next, RNA was transferred to nylon membranes (Hybond™-N, GE Healthcare) and crosslinked as originally described in [209]. The oligonucleotides used as probes for northern hybridization (described in **Table 3**) were 5' end labelled with [γ-^{32}P] ATP (6,000 Ci/mmol; Perkin Elmer). For primer extension analysis, equal amounts of the above RNA samples were subjected to reverse transcription using as primer the oligonucleotide probe g (C_1/C_2; **Table 3**) 5' end labelled with [γ-^{32}P] ATP. The resulting DNA was separated by electrophoresis in a 7% polyacrylamide-8 M gel and transfer to a Whatman filter paper as also described in [209]. Nylon membranes or Whatman filter papers were exposed overnight to Fuji screens (BAS-IP MS; GE Healthcare); finally, RNA levels were visualised using a Typhoon™ FLA-9000 imaging system (GE Healthcare) and quantified using the GelQuant.NET software.

Pulse-chase labelling of pre-rRNA

Pulse-chase labelling of pre-rRNA was performed as described previously [210]. The JFY355 strain (*GAL::RPL15*) was first transformed with an empty YCplac33 plasmid (*CEN URA3*) in order to conferred cells prototrophy for uracil. Cells were grown in liquid SGal-Ura medium until mid-log phase, then eL15 was depleted for 3 h by shifting media to SD-Ura; About 40 OD_{600} units of cells were pulsed for 2 min with 100 µCi of [5,6-^{3}H] uracil (45-50 Ci/mmol; Perkin Elmer). The pulse of radioactive uracil was stopped with an excess of unlabelled uracil (1 mg/ml). The chase was carried out at different times: 0,

5, 15, 30 and 60 min after pulse. Cells were washed with water and frozen in liquid nitrogen.

The hot-acidic phenol:chloroform method, as previously described, was used to extract total RNA from the different samples. The incorporation of labelled uracil was measured using a scintillation counter and about 3,000 cpm per RNA sample were loaded and electrophoretically separated in a 1.2% agarose-6% formaldehyde gel or a 7% polyacrylamide-8 M urea gel. RNA was then transferred to nylon membranes (Hybond^{TM}-N, GE Healthcare), fixed using a crosslinker and exposed to a BAS-IP TR2040E tritium screen (GE Healthcare) for two weeks. Then, the screen was revealed using a Typhoon^{TM} FLA-9000 imaging system (GE Healthcare).

Fluorescence microscopy

In order to test pre-ribosomal particle export, the *GAL::RPL15* strain (JFY355) was transformed with plasmids expressing the nucleolar reporter mRFP-Nop1 and yEGFP-tagged uL23 or uS3 r-proteins. Transformants were grown in selective liquid SGal-Ura medium until mid-log phase and then shifted to liquid SD-Ura medium for 3 h. Cells were washed with PBS buffer (140 mM NaCl, 8 mM Na_2HPO_4, 1.5 mM KH_2PO_4, 2.75 mM KCl, pH 7.3), and examined using an Olympus BX61 fluorescence microscope equipped with a digital camera. Images were acquired and analysed using the Olympus cellSens software and processed with Adobe Photoshop 23.1 (Adobe Systems Inc.).

Purification of Noc2-TAP containing pre-ribosomal particles

The JFY440 and JFY559 strains, which express a chromosomally encoded Noc2-TAP fusion protein and harbour either a *GAL::RPL15A* or a *GAL::RPL36B* allele, as a sole source of eL15 or eL36, respectively, were grown in liquid YP(A)Gal medium until mid-log phase and shifted during 3 h to YP(A)D in order to shut down the expression of *RPL15A* or *RPL36B,* respectively. About 800 OD_{600} units were collected for each strain in each (non-depleted or depleted) condition. Then, cells were washed with 10 ml of P1 buffer (20 mM Tris-HCl, pH 8.0, 150 mM potassium acetate, 5 mM $MgCl_2$, 1 mM DTT and

0.2% (w/v) Triton X-100) and resuspended in 1.5 ml per gram of cells of P1 buffer adding 1 mM PMSF and 0.4 U/μl RNasin® RNase inhibitor. Cells were lysed by vigorous shaking (3 cycles of 30 s of shake and 30 s of pause) with glass beads (0,75-1 mm diameter, 1.4 g per 800 μl of cell suspension) in a Precellys® Evolution refrigerated shaker (Bertin Instruments). Cell lysates were clarified by two consecutive steps of centrifugation at 13,000 rpm. Protein concentration was measured by the Bradford assay and 50 mg per sample were added to 200 μl of IgG-coupled magnetic bead slurry equilibrated in P1 buffer and incubated in rotation during 2 h at 4 °C. Beads were washed 4 times with 1 ml of P1 buffer and twice with 1 ml of AC buffer (100 mM ammonium acetate, pH 7.4, 0.1 mM $MgCl_2$) using a magnetic rack. Then, bound proteins were eluted from beads by two incubations with 500 mM NH_4OH. Eluted samples were frozen in liquid nitrogen and lyophilised overnight.

Mass spectrometry analyses

The Noc2-TAP containing particles were processed and analysed by iTRAQ (isobaric tags for relative and absolute quantitation) using the iTRAQ® Reagents Multiplex Kit (Sigma-Aldrich) as previously described [237]. Lyophilised samples were resolved in 60 μl of dissolution buffer, provided in the kit. Then, 2 μl of reducing reagent were added and samples incubated 2 h at 60 °C with gentle shaking at 500 rpm. One μl of Cysteine Blocking reagent (provided in the kit) was added and incubated 10 min at room temperature. Samples were digested overnight at 37 °C by adding 5.5 μl of Trypsin (1 mg/ml). Then, 70 μl of reconstituted iTRAQ® reagents were added to each sample and incubated 1 h at room temperature. Samples were conveniently combined, frozen in liquid nitrogen and lyophilised during 5 h. Lyophilised samples were dissolved in 30 μl of 0.1% trifluoroacetic acid and clarified by two consecutive steps of centrifugation at 13,000 rpm. Samples were separated by HPLC in a 384 MALDI plate and analysed by MALDI-TOF mass spectrometry. iTRAQ® ratios were calculated as depleted *versus* non-depleted samples and normalized to the Noc2 ratio exactly as previously described [237,238]. Only proteins identified by more than one peptide were taken into account in the Results section.

Table 1. Yeast strains used in this work

Strain	Relevant Genotype	Source
BY4741	*MAT***a** *his3Δ1 leu2Δ0 met15Δ0 ura3Δ0*	Euroscarf
BY4742	*MATα his3Δ1 leu2Δ0 lys2Δ0 ura3Δ0*	Euroscarf
TY1879	As BY4742 but *noc2::NOC2*-TAP-*URA3*	[239]
Y21584	*MAT***a**/*MAT*α *his3Δ1/his3Δ1 leu2Δ0/leu2Δ0 met15Δ0/MET15 LYS2/lys2Δ0 ura3Δ0/ura3Δ0 RPL15A/rpl15A*::kanMX4	Euroscarf
Y26562	*MAT***a**/*MAT*α *his3Δ1/his3Δ1 leu2Δ0/leu2Δ0 met15Δ0/MET15 LYS2/lys2Δ0 ura3Δ0/ura3Δ0 RPL15B/rpl15B::*kanMX4	Euroscarf
JFY144	As BY4741 but *rpl15A::*kanMX4 [YCplac33-RPL15A]	This study
JFY149	As BY4742 but *rpl15B::*kanMX4	This study
JFY168	As BY4741 but *rpl15A::*kanMX4 *rpl15B*::kanMX4 [YCplac33-RPL15A]	This study
JFY355	As BY4741 but *rpl15A*::kanMX4 *rpl15B*::kanMX4 [YCplac111-GAL-RPL15A]	This study
JFY440	As JFY355 but *noc2::NOC2*-TAP-*URA3*	This study
Y20779	*MAT***a**/*MAT*α *his3Δ1/his3Δ1 leu2Δ0/leu2Δ0 met15Δ0/MET15 LYS2/lys2Δ0 ura3Δ0/ura3Δ0 RPL36A/rpl36A::*kanMX4	Euroscarf
Y27724	*MAT***a**/*MAT*α *his3Δ1/his3Δ1 leu2Δ0/leu2Δ0 met15Δ0/MET15 LYS2/lys2Δ0 ura3Δ0/ura3Δ0 RPL36B/rpl36B::*kanMX4	Euroscarf
JFY156	As BY4741 but *rpl36A::*kanMX4	This study
JFY178	As BY4742 but *rpl36B*::kanMX4	This study
JFY519	As BY4741 but *rpl36A*::kanMX4 *rpl36B*::kanMX4 [pAS25-RPL36B]	This study
JFY559	As JFY519 but *noc2::NOC2-TAP-URA3*	This study

Table 2. Plasmid vectors used in this work

Name	Relevant information	Source
YCplac33	*CEN, URA3*	[212]
YCplac111	*CEN, LEU2*	[212]
YCplac33-RPL15A	*RPL15A, CEN, URA3*	This study
YCplac111-GAL-RPL15A	*GAL-RPL15A, CEN, LEU2*	This study
pRS316-RPL25-eGFP NOP1-mRFP	*RPL25*-γEGFP, mRFP-*NOP1*, *CEN URA3*	[213]
pRS316-RPS3-eGFP NOP1-mRFP	*RPS3*-γEGFP, mRFP-*NOP1*, *CEN, URA3*	[213]
pAS25-RPL36B	*GAL-HA-RPL36B, CEN, URA3*	This study
YCplac111-HA-RPL36B	*HA-RPL36B, CEN, LEU2*	This study

Table 3. Oligonucleotides used in this work

Name	5'-3' sequence	Use
L15A UP	GCATGCTCACTCTCTTGATTAACCCA	Cloning and PCR verification
L15A DOWN	GAATTCCCTTGGCTAAGTCTAATAAA	Cloning and PCR verification
L15A-pAS24 UP	GCATGCATGGGTGCCTACAAATATTT	Cloning and sequencing verification
L15A-pAS24 DOWN	AAGCTTGATACGAACATTGTTCTCTA	Cloning
L15A SEC2	AGGTCTCTTTCTGTTACCAC	Sequencing verification
L15A SEC3	TGAACTCCTACTGGGTTAAC	Sequencing verification
L15B UP	GCATGCAAGCGGAAGCGGAAGT	PCR verification
L15B DOWN	AAGCTTGCCTTTAATGCCAATCTGT	PCR verification
L36B-pAS25 UP	GTCGACATGGCTGTCAAGACTGGTAT	Cloning
L36B-pAS25 DOWN	GCATGCGGGCTGGTTATGAAACAACG	Cloning
L36A UP	AATATAGGTCAGTAGGGAAG	PCR verification
L36A DOWN	CCACCGTATAGTAAACGATT	PCR verification
L36B UP	GAATTCAAAACCACCAACTA	PCR verification
L36B DOWN	TCTAGATTCCACAGAGGACATTGTAA	PCR verification
NOC2 UP	CGTGAAGTTAAGGAAGAAAAGGCC	PCR verification
NOC2 DOWN	GCTTGGAGTGCTCACATGTTAGC	PCR verification
Probe b (18S)	CATGGCTTAATCTTTGAGAC	18S rRNA hybridization
Probe c (3-D/A2)	GACTCTCCATCTCTTGTCTTCTTG	Pre-rRNA hybridization
Probe d (A2/A3)	TGTTACCTCTGGGCCC	Pre-rRNA hybridization
Probe e (5.8S)	TTTCGCTGCGTTCTTCATC	5.8S rRNA hybridization
Probe f (E/C2)	GGCCAGCAATTTCAAGTTA	Pre-rRNA hybridization
Probe g (C1/C2)	GAACATTGTTCGCCTAGA	Pre-rRNA hybridization and primer extension
Probe h (25S)	CTCCGCTTATTGATATGC	25S rRNA hybridization
Probe 5S	GGTCACCCACTACACTACTCGG	5S rRNA hybridization

RESULTS

Yeast eL15 is required for LSU production

Yeast eL15 is an essential r-protein ([226] and **Figure 2**) of 204 amino acids with a predicted molecular mass of 24.5 kDa. As most yeast r-proteins, eL15 is encoded by two genes, *RPL15A* (YLR029C) and *RPL15B* (YMR121C). The coding regions of these two genes are nearly identical, differing in few nucleotides that result in two practically identical eL15A and eL15B r-proteins, differing in two amino acid, which curiously involve amino acids of different properties (polar to negatively charged or *vice versa*) in the same position. Thus, eL15A contains a glutamine in position 11 and an aspartic acid in position 153 while eL15B contains a glutamic acid in position 11 and an asparagine in position 153.

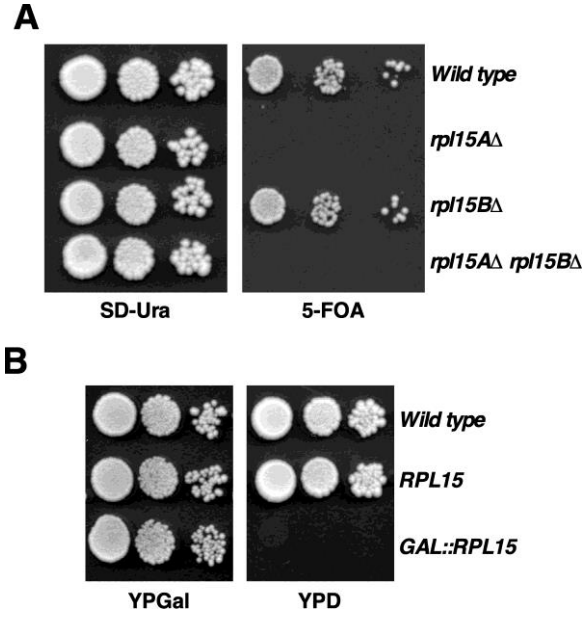

Figure 2. Growth analysis of rpl15 deleted strains. (**A**) Growth test of the *rpl15A* and *rpl15B* null mutants compared to their wild-type control strain. Isogenic strains BY4741 (*Wild type*), JFY144 (*rpl15AΔ*), JFY149 (*rpl15BΔ*) and JFY168 (*rpl15AΔ rpl15BΔ*), harbouring an YCPlac33-RPL15A plasmid were grown in liquid SD-Ura medium to mid-log phase at 30 °C, diluted to an OD_{600} of 0.05 and spotted in 10-fold serial dilutions onto SD-Ura and SD containing 5-FOA plates for counterselection of the plasmid. Plates were incubated 3 days at 30 °C. **(B)** Depletion of eL15. Growth comparison of the isogenic strains BY4741 (*Wild type*), JFY168 harbouring the YCplac33-RPL15A plasmid (*RPL15*) and JFY355 harbouring the YCplac111-GAL-RPL15A plasmid (*GAL::RPL15*). Cells were grown in YP(A)Gal to mid-log phase at 30 °C, diluted to an OD_{600} of 0.05 and spotted in 10-fold serial dilutions onto YP(A)Gal and YPD plates, which were incubated 3 days at 30 °C.

Interestingly, as shown in **Figure 2A**, *RPL15A* is an essential gene while *RPL15B* is apparently fully dispensable under laboratory conditions, in agreement with previous reports [30,226]. Moreover, it has been demonstrated that both *RPL15* genes are unequally expressed: while *RPL15A* is expressed under normal growth conditions, *RPL15B* is not expressed likely because its promoter lacks essential elements for binding of transcriptional factors [226]. Therefore, to properly study the effects of the loss-of-function of eL15 in ribosome biogenesis, avoiding an undesirable suppression event due to the presence of *RPL15B*, in this work we constructed a strain with both *RPL15* genes deleted and expressing as the sole source of eL15, a plasmid-encoded variant of eL15A under the control of a *GAL* promoter (hereafter, *GAL::RPL15* strain). The presence of this plasmid was able to sustain wild-type growth on YP(A)Gal plates, but was unable to do it on YP(A)D plates. As a control, we also cloned the *RPL15A* gene expressed from its own promoter on a centromeric plasmid, which allowed apparent wild-type growth in both YP(A)Gal and YP(A)D medium (**Figure 2B**). After shifting a culture of the *GAL::RPL15* strain in mid-log phase from liquid YP(A)Gal to YP(A)D medium, the growth rate significantly slowed down in few hours and cultures stopped growing in less than 6 h in YP(A)D medium (**Figure 3A**). However, western blot revealed practically no reduction on the protein levels of eL15 when the *GAL::RPL15* strain was subjected to a shift from galactose- to glucose-containing rich medium for even 12 h (**Figure 3B**), likely reflecting the stability of pre-existing ribosomes (see also **Figure 6A**).

To start examining the general effects of eL15 depletion in ribosome biogenesis, we analysed polysome profiles from cells of the *GAL::RPL15* strain grown in YP(A)Gal or shifted for 3 h to YP(A)D. When grown in YP(A)Gal, the strain showed a normal polysome profile, however, when shifted to YP(A)D for 3 h, it showed an aberrant profile, consisting of a clear decrease in the levels of free LSUs *versus* SSUs, a decrease in the 80S peak and the appearance of half-mer polysomes (**Figure 4**). Half-mer polysomes correspond to mRNAs associated with integral numbers of ribosomes plus a stalled 48S pre-initiation complex at the initiation codon [240,241]. They have been linked to translation initiation and/or LSU accumulation defects (e.g. [241-244])**.** As eL15 is a r-protein, we assumed that half-mer polysomes arose from a decrease in LSU accumulation, thus, calculating the overall LSU/SSU ratio of cells could help confirming

this assumption. To do so, we estimated the relative amount of each r-subunit by analysing cell extracts under ribosomal dissociation conditions using low Mg^{2+} run-off sucrose gradients. These experiments revealed a 25% reduction in the amount of LSUs *versus* that of SSUs upon 3 h depletion of eL15. Taken together, these results indicate that eL15 is an essential protein required for normal accumulation of LSUs.

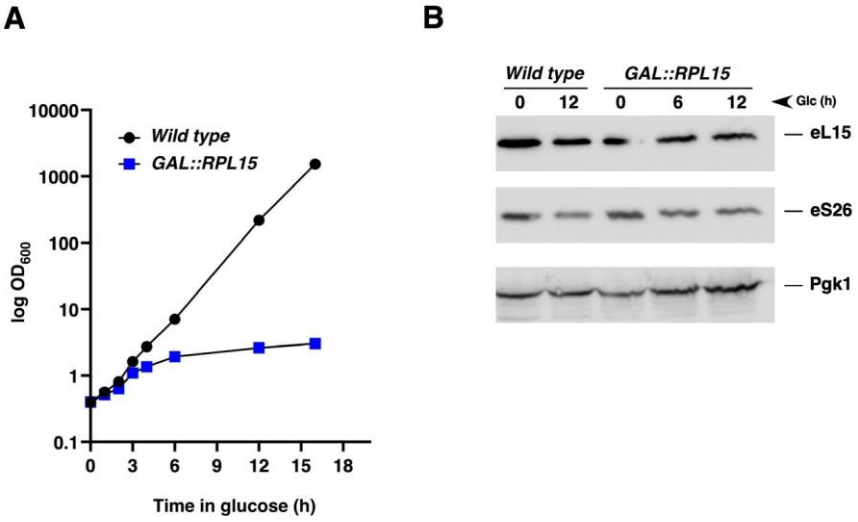

Figure 3. *In vivo* depletion of eL15 inhibits cell growth. (**A**) The strains BY4741 (*Wild type;* filled black circles) and JFY355 harbouring the YCplac111-GAL-RPL15A plasmid (*GAL::RPL15,* filled blue squares) were grown in liquid YP(A)Gal medium to mid-log phase at 30 °C, diluted to an OD_{600} of 0.4 and shifted to YP(A)D medium. The OD_{600} was measured at the indicated times. (**B**) Detection of eL15 by western blotting. The above strains were grown in liquid YP(A)Gal and shifted to YP(A)D medium for up to 12 h. Cell extracts were prepared from samples harvested at the indicated times and assayed by western blotting. Equal amounts of total protein (ca. 70 µg) were loaded in each lane. Polyclonal rabbit anti-eL15 and anti-eS26 were used to detected eL15 and eS26, respectively. Pgk1, detected with anti-Pgk1 monoclonal antibodies, were used as a loading control.

Depletion of eL15 impairs export of pre-60S r-particles from the nucleus to the cytoplasm

As eL15 is assembled in the nucle(ol)us ([92] and J.F.-F., unpublished results), we were interested to test whether the depletion of eL15 impaired LSU export from the nucleus to the cytoplasm. Nuclear export retention of pre-60S r-particles is common to most loss-of-function LSU assembly factors and/or LSU r-proteins (e.g. [118,245-247]) and it has been interpreted as the consequence of a quality control mechanism that retains in the nucle(ol)us defective pre-60S r-particles unable to acquire nuclear export competence; this control mechanism impedes this way the involvement of malfunctioning LSUs in cytoplasmic translation [77,247,248]. To test whether eL15

depletion also impaired nuclear export of pre-60S r-particles, we assessed the subcellular localization of the LSU reporter uL23-yEGFP in the *GAL::RPL15* strain before or after a shift to glucose-containing medium for 3 h. As expected for the steady-state levels of a r-protein, uL23-yEGFP was predominantly localised in the cytoplasm of *GAL::RPL15* cells grown in selective galactose-containing medium (**Figure 5**), indicating that nascent pre-60S r-particles were efficiently exported to the cytoplasm. In contrast, when *GAL::RPL15* cells were shifted to selective glucose-containing medium for 3 h, uL23-yEGFP was found to accumulate in the nucleus, mostly restricted to the nucleolus, which was detected with the nucleolar marker mRFP-Nop1 (**Figure 5**). We did not observe nucleolar accumulation of the uL23-yEGFP reporter in the isogenic wild-type control grown in either galactose- or glucose-containing medium (**data not shown**). Moreover, neither nuclear accumulation was observed when we studied the localisation of the SSU reporter uS2-yEGFP following eL15 depletion (**data not shown**). Assuming that assembly of uL23 r-protein is not strictly dependent on previous assembly of eL15 (see later **Figure 9**), these results strongly suggest that both intra-nuclear and nucleo-cytoplasmic transport of pre-60S r-particles is impaired early after depletion of eL15; this block is apparently specific as the equivalent transport of pre-40S r-particles is unaffected following depletion of eL15.

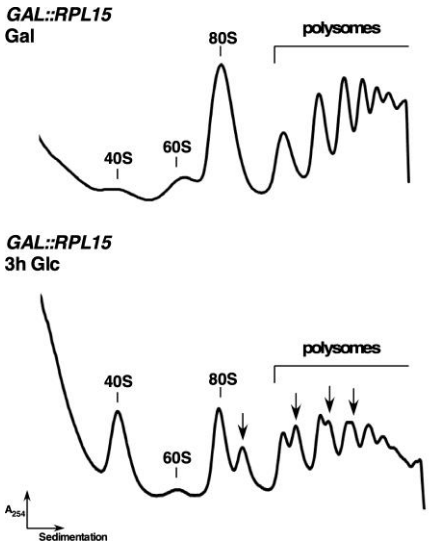

Figure 4. The depletion of eL15 results in a shortage of 60S ribosomal subunits. The strain JFY355 (*rpl15AΔ rpl15BΔ* [YCplac111-GAL-RPL15A]) was grown at 30 °C in YP(A)Gal medium until mid-log phase and shifted to YP(A)D medium for 3 h to deplete eL15 r-protein. Cell extracts were prepared and 10 A_{260} units were subjected to polysome profile analysis in 7-50% sucrose gradients. The peaks of free 40S and 60S r-subunits, 80S free couples/monosomes and polysomes are indicated. Half-mer polysomes are labelled by arrows.

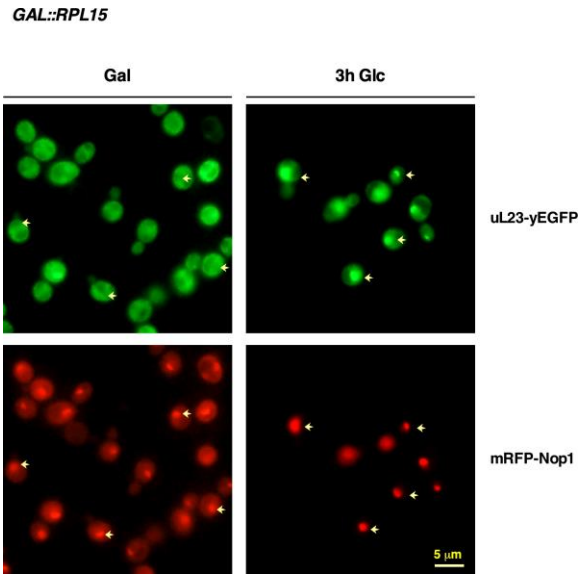

Figure 5. Depletion of eL15 leads to nuclear retention of pre-60S ribosomal particles upon eL15 depletion. JFY355 (*rpl15AΔ rpl15BΔ* [YCplac111-GAL-RPL15A]) cells co-expressing the 60S r-subunit reporter uL23-yEGFP and the nucleolar marker mRFP-Nop1 from a plasmid were grown at 30 °C in liquid SGal-Leu-Ura medium until mid-log phase and shifted to SD-Leu-Ura for 3 h. The subcellular localisations of the GFP-tagged r-protein and the mRFP-Nop1 marker were analysed by fluorescence microscopy. Arrows point to nucleolar fluorescence. Approximately 200 cells were examined and practically all cells gave the results shown in the pictures.

Depletion of eL15 leads to an impairment in $27SA_3$ pre-rRNA processing

As the transport of pre-60S r-particles lacking eL15 r-protein was blocked into the nucleus, we wondered whether or not eL15 was also required for pre-rRNA processing. Thus, we first analysed changes in steady-state levels of pre- and mature rRNAs in isogenic wild-type and *GAL::RPL15* strains grown in YP(A)Gal medium or at various time points after a shift to YP(A)D medium by northern blotting and primer extension. As shown in **Figure 6A**, ongoing depletion of eL15 resulted in a strong accumulation of 35S pre-rRNA and a concomitant increase of 23S pre-rRNA; however, levels of 20S pre-rRNA remained apparently unaffected. Accordingly, levels of $27SA_2$ pre-rRNA slightly diminished, while interestingly, those of 27SB pre-rRNAs clearly decreased. In agreement with the high stability of mature ribosomes, levels of 25S and 18S rRNAs remained practically unaffected during the 6 h shift of duration of the experiment, suggesting that likely these levels corresponded mainly to pre-existing rather than nascent mature LSUs. Analysis of low-molecular mass pre- and mature rRNAs revealed

a significant decrease in the levels of 7S pre-rRNAs, without alteration in either the levels of 5.8S and 5S rRNAs or the ratio of $5.8S_L$ *versus* $5.8S_S$ rRNAs (**Figure 6B**). To unambiguously examine the steady-state levels of each 27S pre-rRNA intermediate, we also performed primer extension experiments. As shown in **Figure 6C**, our results showed that upon depletion of eL15, levels of $27SA_2$ pre-rRNA did not practically change. However, a clear increase in $27SA_3$ pre-rRNA was observed. This increase was accompanied by a slight accumulation of $27SB_L$ pre-rRNA but a significant reduction in $27SB_S$ and 25.5S pre-rRNAs.

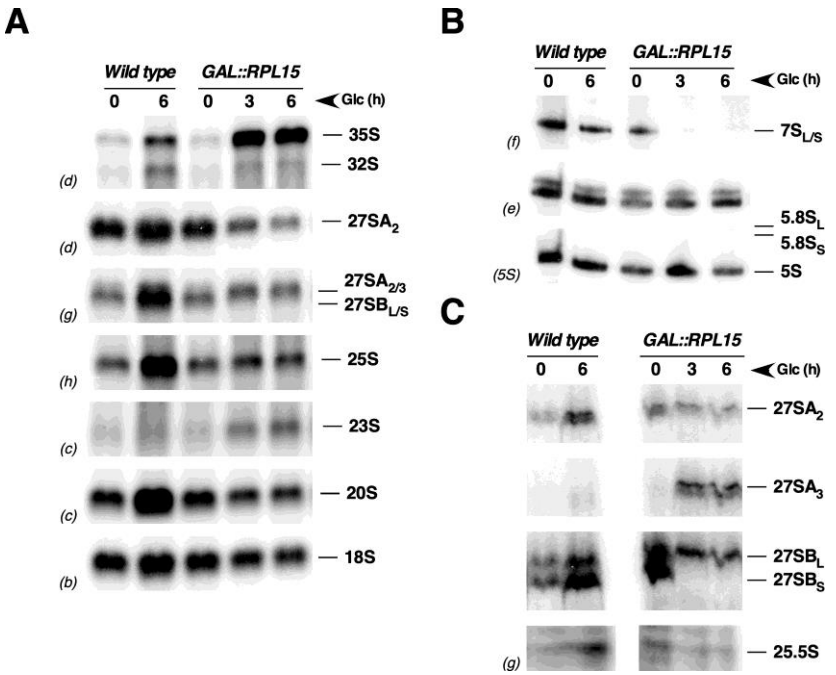

Figure 6. Depletion of eL15 negatively affects the steady-state levels of pre- and mature rRNA species. The strains BY4741 (*Wild type*) and JFY355 (*GAL::RPL15*) were grown in YP(A)Gal medium at 30 °C and shifted to YP(A)D medium. Total RNA was extracted from the cultures at the indicated times after the shift and ca. 5 µg were used for northern blotting or primer extension analysis. (**A**) Northern blot analysis of high-molecular-mass or (**B**) low-molecular-mass pre- and mature rRNAs. Probes used for northern blotting, between parentheses, are indicated and described in **Table 3**. (**C**) Primer extension analysis using the probe g, which is complementary to sequences in ITS2. This probe allows detection of $27SA_2$, $27SA_3$, both 27SB pre-rRNAs and 25.5S pre-rRNA.

We also assayed the kinetics of synthesis and turnover of pre-rRNAs by 5,6-^{3}H-uracil pulse-chase labelling experiments. For this purpose, the *GAL::RPL15* strain and an isogenic wild-type control were first transformed with the YCplac33 (*CEN URA3*) plasmid; then, transformants were grown in SGal-Ura medium and shifted to SD-Ura medium for 3 h. Cells were pulsed with tritiated uracil for 2 min and chased with an

excess of unlabelled uracil for 60 min. Total RNA was extracted from cells after the pulse and at different times (5, 15, 30 and 60 min) after the initiation of the chase, separated by gel electrophoresis, transferred to a nylon membrane and visualised using imaging screens. As shown in **Figure 7A**, in wild-type cells, the 35S pre-rRNA was rapidly converted to 20S and $27SA_2$ pre-rRNAs, which were efficiently converted to mature 18S and 25S rRNAs, respectively. In contrast, in *GAL::RPL15* cells, processing of 35S pre-rRNA was delayed although substantial amounts of 20S pre-rRNA and mature 18S rRNA were produced. However, only traces of 27S pre-rRNAs were visualised and no mature 25S rRNA could be detected (**Figure 7A**). Analysis of low-molecular mass RNAs revealed no 5.8S rRNA production but no alteration on the synthesis of mature 5S rRNA and tRNAs in the *GAL::RPL15* cells compared to the isogenic wild-type control (**Figure 7B**).

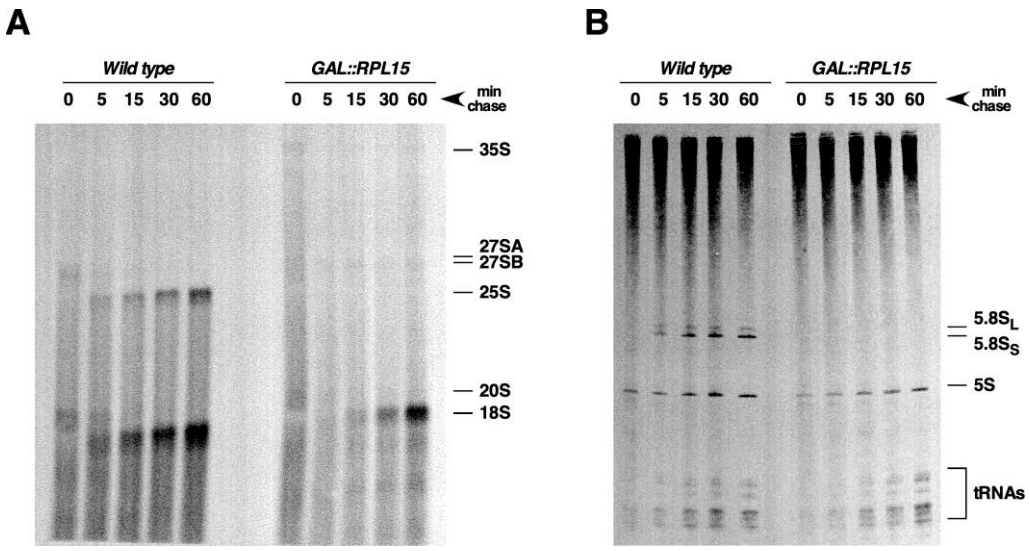

Figure 7. Depletion of eL15 induces turnover of pre-rRNAs. Wild type BY4741 (*Wild type*) and JFY355 (*rpl15AΔ rpl15BΔ* [YCplac111-GAL-RPL15A]) (*GAL::RPL15*) strains were transformed with an empty YCplac33 (*CEN URA3*) plasmid, grown at 30 °C in SGal-Ura to mid-log phase and shifted to SD-Ura for 3 h. Cells were pulse-labelled with [5,6-^{3}H] uracil for 2 min followed by a chase with a large excess of SD-Ura for the indicated times. Total RNA was extracted from each sample and 3,000 cpm was loaded and separated on (**A**) a 1.2% agarose-6% formaldehyde gel or (**B**) a 7% polyacrylamide-8M urea gel, blotted to nylon membranes and exposed to a screen. The positions of the different pre- and mature rRNAs are indicated.

Together, these results indicate that eL15 is required for conversion of 27S pre-rRNAs into mature 25S and 5.8S rRNAs, more specifically for processing of $27SA_3$ pre-rRNA into $27SB_S$ pre-rRNA. Although $27SB_L$ pre-rRNA continues to be produced, it fails to be converted to $7S_L$ pre-rRNA. Furthermore, upon depletion of eL15, there might be

a considerable turnover of pre-rRNAs to mature 25S and 5.8S rRNAs, most likely due to abortive formation of early pre-60S r-particles unable to assemble eL15.

eL15 is required for assembly of neighbouring 60S r-proteins

To further study the role of eL15 in LSU biogenesis, we aim to characterise how the depletion of eL15 affected the assembly of other r-proteins within pre-60S r-particles. For this, we used a *GAL::RPL15* strain with a chromosomally TAP-tagged Noc2. Noc2 is an early pre-60S r-particle assembly factor that is co-transcriptionally recruited to nascent rRNA precursors and is present from very early nucleolar to intermediate nucleolar pre-60S r-particles, dissociating concomitantly to 27SB pre-rRNA processing at site C_2 [91,96,249,250].

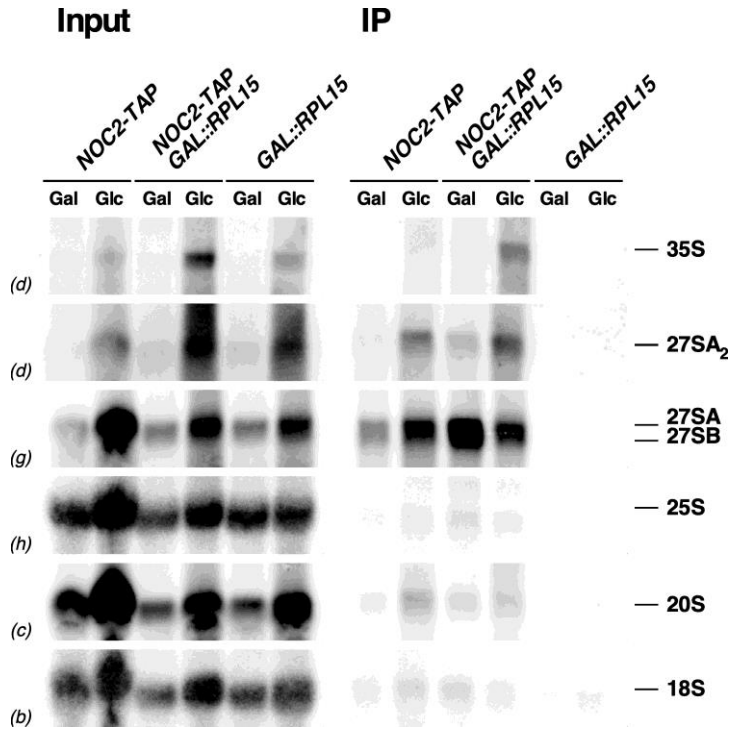

Figure 8. Pre-rRNA composition of Noc2-TAP affinity purified particles before or after *in vivo* depletion of eL15. Strains TY1879 (*NOC2-TAP*), JFY355 (*GAL::RPL15*), and JFY440 (*NOC2-TAP GAL::RPL15*) were grown at 30 °C in YP(A)Gal to mid-log phase (Gal) and shifted to YP(A)D for 3 h (Glc) to shut down the expression of eL15. Total cell extracts were prepared for each strain and each condition and the complexes associated with Noc2-TAP affinity purified. Total RNA was extracted from the affinity-purified samples (lanes IP) and from an amount of total extracts corresponding to 1/50 of that used for purification (lanes Input), separated on a denaturing agarose gel and subjected to northern blotting. Pre- and mature rRNAs were detected using the oligonucleotide probes indicated between parentheses.

We affinity purified pre-ribosomal particles before or after 3 h of depletion of eL15 and then studied the relative abundance of pre- and mature rRNAs of the particles by northern blot analysis (**Figure 8**). As expected, under permissive growth conditions (galactose-containing medium), Noc2-TAP containing particles enriched $27SA_2$ and mostly 27SB pre-rRNAs, which was consistent with the specific presence of early to middle pre-60S r-particles in the purified samples. The background levels of mature 25S and 18S rRNAs reflected that there was no significant contamination of mature r-subunits in our purification experiments. Moreover, depletion of eL15 also allowed co-purification of early 90S pre-ribosomal particles, as deduced from the presence of 35S pre-rRNA in the purified samples (**Figure 8**).

We also studied changes in the protein composition of TAP-tagged Noc2-containing particles purified from eL15 depleted *versus* non-depleted cells by iTRAQ analysis. When focused on r-proteins (see **Figure 9A**), our data indicated that, as expected, eL15 itself was the r-protein whose levels were most highly decreased. The levels of few other LSU r-proteins were significantly reduced, specially eL36, which is interestingly located together to eL8 adjacent to eL15 and bound to 5.8S/25S rRNA domain I from the moment of formation of early pre-60S r-particles [7,92]; (see also **Figures 1** and **10**). The other r-proteins whose levels remarkably decreased were eL13, eL14 and uL24 (**Figure 9A**). As for eL36, eL13 localises relatively close to eL15 in mature LSUs and early pre-60S r-particles (**Figures 10** and **11**); uL24 is not as close as eL36 or eL13 to eL15, but, interestingly, it also interacts with mature 5.8S rRNA ([7]; see also **Figure 10** and **11**). Thus, these results indicate that the efficient assembly of eL15 is required for stable assembly of adjacent r-proteins, such as eL36 and eL13, or associated to domain I of 25S/5.8S rRNA as uL24. In consonance with this, depletion of eL36 results in practically identical pre-rRNA processing defects than those detected upon depletion of eL15 [251]. In contrast, depletion of eL13 leads to a modest $27SA_3$ pre-rRNA processing defect while deletion of both paralogs of uL24 does not induce major pre-rRNA processing phenotypes [252-254]. The relationship between eL14 and eL15 r-proteins is unclear (see the Discussion section), as they do not map close each other in either mature or early pre-60S r-particles [255] (see also **Figure 10** and **11**).

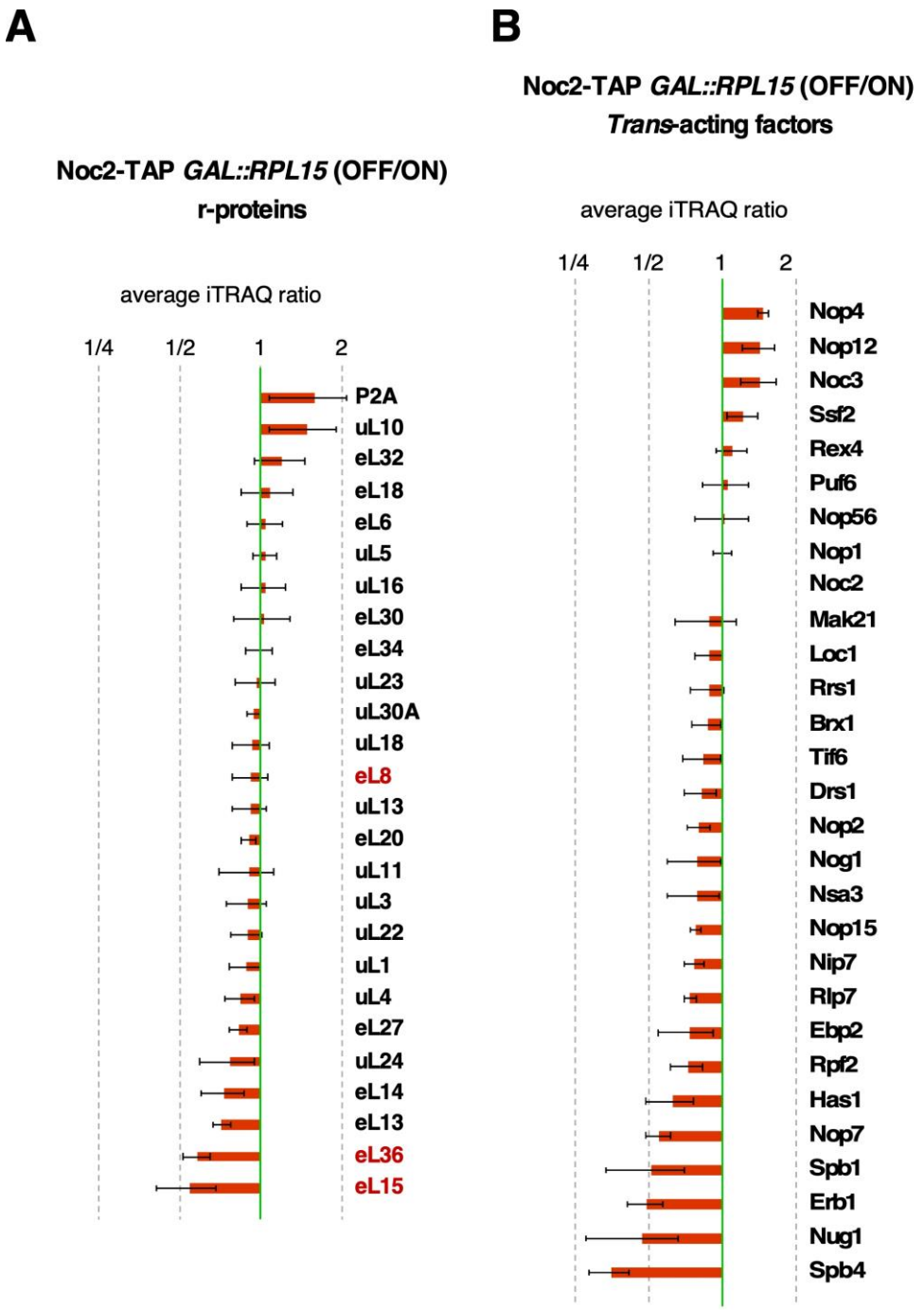

Figure 9. Changes in composition of pre-ribosomal particles upon depletion of eL15. Strain JFY440 (*NOC2-TAP GAL::RPL15*) was grown at 30 °C in YP(A)Gal to mid-log phase and shifted to YP(A)D for 3 h (Glc) to shut down the expression of eL15. Whole cell extracts were prepared, Noc2-TAP-associated ribosomal particles were affinity-purified and protein abundance was analysed by iTRAQ semiquantitative mass spectrometry. The ratios of the proteins purified after *versus* before depletion of eL15 are shown. The average of three independent experiments with their standard deviation is shown. Only proteins identified by more than one peptide are indicated. Ratios were normalized to that of Noc2, the bait protein, whose ratio was set arbitrarily to one. (**A**) Relative enrichment/deprivation of r-proteins purified upon depletion of eL15. (**B**) Relative enrichment/deprivation of protein *trans*-acting factors purified upon depletion of eL15.

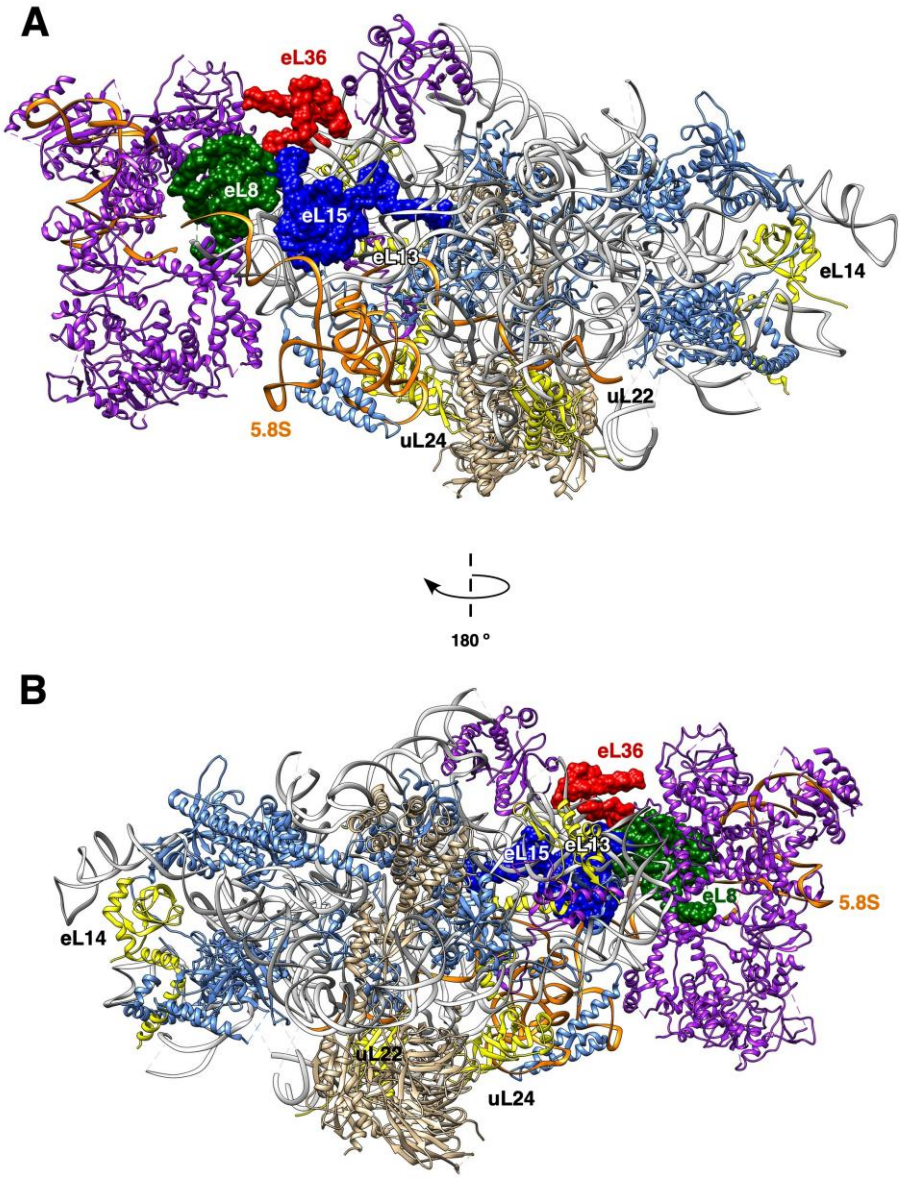

Figure 10. Location of eL15 and its r-protein neighbourhood on early pre-60S ribosomal particles (state A). The cartoons show the representation rendered with UCSF Chimera of data from the cryo-EM map of so-called state A of maturation of pre-60S r-particles (PDB ID: 6EM3; [92]). Particles are shown from the intersubunit interface (**A**) or solvent exposed interface (**B**). Only the surfaces of eL8 (green), eL15 (blue) and eL36 (red) are shown. Co-depleted r-proteins other than eL15 and eL36 upon depletion of eL15 or eL36 are shown in yellow. The rest of r-proteins are coloured in pale blue. *Trans*-acting factors are shown in purple if their composition was affected or in khaki if was not affected upon depletion of eL15 or eL36. Pre-rRNA is shown in pale grey, and 5.8S rRNA and a region of ITS2 in orange.

Our iTRAQ analyses also showed that two r-proteins, uL10 and P2A, increased when compared the composition of Noc2-TAP particles purified from either eL15 depleted or non-depleted cells. These two r-proteins have been described to

predominantly assemble in the cytoplasm (e.g. [256,257]), thus, their increased levels would likely reflect the artefactual result of some minor contamination of LSU in the samples from depleted cells.

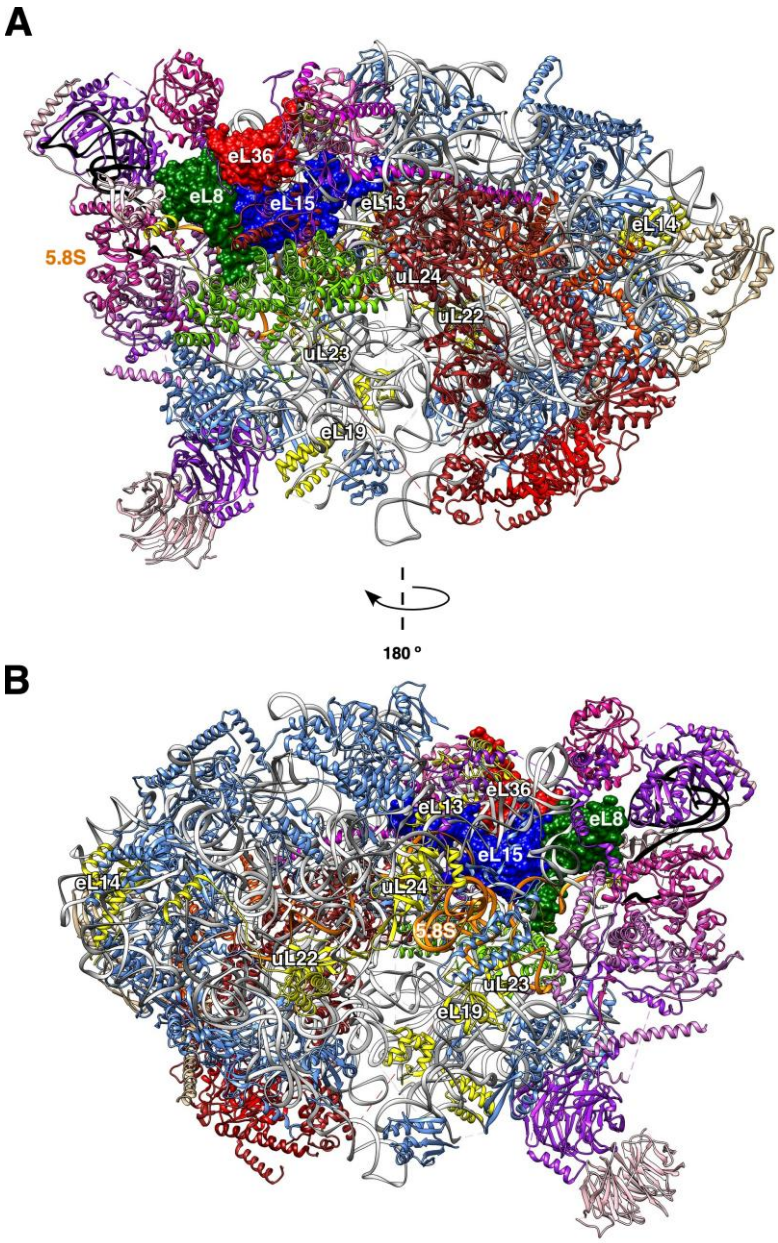

Figure 11. Location of eL15 and its r-protein neighbourhood on early pre-60S ribosomal particles (state E). The cartoons show the representation rendered with UCSF Chimera of data from the cryo-EM map of so-called state E of maturation of pre-60S r-particles (PDB ID: 6ELZ; [92]). Particles are shown from the intersubunit interface (**A**) or solvent exposed interface (**B**). Only the surfaces of eL8 (green), eL15 (blue) and eL36 (red) are shown. Co-depleted r-proteins other than eL15 and eL36 upon depletion of eL15 or eL36 are shown in yellow. The rest of r-proteins are coloured in pale blue. *Trans*-acting factors from the group of A_3-factors and B-factors are coloured in tones of purple/pink or red, respectively. Note that the composition of these factors was negatively affected upon depletion of eL15 or eL36. Noc3 is shown in green. Other *trans*-acting factors are coloured in khaki. Pre-rRNA is shown in pale grey and 5.8S rRNA in orange. The resolved region of ITS2 is coloured in black.

eL15 is required for association of A_3- and B-factors with pre-60S r-particles

We also determined how the depletion of eL15 affected the association of protein assembly factors with Noc2-TAP purified particles (**Figure 9B**). Factors that showed reduced association can be grouped into two major categories. First, many of these factors belonged to the group so-called A_3-factors, namely assembly factors that are required for removal of ITS1 from $27SA_3$ pre-rRNA to form $27SB_S$ pre-rRNA; this group comprises Brx1, Drs1, Ebp2, Erb1, Has1, Nop7, Nop12, Nop15, Nsa3/Cic1, Pwp1, Rlp7, and Ytm1 (for a review, see [36]). Depletion of any of these factors leads to increased levels of $27SA_3$ pre-rRNA and decreased amounts of 27SB pre-rRNAs [36], situation similar to that occurring upon depletion of eL15. Nine out of the twelve A_3-factors (Brx1, Drs1, Ebp2, Erb1, Has1, Nop7, Nop15, Nsa3 and Rlp7) were significantly reduced upon depletion of eL15, as deduced from our iTRAQ analysis (**Figure 9B**). The second group was formed by the so-called B-factors, which includes assembly factors required for 27SB pre-rRNA cleavage at site C_2; this group comprises Dbp10, Mak11, Nip7, Nog1, Nog2, Nop2, Nsa2, Rlp24, Rpf2, Rsr1, Spb4, and Tif6. Upon depletion of these factors, 27SB pre-rRNAs accumulated and little downstream 25.5S and 7S pre-rRNAs were formed (for a review, see again [36]). Seven out of the twelve B-factors (Nip7, Nog1, Nop2, Rpf2, Rrs1, Spb4, and Tif6) were significantly reduced upon depletion of eL15, as also deduced from our iTRAQ analysis (**Figure 9B**). Other factors including Sbp1, whose depletion resembles that of a B-factor [258], and Nug1, which is neither a A_3- nor a B-factor functionally linked to Dbp10 [147,259], also significantly decreased. Interestingly, some of these factors form small complexes such as Nip7 with Nop2 [114], Nop7 with Drs1, Erb1 and Ytm1 [105,110,260], Has1 with Rlp7 and Nop15 [107], and Rpf2 with Rrs1 [131].

In turn, few factors enriched upon depletion of eL15, basically Nop4/Nop77, Nop12 and Noc3 (**Figure 9B**). Nop4, which binds near the 5' end of 5.8S rRNA [261], has been recently shown to be an important organiser of primordial pre-60S r-particles [79]. Likely, in normal conditions, Nop4 binds and releases pre-60S r-particles before the recruitment of eL15 r-protein so it enriches to pre-60S r-particles in circumstances where eL15 has not been incorporated. Nop12, together with Nop13 and Pwp1 [262,263], is required for proper folding of 5.8S rRNA [261,264]. Interestingly, Nop12

has been shown to cross-linked within ITS2 and 5.8S rRNA, close to the eL15 r-protein binding site [92,261]. Noc3 forms a dimer with Noc2, which during maturation replaces the Noc1-Noc2 complex in early pre-60S r-particles [249]; Noc3 binds close to the eL15 r-protein binding site at early pre-60S r-particles [92]. Strikingly, as shown in **Figures 12** and **13**, most of the assembly factors identified in our iTRAQ analysis have been found to be component of stable early pre-60S ribosomal intermediates (state A to state D intermediates) resolved at high resolution by cryo-EM analysis [92].

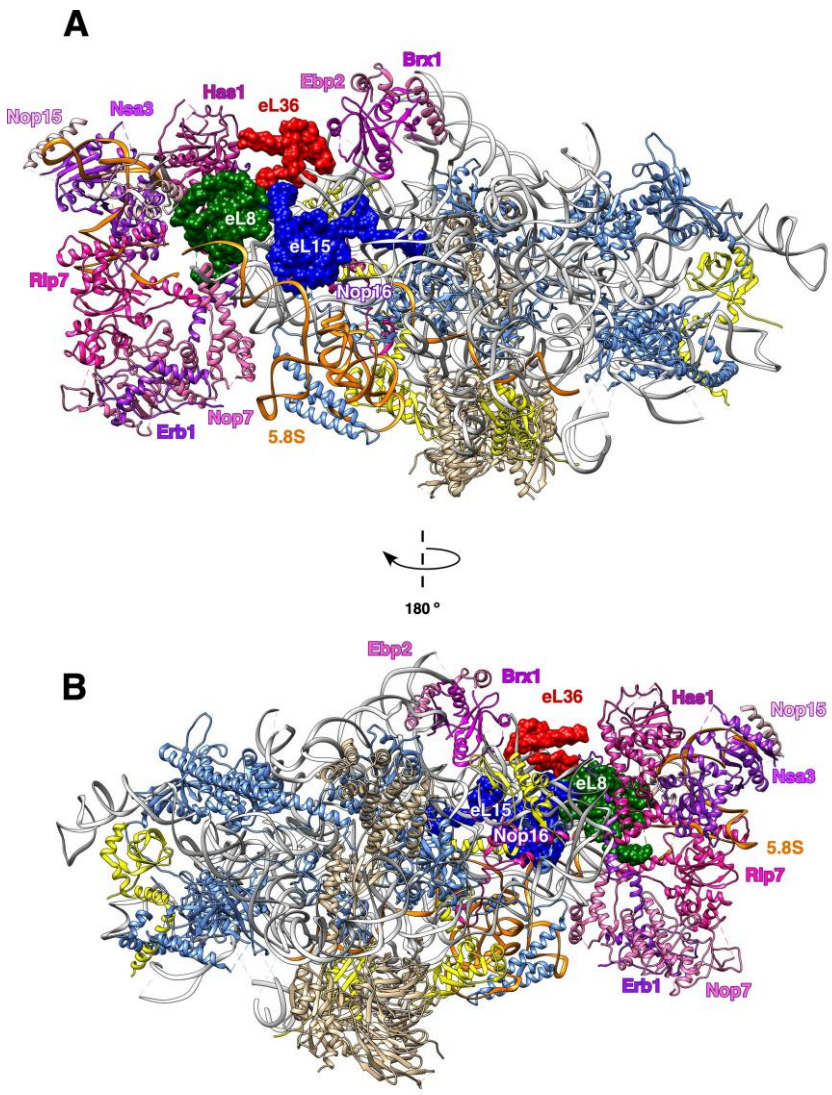

Figure 12. *Trans*-acting factors affected upon depletion of eL15 on early pre-60S ribosomal particles (state A). The cartoons and legend of colour is exactly the same used in Figure 10. Particles are shown from the intersubunit interface (**A**) or solvent exposed interface (**B**). The A_3-factors are highlighted in different tones of purple/pink. Other factors are coloured in khaki. Pre-rRNA is shown in pale grey and 5.8S rRNA included a region of ITS2 in orange. Only the surfaces of eL8 (green), eL15 (blue) and eL36 (red) are shown. Co-depleted r-proteins other than eL15 and eL36 upon depletion of eL15 or eL36 are shown in yellow. The rest of r-proteins are coloured in pale blue.

Taken together, we conclude that depletion of eL15 aborts formation of early stable pre-60S r-particles as those identified by the snapshots states A and D resolved by cryo-EM analysis. These particles cannot properly progress in their maturation through removal of ITS1 (cleavage at site A_3) and ITS2 (processing at B_1 sites), which explain the pre-rRNA processing and nucleo-cytoplasmic export defects observed upon depletion of eL15.

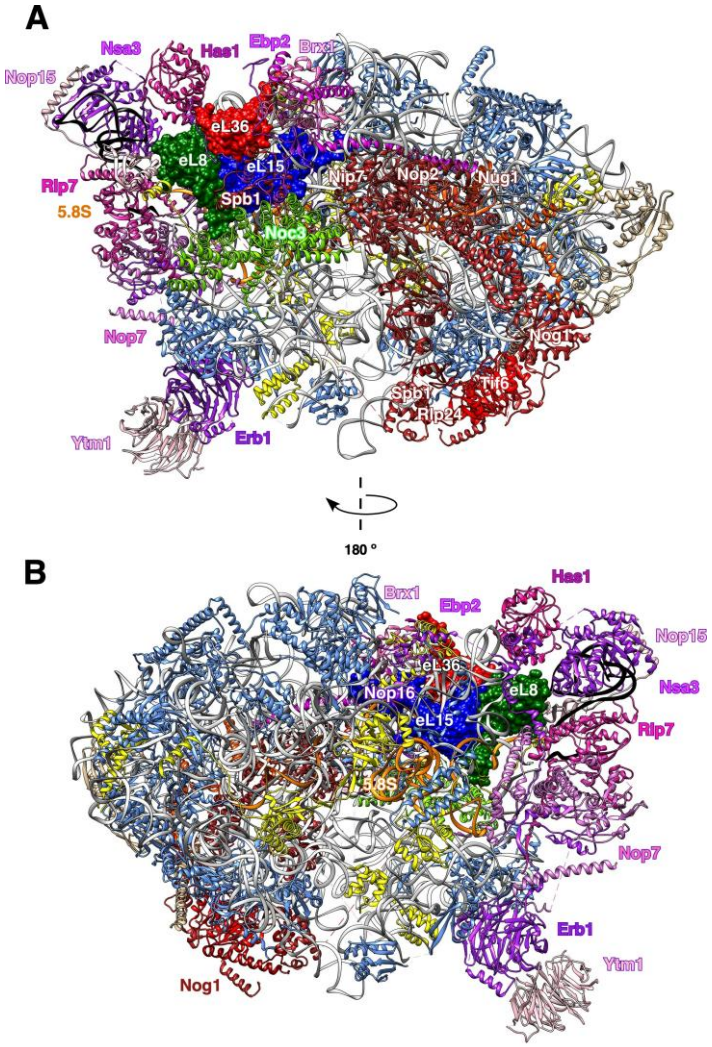

Figure 13. *Trans*-acting factors affected upon depletion of eL15 on early pre-60S ribosomal particles (state E). The cartoons and legend of colour is exactly the same used in Figure 11. Particles are shown from the intersubunit interface (**A**) or solvent exposed interface (**B**). The A_3-factors are highlighted in different tones of purple/pink and the B-factor in different tones of red. The rest of factors are coloured in khaki. Pre-rRNA is shown in pale grey, 5.8S rRNA in orange and a region of ITS2 in black. Only the surfaces of eL8 (green), eL15 (blue) and eL36 (red) are shown. Co-depleted r-proteins other than eL15 and eL36 upon depletion of eL15 or eL36 are shown in yellow. The rest of r-proteins are coloured in pale blue.

Hierarchical and interdependent assembly of the eL15 neighbourhood environment

We compared our iTRAQ results with those of the literature and found remarkable similarities with those previously shown upon depletion of eL8. These studies reported that depletion of eL8 leads to practically identical 27S pre-rRNA processing than depletion of eL15. More interestingly, depletion of eL8 also negatively impacts the assembly of both eL15 and eL36 r-proteins, as well as prevents the stable association of A_3- and B-factors with pre-60S r-particles [239,252,265]. However, although another study showed that eL36 is also required for processing of $27SA_3$ pre-rRNA [251], no data was available for the dynamics of association of r-proteins and protein assembly factors with pre-ribosomal intermediates upon depletion of eL36. Thus, to further study the relationship between this triad of interconnected r-proteins, we also compared the changes in pre-rRNA and protein composition of Noc2-TAP containing particles before or after depletion of eL36. To do so, we first constructed a *GAL::RPL36* strain (see Materials and Methods). This strain showed similar growth to that of an isogenic wild-type strain on YP(A)Gal plates but was unable to grow on YP(A)D plates (**Figure 14A**). Reproducibly, after shifting a culture of the *GAL::RPL36* strain at mid-log phase from liquid YP(A)Gal medium to YP(A)D medium, the growth progressively decreased stopping 6 to 9 h after the shift (**Figure 14B**).

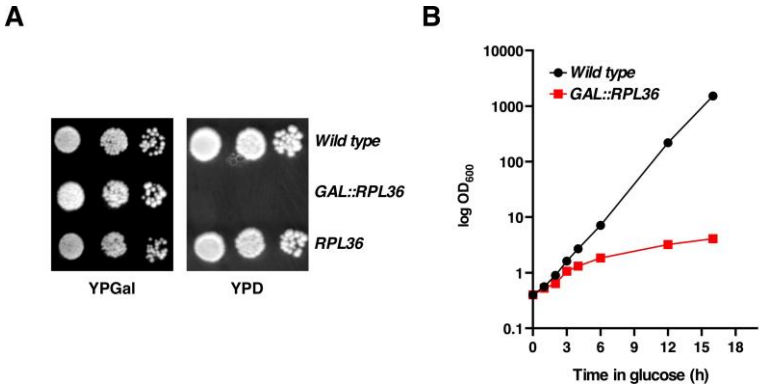

Figure 14. *In vivo* depletion of eL36 inhibits cell growth. (**A**) Growth comparison of the isogenic strains BY4741 (*Wild type*) and JFY519 harbouring the pAS25-RPL36B plasmid (*GAL::RPL36*) or YCplac111-HA-RPL36B (*RPL36*). Cells were grown in YP(A)Gal to mid-log phase at 30 °C, diluted to an OD_{600} of 0.05 and spotted in 10-fold serial dilutions onto YP(A)Gal and YPD plates, which were incubated 3 days at 30 °C. (**B**) Growth curves of the above strains (*Wild type;* filled black circles. *GAL::RPL36,* filled red squares) in YP(A)D medium at 30 °C. Cells were first grown in liquid YP(A)Gal medium to mid-log phase at 30 °C, diluted to an OD_{600} of 0.4 and shifted to YP(A)D. The OD_{600} was measured at the indicated times. Note that the data corresponding to the wild-type strain are the previously shown in Figure 3.

We first analysed the pre- and mature rRNAs that associate with Noc2-TAP by northern blotting. As shown in **Figure 15**, Noc2-TAP was able to efficiently co-purified 27SB pre-rRNAs both before and after *in vivo* depletion of eL36, indicative for its association with early to intermediate pre-60S r-particles.

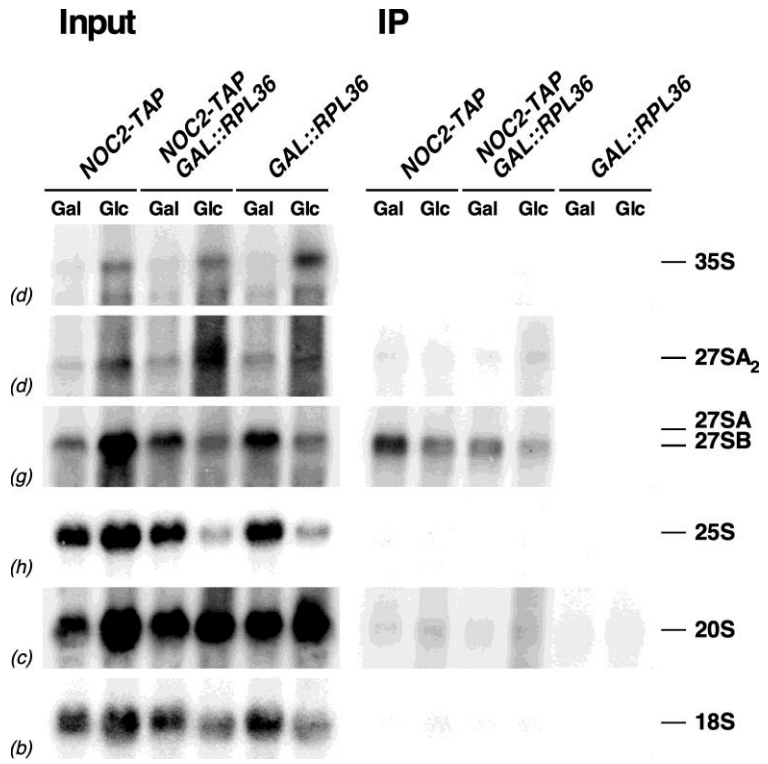

Figure 15. Pre-rRNA composition of Noc2-TAP affinity purified particles before or after in vivo depletion of eL15. Strains TY1879 (*NOC2-TAP*), JFY519 (*GAL::RPL36*), and JFY559 (*NOC2-TAP GAL::RPL36*) were grown at 30 °C in YP(A)Gal to mid-log phase (Gal) and shifted to YP(A)D for 3 h (Glc) to shut down the expression of eL36. Total cell extracts were prepared for each strain and each condition and the complexes associated with Noc2-TAP affinity purified. Total RNA was extracted from the affinity-purified samples (lanes IP) and from an amount of total extracts corresponding to 1/50 of that used for purification (lanes Input), separated on a denaturing agarose gel and subjected to northern blotting. Pre- and mature rRNAs were detected using the oligonucleotide probes indicated between parentheses.

When r-proteins were assessed by iTRAQ mass spectrometry, as shown in **Figure 16A**, and as expected, eL36 itself was the r-protein whose levels were most severely diminished from Noc2-TAP-containing particles upon depletion of eL36. The levels of other r-proteins were also significantly reduced, specially uL1 uL22, eL14, eL19, uL24, eL13 and uL23. The uL1 r-protein forms the uL1-stalk together with the tip of helix H76 of 25S rRNA, whose base interacts with eL36 [266]. As above described, eL13 maps close

to eL15, and thus to eL36. uL24, but also uL22, uL23 and eL19 are located in the nearby environment of eL36 in both mature LSUs and early pre-60S r-particles ([255]; see also **Figures 10** and **11**). As for eL15, the relationship of eL14 with the depletion of eL36 is also unclear. Curiously, neither eL15 nor eL8 were among the top five most affected r-proteins, in contrast to the results obtained upon depletion of eL15 (see above) or of eL8 [239,252,265]. This fact suggests a hierarchical manner for the assembly of these triad of r-proteins (see Discussion).

Few r-proteins were enriched upon depletion of eL36 (**Figure 16A**); as observed upon depletion of eL15, these included P2A and uL10, most likely due to some contamination of mature LSUs in particles purified from depleted cells.

We also studied how the depletion of eL36 affected the association of protein ribosome assembly factors with Noc2-TAP purified particles. Similarly, as occurred upon depletion of eL15 or eL8, most A_3-factors (10 out of 12 factors: Brx1, Drs1, Ebp2, Erb1, Has1, Nop7, Nop15, Nsa3, Rlp7, and Ytm1) and B-factors (9 out of 12 factors: Dbp10, Nip7, Nog1, Nop2, Rlp24, Rpf2, Rsr1, Sbp4, and Tif6) were greatly diminished in our iTRAQ analysis upon depletion of eL36 (**Figure 16B**). Other factors such as Spb1 or Nug1 were also affected upon depletion of eL8, eL15 and eL36 (this work; [239]). Interestingly, the most negatively affected factor after depletion of eL36 was Nop16 (**Figure 16B**), which also showed reduced levels upon depletion of eL8 [239]. This behaviour might be linked to the interaction of Nop16 with eL8 and eL13 and its role interconnecting RNA elements within 5.8S/25S rRNA domain I (see **Figure 13**).

Few assembly factors were overrepresented in Noc2-TAP particles following depletion of eL36, among them Pwp1, Noc3, Nop12 and Noc4; interestingly, most of these factors also increased upon depletion of eL15 (see **Figure 9**) or eL8 [239]. As suggested above, these factors must associate with pre-60S r-particles before the stable assembly of any of this triad of r-proteins and leave them only once the assembly of the r-proteins occurs (i.e. [79]).

Altogether, these results suggest that depletion of eL36, as well as that of eL15 (this study) and eL8 [239] prevent the stable formation of early pre-60S r-particles. In the absence of any of these r-proteins, the association of most assembly factors that

bind domain I such as Nop16 and A_3-factors, the subsequent association of particular B-factors and the assembly of a set of r-proteins that mainly lie close to them fail. Moreover, the assembly of eL8, eL15 and eL36 seems to occur in an interdependent manner but apparently following a particular hierarchy (see Discussion).

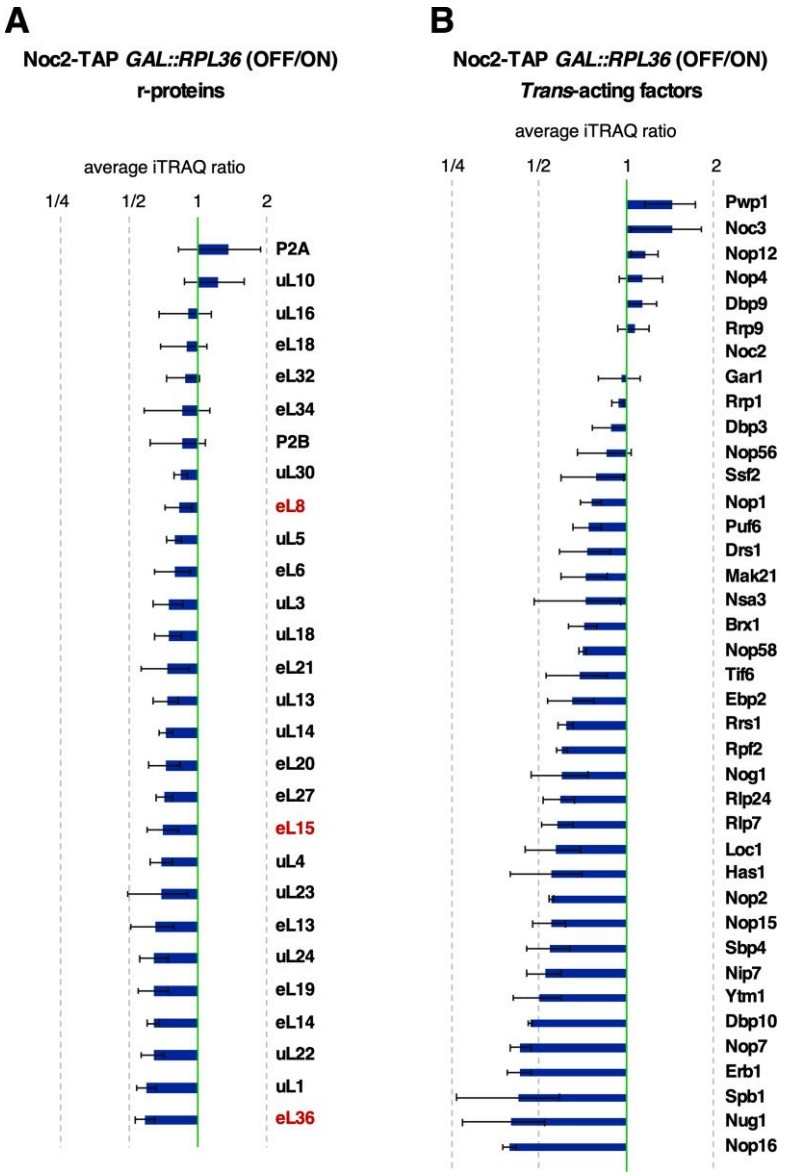

Figure 16. Changes in composition of pre-ribosomal particles upon depletion of eL36. Strain JFY559 (*NOC2-TAP GAL::RPL36*) was grown at 30 °C in YP(A)Gal to mid-log phase and shifted to YP(A)D for 3 h (Glc) to shut down the expression of eL36. Whole cell extracts were prepared, Noc2-TAP-associated ribosomal particles were affinity-purified and protein abundance was analysed by iTRAQ semiquantitative mass spectrometry. The ratios of the proteins purified after *versus* before depletion of eL36 are shown. Data are the average of three independent experiments with their standard deviation. Only proteins identified by more than one peptide are indicated. Ratios were normalized to that of Noc2, the bait protein, whose ratio was set arbitrarily to one. (**A**) Relative enrichment/deprivation of r-proteins purified upon depletion of eL36. (**B**) Relative enrichment/deprivation of protein *trans*-acting factors purified upon depletion of eL36.

DISCUSSION

We are interested in understanding the role of yeast r-proteins in the assembly and function of ribosomes. Although the contribution of practically all r-proteins from both r-subunits in pre-rRNA processing and nucleo-cytoplasmic transport have been successfully studied (e.g. [223,267], for a review, see [218]), few r-proteins still await characterization or have been poorly studied. In this work, we have undertaken the functional analysis in ribosome assembly of one of them, the yeast eL15 r-protein. eL15 is an essential protein conserved in both archaea and eukaryotes, although the eukaryotic eL15 r-protein contains a specific C-terminal extension, which is absent in the archaeal orthologs [7,189]. In yeast, eL15 is encoded by duplicated genes, *RPL15A* and *RPL15B*, but while *RPL15A* is an essential gene, *RPL15B* is apparently fully dispensable for growth under laboratory conditions. Indeed, it has been reported that *RPL15B* is transcriptionally inactive [226]. Yeast eL15A and eL15B proteins have practically identical sequences, differing only in two amino acids, Q11 and D153 in eL15A *versus* N11 and E153 in eL15B. Whether or not these particular residues are involved in distinct functional-relevant interactions/repulsions with nearby residues of other r-proteins, ribosomal assembly factors or rRNA remains unknown. Interestingly, both eL15 variant proteins are functional, as nicely demonstrated by the expression of either an plasmid-encoded eL15B r-protein from the promoter region of the *RPL15A* gene or by the expression of an eL15A[Q11N D153E] point mutant as the sole sources of eL15 [226]. Regarding the eukaryote-specific C-terminal extension of eL15, it has also been shown that while the last four amino acids of eL15A can be deleted without no effect on function, deletion of last 12 amino acids is fully detrimental for growth, in part due to an interference with the nuclear import of the truncated protein since a predicted bipartite NLS with significant high score is found within this region [226,268].

In this work, we have addressed the role of the eL15 r-protein using a *GAL::RPL15* strain that conditionally expresses eL15A. As expected for an essential 60S r-protein, depletion of eL15 led to a strong deficit of 60S r-subunits (see **Figure 4**). Study of pre-rRNA processing upon eL15 depletion clearly indicates that this deficit was due to a main impairment of the 27S pre-rRNAs conversion into mature 25S and 5.8S rRNAs. Thus,

northern and primer extension analyses showed that while the steady-state levels of $27SA_2$ pre-rRNA remained practically invariable or slightly decreased upon depletion of eL15, those of $27SA_3$ pre-rRNA accumulated. Moreover, levels of the subsequent $27SB_S$ pre-rRNA rapidly and considerably decreased but those from $27SB_L$ pre-rRNA, which derived directly from $27SA_2$ pre-rRNA, did not do it (see **Figure 6**). Nevertheless, the $27SB_L$ pre-rRNA species seemed not to be productively processed, as neither 7S pre-rRNA form were produced. Consistently, no change in the ratio $5.8S_L$:$5.8S_S$ could be observed following eL15 depletion, contrary to what occurs with loss-of-function mutations of components of RNase MRP, which is the A_3-site endonuclease (e.g. [269,270]). We conclude, therefore, that both processing of $27SA_3$ to $27SB_S$ pre-rRNA at ITS1 and maturation of both species of 27SB pre-rRNA at ITS2 are impaired upon depletion of eL15. Northern analysis also revealed that depletion of eL15 mildly compromised early processing of 35S pre-rRNA since both, this intermediate and an aberrant 23S pre-rRNA, accumulated with ongoing eL15 depletion. Moreover, as deduced by pulse-chase experiments, although some 35S pre-rRNA was detected and normal amounts of 20S pre-rRNA and mature 18S rRNA were produced, all intermediates destined for mature 25S and 5.8S rRNAs and these mature rRNAs themselves underwent significant turnover following eL15 depletion (see **Figure 7**). In addition to pre-rRNA processing defects, very rapidly upon eL15 depletion (3 h), there was an accumulation of pre-60S r-particle intermediates in the nucle(ol)us as deduced by the nucle(ol)ar accumulation of the uL23-yEGFP reporter in these conditions (see **Figure 5**). This result suggests that abortive pre-60S r-particles containing uL23-yEGFP but lacking eL15 were being retained in the nucle(ol)us due to impaired intra-nuclear and nucleo-cytoplasmic export, most likely due to the fact that they could not gain export competence.

Similar pre-rRNA processing defects, namely accumulation of $27SA_3$ and $27SB_L$ pre-rRNAs, rapid turnover of 27S pre-rRNA intermediates to mature 25S and 5.8S rRNAs, delayed pre-rRNA processing at the early A_0-A_2 sites and nucle(ol)ar accumulation of pre-60S r-particles, have previously been observed upon depletion of other 60S r-proteins and protein assembly factors involved in 60S r-subunit biogenesis. Thus, practically identical defects to those herein described upon eL15 depletion have been

reported upon depletion of eL8 [239,252] and eL36 [251] or upon depletion of the subset of 60S r-subunit assembly factors known as A_3-factors ([105,107-109,113,251,260,261,264,271-280], for a review see [36]). Alike pre-rRNA processing defects have been reported upon mutation in or depletion of other r-proteins, such as uL4 [254,281], eL6 [254], eL7 [239], eL14 [246], uL13 [91,252,282], eL18 [252,265], eL20 [252,265] and eL33 [252,283]; depletion of eL13 leads to accumulation of $27SA_3$ pre-rRNA without a parallel decrease in the levels of $27SB_S$ pre-rRNA [252,254].

In order to rationale why these ribosome biogenesis phenotypes emerge upon depletion of eL15, which is an early assembling r-protein (e.g. [91,92]), and distinguish which ones are general and which ones specific of the loss of this particular r-protein, we studied the pre-rRNA and protein composition of early pre-ribosomal particles purified with the *trans*-acting factor Noc2 fused to a C-terminal TAP tag before and after depletion of eL15. This approach has been successfully carried out in previous analyses after depletion of or mutation in many ribosome assembly factors and other different r-proteins, included eL8 (e.g. [91,107,223,237-239,246,254,265,274,284-286]). For comparative studies, we performed similar experiments upon depletion of eL36, which is together with eL8, the closest neighbouring r-protein to eL15 in mature ribosomes [7]. We used the TAP-tagged Noc2 factor for performing the affinity-purification analyses of pre-ribosomal particles containing or lacking each r-protein. Noc2 is present in 90S and early pre-60S r-particles as member of the consecutive Noc2-Noc1-Rrp5 and Noc2-Noc3 subcomplexes [96,249], thus, being suitable to reveal those compositional changes related to the pre-rRNA processing defects observed upon the depletion of eL15 or eL36. Importantly, a Noc2-TAP construct was also used as the purification bait for akin analyses performed following depletion of eL8 [239,265], which allowed us to directly compare our results with those obtained for eL8. As proven in our co-IP analyses (see **Figures 8** and **15**), Noc2-TAP was still able to associate with pre-ribosomal intermediates upon eL15 or eL36 depletion; most likely, these particles correspond to those that were retained in the nucle(ol)us upon depletion of eL15 (see **Figure 5**). Indeed, as our analysis confirmed, uL23 seems to still be stably associated with Noc2-TAP-containing particles after the depletion of eL15 (**Figure 9**). Moreover, both northern hybridisation and iTRAQ mass spectrometry experiments suggest that, upon depletion of eL15 or eL36, there was

a tendency for accumulation of early Noc2-containing pre-ribosomal particles, likely formed before the occurrence of $27SA_3$ pre-rRNA processing. Thus, 35S pre-rRNA accumulated in these conditions (**Figures 8** and **15**) and factors such as Pwp1, Nop4, Nop12, Rex4 or Dbp9 are present in greater amounts in pre-ribosomal particles purified from the depleted condition (**Figures 9** and **16**), fact that was also reported to occur upon depletion of eL8 [239,265]. Consistently, Pwp1 and Nop12, which both are members of the same subcomplex [263,264], Nop4, and Dbp9 have been recently identified in the so-called primordial pre-60S r-particles that represent the earliest intermediates on the road to mature 60S r-subunits [79]. Likewise, Rex4 has been described to be functionally associated to Rrp5, another ribosome assembly factor linked to emerging pre-60S r-particles [79].

Regarding the proteins that decrease following depletion of eL15 or eL36 and focusing first into r-proteins, two distinct groups could be highlighted. (i) First, the group comprising the r-proteins eL15, eL36, eL8 and eL13. All these are neighbouring proteins that form a cluster associated with domain I of mature 25S/5.8S rRNAs where they predominantly interact, included the ITS2-proximal stem formed by the base-pairing between the 3' end of 5.8S rRNA and the 5' end of 25S rRNA. Other rRNA residues from domains II, III, V and VI are also minorly bound by these r-proteins [7]. Our results indicate that, in the absence of eL15 or eL36, the cluster of these r-proteins failed to properly assemble, as previously reported upon depletion of eL8 [239,265]. In any case, the semiquantitative iTRAQ analyses indicated that the r-protein showing the strongest decrease corresponded to that being depleted in the experiments, while values for the other r-proteins of the cluster were different depending on the depleted r-protein analysed. Thus, depletion of eL8 leads to a clear, almost equal, decrease on the levels of eL15 and eL36 into Noc2-TAP-containing pre-60S r-particles [239,265]. However, depletion of eL15 affected significantly the association of eL36 with Noc2-TAP-containing pre-ribosomal particles but not that of eL8. Lastly, neither eL8 nor eL15 were among the top reductions upon depletion of eL36. Therefore, we are tempted to speculate that eL8, eL15 and eL36 follow a hierarchical and interdependent assembly to establish a stable core for domain I within early pre-60S particles, being eL8 the hub for assembly of the cluster and eL15 assembling before eL36. Unfortunately, no parallel

analysis has so far been done upon the specific depletion of eL13. In agreement with this hypothesis, it has been described that the abundance of eL8 in early pre-60S r-particles purified using Rrp5-TAP is greater than that of eL15, which in turn is more abundant than eL36 [287]. (ii) The second group of r-proteins that inefficiently assemble upon depletion of eL8 [239,265], eL15 or eL36 (this work) is comprised by uL24 and uL22, which are r-proteins that also predominantly bind the domain I of 25S/5.8S rRNA, and eL14 that bind domains II and VI of 25S rRNA [7]. Whether or not this failure is the direct consequence of the inability of the former cluster of r-proteins to assemble is still unclear (see later).

We have also studied the failure of association of ribosome assembly factors with pre-ribosomal particles purified *via* TAP-tagged Noc2 upon depletion of eL15 or eL36 r-proteins. Strikingly, our iTRAQ analyses clearly indicate that the assembly of both eL15 and eL36 was crucial for the association with pre-ribosomal particles of the so-called A_3-factors, which are required for the conversion of $27SA_3$ to $27SB_S$ (for a review, see [36]). Indeed, 9 out of the 12 ribosome assembly proteins defined as A_3-factors were found significantly diminished from the Noc2-containing pre-60S r-particles upon depletion of either eL15 or eL36 (**Figures 9** and **16**), result that was also described upon the failure of eL8 assembly by the Woolford and Milkereit groups [239,265]. It has also been previously reported that the association of A_3-factors with pre-ribosomal particles is hierarchical and interdependent [36,261,274,285]. Thus, the association of Ebp2 is required for that of a group of 7 mutually interdependent A_3-factors (Erb1, Nop7 Nop15, Nsa3, Rpl7 and Ytm1) that are, in turn, necessary for association of Drs1 and Has1. As previously reported for eL8 [239], our results suggest that assembly of eL15 and eL36 is also required to materialise the initiation of this hierarchical process. However, as also our results show, the association of two other A_3-factors, Pwp1 and Nop12, seems to occur upstream of this series of events, consistently with the fact that upon depletion of one of the interdependent A_3-factor such as Rlp7, both, Pwp1 and Nop12, are still efficiently recruited to early pre-60S r-particles [264]. Moreover, our results also confirm that the different components of the Pwp1 subcomplex, although able to form a free stable complex [263], could have differences in their binding possibilities to pre-ribosomal particles. As the recruitment of the A_3-factors precedes pre-rRNA processing

from sites A_3 to B_{1S}, consequently, the 27S pre-rRNA processing defects that we reported here upon depletion of either eL15 or eL36 might be interpreted as the consequence of the failure of association of this functional group of factors; in other words, depletion of these r-proteins does not directly impair pre-rRNA processing at site A_3. In contrast, it has also been reported examples of r-proteins, such as eL7, eL14 and some others from the eL14 functional cluster (uL13, eL20, eL32, eL33), that bind predominantly domain II of 25S/5.8S rRNA and whose depletion leads to $27SA_3$ pre-rRNA processing defects without a parallel influence on the recruitment of the A_3-factors to pre-ribosomal particles [239,246,265].

There is a second group of ribosome assembly factors that failed to associate with Noc2-containing pre-ribosomal particles upon the depletion of eL15 or eL36. This includes Nug1, Spb1, Spb4, Tif6, the subcomplex formed by Nip7 and Nop2 and the subcomplex formed by Rpf2 and Rrs1, among others (**Figures 9** and **16**), which all have in common that belong to the category of ribosome assembly proteins known as B-factors that are required for cleavage of 27SB pre-rRNA at site C_2 [36,114]. A similar result was also observed upon the depletion of eL8 [239,265]. Association of B-factors with pre-ribosomal particles has been described to occur through parallel pathways that converge to recruit the GTPase Nog2 [36,114]; in contrast with the result described upon depletion of eL8 [239], unexpectedly, we did not identified Nog2 among the factors that clearly diminished upon depletion of eL15 or eL36, perhaps as the consequence that our iTRAQ mass spectrometry analysis was not exhaustive enough or too stringent (only included proteins identified by more than one peptide). In no case, the failure of association of B-factors with pre-ribosomal particles is the obligate consequence of the requirement of previous association of the A_3-factors; thus, different examples have been reported where B-factors fail to be recruited with pre-ribosomal particles without apparent previous block on the association of A_3-factors (e.g. eL14 [246]).

Biochemical and structural studies have revealed that eukaryotic 60S r-subunits *in vivo* assemble following a sequential but imperfect 5'-3' co-transcriptional plan; rRNAs are folded in a hierarchical and cooperative manner to form monolithic structures where the different rRNA domains are highly intertwined (e.g. [92,93,102,288], see [38,40,77] for reviews). Earliest steps of 60S r-subunit assembly imply the co-transcriptional

assembly of primary binding 60S r-proteins including uL4 and eL8 [79] and the association of different ribosome assembly factors with nascent 35S or 27S pre-rRNAs, among others, those from the Rrp5-Noc1-Noc2 module [97,289], the Dbp6-subcomplex components Npa1/Urb1, Npa2/Urb2, Nop8, Rsa3 and the RNA helicase Dbp6 [98,99], other RNA helicases such as Mak5, Dbp7 and Dbp9 [290], Nop4 [261,291], different snoRNP complexes including those containing snR190 and snR37 [79], the Pwp1-subcomplex formed by Pwp1, Nop12, Brx1 and Ebp2 [263] and the methyltransferases Upa1 and Upa2 [79]. These earliest pre-60S r-particles remains elusive from the structural point of view, most likely due to their high degree of flexibility (e.g. [79]). As previously discussed, distinct factors from these particles are among those ones that increase in the Noc2-containing particles following depletion of either eL15 or eL36 in our experiments and of eL8 in the literature [239,265]. It seems that earliest pre-60S r-particles progress through the folding of complete domain I of 25S rRNA with 5.8S rRNA, and regions of domain II, IV and unprocessed ITS2 to form stable structures that, in this case, could have been revealed by cryo-EM analyses [92,93,102]. In these particles, named as state A intermediates in one of these studies [92], the rest of 25S rRNA domains and 5S RNP remain flexible. Additional steps of early 60S r-subunit assembly involve the compaction of the rest of domain VI and the subsequent folding of domain III and part of domain V, and finally of domain IV and the rest of domain V [92,93,102]. The resulting particles correspond to the so-called state E intermediates of the early nucleolar stages of 60S r-subunit synthesis [92]. Interestingly, particles from the state A contains most of the A_3-factors and most of the r-proteins that we have revealed to inefficiently associated with purified Noc2-containing particles upon depletion of either eL15 or eL36 in our experiments and others have revealed upon depletion of eL8 [239,265]. In these particles, the A_3-factors bind ITS2 and the part of domain I that surrounds this spacer forming a structure known as the foot [92,93,102]. Thus, we suggest that improper folding of domain I of 5.8S/25S rRNA is the primary cause of depletion of the r-proteins of the eL8-eL15-eL36 cluster. As a consequence of this impairment, the earliest steps of pre-60S r-subunit assembly delay, thus, leading to the slight accumulation of factors such as, Nop4, Nop12 and Pwp1, and some of the subsequent steps do not take place, thus, leading to inefficient association of most A_3-factors, which occurs normally in a concert and interdependent manner [274]. However,

other events, such as the association of the module formed by Nsa1, Mak16, Rpf1 and Rrp1, which is important to clamp rRNA domains I and II in state A intermediates [92,93,102], seem not to be significantly affected by the depletion of either eL8 [239], eL15 or eL36. Moreover, downstream assembly events *en route* to the formation of state E intermediates, such as the association of groups of other ribosome assembly factors, including distinct B-factors that bind to the side of the pre-60S r-particles opposing the foot structure, do neither apparently occur. Whether this is directly due from the depletion of eL15 or eL36 need further clarification. Indeed, the depletion of most but not all A_3-factors, which does not or minorly affects the assembly of eL8, eL15 or eL36, is sufficient to significantly impair the association of many B-factors with early pre-60S r-particles (e.g. [107,274]). It is interesting to remark that several of these B-factors show, in addition to dependence of distinct A_3-factors for their association with pre-60S r-particles, interdependence among them; for example, association of the B-factors Nip7 and Nop2 is required for recruitment of Rrs1 and Rpf2 to pre-60S intermediates, that, in turn, are needed for association of Spb4 and of Rpl24, Nog1 and Tif6 [114], all significantly reduced in purified Noc2-containing pre-60S r-particles upon depletion of eL15 or eL36 (**Figures 9** and **16**). Depletion of A_3-factors also leads to the assembly failure of other r-proteins from domain I (uL22, uL24, uL29 and eL37) within pre-60S r-particles [274]. Our results show that, at least, two of these r-proteins (uL22 and uL24) inefficiently assemble within Noc2-containing particles upon depletion of eL15 or eL36, result that has been previously revealed for the equivalent depletion of eL8 [239,265]. As above discussed, whether this result is the direct consequence of depleting eL8, eL15 or eL36 r-protein or the indirect effect of the failure of associating the A_3-factors is still unclear.

In summary, our results indicate that the depletion of a set of interdependent r-proteins (eL8, eL15 and eL36) leads to practically identical changes in the composition of early pre-60S r-particles. They also provide a logic reasoning of the common pre-rRNA processing defects detected upon the depletion of any of these r-proteins. We conclude that eL8, eL15 and eL36 are essential to properly fold domain I of 5.8S/25S rRNA both by their direct binding to sequences within this domain and by recruiting the set of A_3-factors to it. These events must facilitate the structuring of 5.8S rRNA from a largely

unfolded to a highly organised status including its 5' and 3' base-pairings to 25S rRNA in helix H2 and the so-called ITS2-proximal stem that contains future helix H10, respectively. Then, the stable and proper folding of rRNA domain I must be reinforced by binding of r-proteins such as uL24 and uL22, whose recruitment to rRNA domain I is also dependent on the earlier assembly of eL8, eL15 and eL36 and the association of A_3-factors, (this work and e.g. [253,265,274,287,292]). All these rearrangements have been demonstrated to be essential for 27S pre-rRNA processing at both ITS1 and ITS2 regions (e.g. [293,294]). Most importantly, upon the failure of the stable formation of 25S/5.8S rRNA domain I, pre-rRNA intermediates are subjected to rapid turnover, most likely as the result of the 5'-3' exonucleolytic activity of Rat1 in misassembled pre-60S intermediates [261,274]. This strategy operates as a logical quality control mechanism that prevents misassembled pre-60S r-particles to further mature into inactive ribosomes.

CONCLUSIONS

1. The non-essential ribosomal protein eL22 is required for efficient production of 60S ribosomal subunits. Specifically, eL22 is important for the correct processing of 27SB pre-rRNA in the nucleus.

2. eL22 has a cytoplasmic role, being important for the correct recycling of the Arx1 and Alb1 ribosomal assembly factors from the cytoplasm to the nucleus.

3. Despite its function on ribosome biogenesis, ribosomes lacking eL22 do not apparently display translation accuracy errors.

4. The ribosomal protein eL15 is essential for the production of pre-60S ribosomal particles at nucleolar stages of ribosome assembly.

5. eL15 is necessary for the processing of $27SA_3$ and 27SB pre-rRNAs. Upon depletion of eL15, pre-60S r-particles are subjected to rapid turnover.

6. eL15 is essential for the formation of domain I of 25S/5.8S rRNA. Its assembly displays a hierarchical interdependence with that of eL8 and eL36. In addition, assembly of eL15 is important for the stable association of A_3- and B-assembly factors with early pre-60S ribosomal particles.

BIBLIOGRAPHY

1. Green, R. & Noller, H.F. Ribosomes and translation. *Annu. Rev. Biochem.* **66**, 679-716 (1997).

2. Shajani, Z., Sykes, M.T. & Williamson, J.R. Assembly of bacterial ribosomes. *Annu. Rev. Biochem.* **80**, 501-526 (2011).

3. Klinge, S., Voigts-Hoffmann, F., Leibundgut, M. & Ban, N. Atomic structures of the eukaryotic ribosome. *Trends Biochem. Sci.* **37**, 189-198 (2012).

4. Greber, B.J. & Ban, N. Structure and function of the mitochondrial ribosome. *Annu. Rev. Biochem.* **85**, 103-132 (2016).

5. Zoschke, R. & Bock, R. Chloroplast translation: structural and functional organization, operational control, and regulation. *Plant Cell* **30**, 745-770 (2018).

6. Schmeing, T.M. & Ramakrishnan, V. What recent ribosome structures have revealed about the mechanism of translation. *Nature* **461**, 1234-1242 (2009).

7. Ben-Shem, A., Garreau de Loubresse, N., Melnikov, S., Jenner, L., Yusupova, G. & Yusupov, M. The structure of the eukaryotic ribosome at 3.0 Å resolution. *Science* **334**, 1524-1529 (2011).

8. Klinge, S., Voigts-Hoffmann, F., Leibundgut, M., Arpagaus, S. & Ban, N. Crystal structure of the eukaryotic 60S ribosomal subunit in complex with initiation factor 6. *Science* **334**, 941-948 (2011).

9. Rabl, J., Leibundgut, M., Ataide, S.F., Haag, A. & Ban, N. Crystal structure of the eukaryotic 40S ribosomal subunit in complex with initiation factor 1. *Science* **331**, 730-736 (2011).

10. Yusupova, G. & Yusupov, M. Crystal structure of eukaryotic ribosome and its complexes with inhibitors. *Philos. Trans. R. Soc. Lond. B Biol. Sci.* **372**(2017).

11. Melnikov, S., Ben-Shem, A., Garreau de Loubresse, N., Jenner, L., Yusupova, G. & Yusupov, M. One core, two shells: bacterial and eukaryotic ribosomes. *Nat. Struct. Mol. Biol.* **19**, 560-567 (2012).

12. Reuveni, S., Ehrenberg, M. & Paulsson, J. Ribosomes are optimized for autocatalytic production. *Nature* **547**, 293-297 (2017).

13. Tye, B.W., Commins, N., Ryazanova, L.V., Wuhr, M., Springer, M., Pincus, D. & Churchman, L.S. Proteotoxicity from aberrant ribosome biogenesis compromises cell fitness. *eLife* **8**, e43002 (2019).

14. Pillet, B., Mitterer, V., Kressler, D. & Pertschy, B. Hold on to your friends: Dedicated chaperones of ribosomal proteins: dedicated chaperones mediate the safe transfer of ribosomal proteins to their site of pre-ribosome incorporation. *Bioessays* **39**, 1-12 (2017).

15. Sung, M.K., Porras-Yakushi, T.R., Reitsma, J.M., Huber, F.M., Sweredoski, M.J., Hoelz, A., Hess, S. & Deshaies, R.J. A conserved quality-control pathway that mediates degradation of unassembled ribosomal proteins. *eLife* **5**, e19105 (2016).

16. Sung, M.K., Reitsma, J.M., Sweredoski, M.J., Hess, S. & Deshaies, R.J. Ribosomal proteins produced in excess are degraded by the ubiquitin-proteasome system. *Mol. Biol. Cell* **27**, 2642-2652 (2016).

17. Lafontaine, D.L. A 'garbage can' for ribosomes: how eukaryotes degrade their ribosomes. *Trends Biochem. Sci.* **35**, 267-277 (2010).

18. Cole, S.E., LaRiviere, F.J., Merrikh, C.N. & Moore, M.J. A convergence of rRNA and mRNA quality control pathways revealed by mechanistic analysis of nonfunctional rRNA decay. *Mol. Cell* **34**, 440-450 (2009).

19. Grousl, T., Ivanov, P., Frydlova, I., Vasicova, P., Janda, F., Vojtova, J., Malinska, K., Malcova, I., Novakova, L., Janoskova, D., Valasek, L. & Hasek, J. Robust heat shock induces eIF2alpha-phosphorylation-independent assembly of stress granules containing eIF3 and 40S ribosomal subunits in budding yeast, *Saccharomyces cerevisiae*. *J. Cell. Sci.* **122**, 2078-2088 (2009).

20. Fujii, K., Kitabatake, M., Sakata, T., Miyata, A. & Ohno, M. A role for ubiquitin in the clearance of nonfunctional rRNAs. *Genes Dev.* **23**, 963-974 (2009).

21. Fujii, K., Kitabatake, M., Sakata, T. & Ohno, M. 40S subunit dissociation and proteasome-dependent RNA degradation in nonfunctional 25S rRNA decay. *EMBO J.* **31**, 2579-2589 (2012).

22. Kraft, C., Deplazes, A., Sohrmann, M. & Peter, M. Mature ribosomes are selectively degraded upon starvation by an autophagy pathway requiring the Ubp3p/Bre5p ubiquitin protease. *Nat. Cell Biol.* **10**, 602-610 (2008).

23. Heeseon An, H. & Harper, J.W. Ribosome abundance control via the ubiquitin-proteasome system and autophagy. *J. Mol. Biol.* **432**, 170-184 (2020).

24. Melnikov, S., Manakongtreecheep, K. & Soll, D. Revising the structural diversity of ribosomal proteins across the three domains of life. *Mol. Biol. Evol.* **35**, 1588-1598 (2018).

25. Pausch, P., Singh, U., Ahmed, Y.L., Pillet, B., Murat, G., Altegoer, F., Stier, G., Thoms, M., Hurt, E., Sinning, I., Bange, G. & Kressler, D. Co-translational capturing of nascent ribosomal proteins by their dedicated chaperones. *Nat. Commun.* **6**, 7494 (2015).

26. Fernández-Pevida, A., Martín-Villanueva, S., Murat, G., Lacombe, T., Kressler, D. & de la Cruz, J. The eukaryote-specific N-terminal extension of ribosomal protein S31 contributes to the assembly and function of 40S ribosomal subunits. *Nucleic Acids Res.* **44**, 7777-7791 (2016).

27. Mazumder, B., Sampath, P., Seshadri, V., Maitra, R.K., DiCorleto, P.E. & Fox, P.L. Regulated release of L13a from the 60S ribosomal subunit as a mechanism of transcript-specific translational control. *Cell* **115**, 187-198 (2003).

28. Deisenroth, C. & Zhang, Y. Ribosome biogenesis surveillance: probing the ribosomal protein-Mdm2-p53 pathway. *Oncogene* **29**, 4253-4260 (2010).

29. Kellis, M., Birren, B.W. & Lander, E.S. Proof and evolutionary analysis of ancient genome duplication in the yeast *Saccharomyces cerevisiae*. *Nature* **428**, 617-624 (2004).

30. Steffen, K.K., McCormick, M.A., Pham, K.M., Mackay, V.L., Delaney, J.R., Murakami, C.J., Kaeberlein, M. & Kennedy, B.K. Ribosome deficiency protects against ER stress in *Saccharomyces cerevisiae*. *Genetics* **191**, 107-118 (2012).

31. Ghulam, M.M., Catala, M. & Abou Elela, S. Differential expression of duplicated ribosomal protein genes modifies ribosome composition in response to stress. *Nucleic Acids Res.* **48**, 1954-1968 (2020).

32. Lu, H., Zhu, Y.F., Xiong, J., Wang, R. & Jia, Z. Potential extra-ribosomal functions of ribosomal proteins in *Saccharomyces cerevisiae*. *Microbiol Res* **177**, 28-33 (2015).

33. Genuth, N.R. & Barna, M. The discovery of ribosome heterogeneity and its implications for gene regulation and organismal life. *Mol. Cell* **71**, 364-374 (2018).

34. Ban, N. *et al.* A new system for naming ribosomal proteins. *Curr. Opin. Struct. Biol.* **24**, 165-169 (2014).

35. Warner, J.R. The economics of ribosome biosynthesis in yeast. *Trends Biochem. Sci.* **24**, 437-440 (1999).

36. Woolford, J.L., Jr. & Baserga, S.J. Ribosome biogenesis in the yeast *Saccharomyces cerevisiae*. *Genetics* **195**, 643-681 (2013).

37. Kobayashi, T. Regulation of ribosomal RNA gene copy number and its role in modulating genome integrity and evolutionary adaptability in yeast. *Cell Mol. Life Sci.* **68**, 1395-1403 (2011).

38. Klinge, S. & Woolford, J.L., Jr. Ribosome assembly coming into focus. *Nat. Rev. Mol. Cell. Biol.* **20**, 116-131 (2019).

39. Tartakoff, A.M., Chen, L., Raghavachari, S., Gitiforooz, D., Dhinakaran, A., Ni, C.L., Pasadyn, C., Mahabeleshwar, G.H., Pasadyn, V. & Woolford, J.L., Jr. The nucleolus as a polarized coaxial cable in which the rDNA axis is surrounded by dynamic subunit-specific phases. *Curr. Biol.* **31**, 2507-2519 (2021).

40. Kressler, D., Hurt, E. & Bassler, J. A puzzle of life: crafting ribosomal subunits. *Trends Biochem. Sci.* **42**, 640-654 (2017).

41. de la Cruz, J., Gómez-Herreros, F., Rodríguez-Galán, O., Begley, V., Muñoz-Centeno, M.C. & Chávez, S. Feedback regulation of ribosome assembly. *Curr. Genet.* **64**, 393-404 (2018).

42. Kampen, K.R., Sulima, S.O., Vereecke, S. & De Keersmaecker, K. Hallmarks of ribosomopathies. *Nucleic Acids Res.* **48**, 1013-1028 (2020).

43. Farley-Barnes, K.I., Ogawa, L.M. & Baserga, S.J. Ribosomopathies: old concepts, new controversies. *Trends Genet* **35**, 754-767 (2019).

44. Fernández-Pevida, A., Kressler, D. & de la Cruz, J. Processing of preribosomal RNA in *Saccharomyces cerevisiae*. *Wiley Interdiscip. Rev. RNA* **6**, 191-209 (2015).

45. Koš, M. & Tollervey, D. Yeast pre-rRNA processing and modification occur cotranscriptionally. *Mol. Cell* **37**, 809-820 (2010).

46. Horn, D.M., Mason, S.L. & Karbstein, K. Rcl1 protein, a novel nuclease for 18 S ribosomal RNA production. *J. Biol. Chem.* **286**, 34082-34087 (2011).

47. Wells, G.R., Weichmann, F., Colvin, D., Sloan, K.E., Kudla, G., Tollervey, D., Watkins, N.J. & Schneider, C. The PIN domain endonuclease Utp24 cleaves pre-ribosomal RNA at two coupled sites in yeast and humans. *Nucleic Acids Res.* **44**, 5399-5409 (2016).

48. Cheng, J., Lau, B., La Venuta, G., Ameismeier, M., Berninghausen, O., Hurt, E. & Beckmann, R. 90S pre-ribosome transformation into the primordial 40S subunit. *Science* **369**, 1470-1476 (2020).

49. Henras, A.K., Plisson-Chastang, C., O'Donohue, M.F., Chakraborty, A. & Gleizes, P.E. An overview of pre-ribosomal RNA processing in eukaryotes. *Wiley Interdiscip. Rev. RNA* **6**, 225-242 (2015).

50. Lamanna, A.C. & Karbstein, K. Nob1 binds the single-stranded cleavage site D at the 3'-end of 18S rRNA with its PIN domain. *Proc. Natl. Acad. Sci. USA* **106**, 14259-14264 (2009).

51. Pertschy, B., Schneider, C., Gnadig, M., Schafer, T., Tollervey, D. & Hurt, E. RNA helicase Prp43 and its co-factor Pfa1 promote 20 to 18 S rRNA processing catalyzed by the endonuclease Nob1. *J. Biol. Chem.* **284**, 35079-35091 (2009).

52. Lebaron, S., Schneider, C., van Nues, R.W., Swiatkowska, A., Walsh, D., Bottcher, B., Granneman, S., Watkins, N.J. & Tollervey, D. Proofreading of pre-40S ribosome maturation by a translation initiation factor and 60S subunits. *Nat. Struct. Mol. Biol.* **19**, 744-753 (2012).

53. Strunk, B.S., Novak, M.N., Young, C.L. & Karbstein, K. A translation-like cycle is a quality control checkpoint for maturing 40S ribosome subunits. *Cell* **150**, 111-121 (2012).

54. García-Gómez, J.J., Fernández-Pevida, A., Lebaron, S., Rosado, I.V., Tollervey, D., Kressler, D. & de la Cruz, J. Final pre-40S maturation depends on the functional integrity of the 60S subunit ribosomal protein L3. *PLoS Genet.* **10**, e1004205 (2014).

55. Kos-Braun, I.C. & Koš, M. Post-transcriptional regulation of ribosome biogenesis in yeast. *Microbial Cell* **4**, 179-181 (2016).

56. Oeffinger, M., Zenklusen, D., Ferguson, A., Wei, K.E., El Hage, A., Tollervey, D., Chait, B.T., Singer, R.H. & Rout, M.P. Rrp17p is a eukaryotic exonuclease required for 5' end processing of pre-60S ribosomal RNA. *Mol. Cell* **36**, 768-781 (2009).

57. Johnson, A.W. Rat1p and Xrn1p are functionally interchangeable exoribonucleases that are restricted to and required in the nucleus and cytoplasm, respectively. *Mol. Cell. Biol.* **17**, 6122-6130 (1997).

58. El Hage, A., Koper, M., Kufel, J. & Tollervey, D. Efficient termination of transcription by RNA polymerase I requires the 5' exonuclease Rat1 in yeast. *Genes Dev.* **22**, 1069-1081 (2008).

59. Gasse, L., Flemming, D. & Hurt, E. Coordinated ribosomal ITS2 RNA processing by the Las1 complex integrating endonuclease, polynucleotide kinase, and exonuclease activities. *Mol. Cell* **60**, 808-815 (2015).

60. Fromm, L., Falk, S., Flemming, D., Schuller, J.M., Thoms, M., Conti, E. & Hurt, E. Reconstitution of the complete pathway of ITS2 processing at the pre-ribosome. *Nat. Commun.* **8**, 1787 (2017).

61. Allmang, C., Kufel, J., Chanfreau, G., Mitchell, P., Petfalski, E. & Tollervey, D. Functions of the exosome in rRNA, snoRNA and snRNA synthesis. *EMBO J.* **18**, 5399-5410 (1999).

62. van Hoof, A., Lennertz, P. & Parker, R. Three conserved members of the RNase D family have unique and overlapping functions in the processing of 5S, 5.8S, U4, U5, RNase MRP and RNase P RNAs in yeast. *EMBO J.* **19**, 1357-1365 (2000).

63. Faber, A.W., Van Dijk, M., Raué, H.A. & Vos, J.C. Ngl2p is a Ccr4p-like RNA nuclease essential for the final step in 3'- end processing of 5.8S rRNA in *Saccharomyces cerevisiae*. *RNA* **8**, 1095-1101 (2002).

64. Thomson, E. & Tollervey, D. The final step in 5.8S rRNA processing is cytoplasmic in *Saccharomyces cerevisiae*. *Mol. Cell. Biol.* **30**, 976-984 (2010).

65. Ciganda, M. & Williams, N. Eukaryotic 5S rRNA biogenesis. *Wiley Interdiscip. Rev. RNA* **2**, 523-533 (2011).

66. Sharma, S. & Lafontaine, D.L.J. 'View from a bridge': a new perspective on eukaryotic rRNA base modification. *Trends Biochem. Sci.* **40**, 560-575 (2015).

67. Ojha, S., Malla, S. & Lyons, S.M. snoRNPs: functions in ribosome biogenesis. *Biomolecules* **10**, 783 (2020).

68. Decatur, W.A. & Fournier, M.J. rRNA modifications and ribosome function. *Trends Biochem. Sci.* **27**, 344-351 (2002).

69. Liang, X.H., Liu, Q. & Fournier, M.J. Loss of rRNA modifications in the decoding center of the ribosome impairs translation and strongly delays pre-rRNA processing. *RNA* **15**, 1716-1728 (2009).

70. Rodríguez-Galán, O., García-Gómez, J.J. & de la Cruz, J. Yeast and human RNA helicases involved in ribosome biogenesis: current status and perspectives. *Biochim. Biophys. Acta-Gene Regulatory Mechanisms* **1829**, 775-790 (2013).

71. Pérez-Fernández, J., Román, A., de las Rivas, J., Bustelo, X.R. & Dosil, M. The 90S preribosome is a multimodular structure that is assembled through a hierarchical mechanism. *Mol. Cell. Biol.* **27**, 5414-5429 (2007).

72. Hunziker, M., Barandun, J., Petfalski, E., Tan, D., Delan-Forino, C., Molloy, K.R., Kim, K.H., Dunn-Davies, H., Shi, Y., Chaker-Margot, M., Chait, B.T., Walz, T., Tollervey, D. & Klinge, S. UtpA and UtpB chaperone nascent pre-ribosomal RNA and U3 snoRNA to initiate eukaryotic ribosome assembly. *Nat. Commun.* **7**, 12090 (2016).

73. Zhang, L., Wu, C., Cai, G., Chen, S. & Ye, K. Stepwise and dynamic assembly of the earliest precursors of small ribosomal subunits in yeast. *Genes Dev.* **30**, 718-732 (2016).

74. Chaker-Margot, M., Hunziker, M., Barandun, J., Dill, B.D. & Klinge, S. Stage-specific assembly events of the 6-MDa small-subunit processome initiate eukaryotic ribosome biogenesis. *Nat. Struct. Mol. Biol.* **22**, 920-923 (2015).

75. Kornprobst, M., Turk, M., Kellner, N., Cheng, J., Flemming, D., Kos-Braun, I., Kos, M., Thoms, M., Berninghausen, O., Beckmann, R. & Hurt, E. Architecture of the 90S pre-ribosome: a structural view on the birth of the eukaryotic ribosome. *Cell* **166**, 380-393 (2016).

76. Cheng, J., Kellner, N., Berninghausen, O., Hurt, E. & Beckmann, R. 3.2-Å-resolution structure of the 90S preribosome before A1 pre-rRNA cleavage. *Nat Struct Mol Biol* **24**, 954-964 (2017).

77. Bassler, J. & Hurt, E. Eukaryotic ribosome assembly. *Annu. Rev. Biochem.* **88**, 281-306 (2019).

78. Lau, B., Cheng, J., Flemming, D., La Venuta, G., Berninghausen, O., Beckmann, R. & Hurt, E. Structure of the maturing 90S pre-ribosome in association with the RNA Exosome. *Mol. Cell* **81**, 293-303 (2021).

79. Ismail, S., Flemming, D., Thoms, M., Gomes-Filho, J.V., Randau, L., Beckmann, R. & Hurt, E. Emergence of the primordial pre-60S from the 90S pre-ribosome. *Cell Rep* **39**, 110640 (2022).

80. Chaker-Margot, M. Assembly of the small ribosomal subunit in yeast: mechanism and regulation. *RNA* **24**, 881-891 (2018).

81. Johnson, M.C., Ghalei, H., Doxtader, K.A., Karbstein, K. & Stroupe, M.E. Structural heterogeneity in pre-40S ribosomes. *Structure* **25**, 329-340 (2017).

82. Heuer, A., Thomson, E., Schmidt, C., Berninghausen, O., Becker, T., Hurt, E. & Beckmann, R. Cryo-EM structure of a late pre-40S ribosomal subunit from *Saccharomyces cerevisiae*. *eLife* **6**, e30189 (2017).

83. Scaiola, A., Pena, C., Weisser, M., Bohringer, D., Leibundgut, M., Klingauf-Nerurkar, P., Gerhardy, S., Panse, V.G. & Ban, N. Structure of a eukaryotic cytoplasmic pre-40S ribosomal subunit. *EMBO J.* **37**, e98499 (2018).

84. Fung, H.Y., Fu, S.C., Brautigam, C.A. & Chook, Y.M. Structural determinants of nuclear export signal orientation in binding to exportin CRM1. *Elife* **4**, e10034 (2015).

85. Oeffinger, M., Dlakic, M. & Tollervey, D. A pre-ribosome-associated HEAT-repeat protein is required for export of both ribosomal subunits. *Genes Dev.* **18**, 196-209 (2004).

86. Faza, M.B., Chang, Y., Occhipinti, L., Kemmler, S. & Panse, V.G. Role of Mex67-Mtr2 in the nuclear export of 40S pre-ribosomes. *PLoS Genet.* **8**, e1002915 (2012).

87. Karbstein, K. Quality control mechanisms during ribosome maturation. *Trends Cell Biol.* **23**, 242-250 (2013).

88. Turowski, T.W., Lebaron, S., Zhang, E., Peil, L., Dudnakova, T., Petfalski, E., Granneman, S., Rappsilber, J. & Tollervey, D. Rio1 mediates ATP-dependent final maturation of 40S ribosomal subunits. *Nucleic Acids Res.* **42**, 12189-12199 (2014).

89. Ferreira-Cerca, S., Kiburu, I., Thomson, E., LaRonde, N. & Hurt, E. Dominant Rio1 kinase/ATPase catalytic mutant induces trapping of late pre-40S biogenesis factors in 80S-like ribosomes. *Nucleic Acids Res.* **42**, 8635-8647 (2014).

90. Jenner, L., Melnikov, S., de Loubresse, N.G., Ben-Shem, A., Iskakova, M., Urzhumtsev, A., Meskauskas, A., Dinman, J., Yusupova, G. & Yusupov, M. Crystal structure of the 80S yeast ribosome. *Curr. Opin. Struct. Biol.* **22**, 759-767 (2012).

91. Ohmayer, U., Gamalinda, M., Sauert, M., Ossowski, J., Pöll, G., Linnemann, J., Hierlmeier, T., Pérez-Fernández, J., Kumcuoglu, B., Léger-Silvestre, I., Faubladier, M., Griesenbeck, J., Woolford, J., Tschochner, H. & Milkereit, P. Studies on the assembly characteristics of large subunit ribosomal proteins in *S. cerevisae*. *PLoS One* **8**, e68412 (2013).

92. Kater, L., Thoms, M., Barrio-García, C., Cheng, J., Ismail, S., Ahmed, Y.L., Bange, G., Kressler, D., Berninghausen, O., Sinning, I., Hurt, E. & Beckmann, R. Visualizing the assembly pathway of nucleolar pre-60S ribosomes. *Cell* **171**, 1599-1610 (2017).

93. Sanghai, Z.A., Miller, L., Molloy, K.R., Barandun, J., Hunziker, M., Chaker-Margot, M., Wang, J., Chait, B.T. & Klinge, S. Modular assembly of the nucleolar pre-60S ribosomal subunit. *Nature* **556**, 126-129 (2018).

94. Davis, J.H., Tan, Y.Z., Carragher, B., Potter, C.S., Lyumkis, D. & Williamson, J.R. Modular assembly of the bacterial large ribosomal subunit. *Cell* **167**, 1610-1622 (2016).

95. Eppens, N.A., Rensen, S., Granneman, S., Raué, H.A. & Venema, J. The roles of Rrp5p in the synthesis of yeast 18S and 5.8S rRNA can be functionally and physically separated. *RNA* **5**, 779-793 (1999).

96. Hierlmeier, T. *et al.* Rrp5p, Noc1p and Noc2p form a protein module which is part of early large ribosomal subunit precursors in S. cerevisiae. *Nucleic Acids Res.* **41**, 1191-1210 (2012).

97. Lebaron, S., Segerstolpe, A., French, S.L., Dudnakova, T., de Lima Alves, F., Granneman, S., Rappsilber, J., Beyer, A.L., Wieslander, L. & Tollervey, D. Rrp5 binding at multiple sites coordinates pre-rRNA processing and assembly. *Mol. Cell* **52**, 707-719 (2013).

98. Rosado, I.V., Dez, C., Lebaron, S., Caizergues-Ferrer, M., Henry, Y. & de la Cruz, J. Characterization of *Saccharomyces cerevisiae* Npa2p (Urb2p) reveals a low-molecular-mass complex containing Dbp6p, Npa1p (Urb1p), Nop8p, and Rsa3p involved in early steps of 60S ribosomal subunit biogenesis. *Mol. Cell. Biol.* **27**, 1207-1221 (2007).

99. Joret, C., Capeyrou, R., Belhabich-Baumas, K., Plisson-Chastang, C., Ghandour, R., Humbert, O., Fribourg, S., Leulliot, N., Lebaron, S., Henras, A.K. & Henry, Y. The Npa1p complex chaperones the assembly of the earliest eukaryotic large ribosomal subunit precursor. *PLoS Genet.* **14**, e1007597 (2018).

100. Bhutada, P. *et al.* Rbp95 binds to 25S rRNA helix H95 and cooperates with the Npa1 complex during early pre-60S particle maturation. *Nucleic Acids Res.* **50**, 10053–10077 (2022).

101. Jaafar, M. *et al.* Association of snR190 snoRNA chaperone with early pre-60S particles is regulated by the RNA helicase Dbp7 in yeast. *Nat. Commun.* **12**, 6153 (2021).

102. Zhou, D., Zhu, X., Zheng, S., Tan, D., Dong, M.Q. & Ye, K. Cryo-EM structure of an early precursor of large ribosomal subunit reveals a half-assembled intermediate. *Protein Cell* **10**, 120-130 (2019).

103. Lo, Y.H., Romes, E.M., Pillon, M.C., Sobhany, M. & Stanley, R.E. Structural analysis reveals features of ribosome assembly factor Nsa1/WDR74 Important for localization and interaction with Rix7/NVL2. *Structure* **25**, 762-772 (2017).

104. Kressler, D., Roser, D., Pertschy, B. & Hurt, E. The AAA ATPase Rix7 powers progression of ribosome biogenesis by stripping Nsa1 from pre-60S particles. *J. Cell Biol.* **181**, 935-944 (2008).

105. Miles, T.D., Jakovljevic, J., Horsey, E.W., Harnpicharnchai, P., Tang, L. & Woolford, J.L., Jr. Ytm1, Nop7, and Erb1 form a complex necessary for maturation of yeast 66S preribosomes. *Mol. Cell. Biol.* **25**, 10419-10432 (2005).

106. Dembowski, J.A., Ramesh, M., McManus, C.J. & Woolford, J.L., Jr. Identification of the binding site of Rlp7 on assembling 60S ribosomal subunits in *Saccharomyces cerevisiae*. *RNA* **19**, 1639-1647 (2013).

107. Dembowski, J.A., Kuo, B. & Woolford, J.L., Jr. Has1 regulates consecutive maturation and processing steps for assembly of 60S ribosomal subunits. *Nucleic Acids Res.* **41**, 7889-7904 (2013).

108. Oeffinger, M. & Tollervey, D. Yeast Nop15p is an RNA-binding protein required for pre-rRNA processing and cytokinesis. *EMBO J.* **22**, 6573-6583 (2003).

109. Fatica, A., Oeffinger, M., Tollervey, D. & Bozzoni, I. Cic1p/Nsa3p is required for synthesis and nuclear export of 60S ribosomal subunits. *RNA* **9**, 1431-1436 (2003).

110. Tang, L., Sahasranaman, A., Jakovljevic, J., Schleifman, E. & Woolford, J.L., Jr. Interactions among Ytm1, Erb1, and Nop7 required for assembly of the Nop7-subcomplex in yeast preribosomes. *Mol. Biol. Cell* **19**, 2844-2856 (2008).

111. Thoms, M., Ahmed, Y.L., Maddi, K., Hurt, E. & Sinning, I. Concerted removal of the Erb1-Ytm1 complex in ribosome biogenesis relies on an elaborate interface. *Nucleic Acids Res.* **44**, 926-939 (2016).

112. Wegrecki, M., Neira, J.L. & Bravo, J. The carboxy-terminal domain of Erb1 is a seven-bladed β-propeller that binds RNA. *PLoS One* **10**, e0123463 (2015).

113. Konikkat, S., Biedka, S. & Woolford, J.L., Jr. The assembly factor Erb1 functions in multiple remodeling events during 60S ribosomal subunit assembly in *S. cerevisiae*. *Nucleic Acids Res.* **45**, 4853–4865 (2017).

114. Talkish, J., Zhang, J., Jakovljevic, J., Horsey, E.W. & Woolford, J.L., Jr. Hierarchical recruitment into nascent ribosomes of assembly factors required for 27SB pre-rRNA processing in *Saccharomyces cerevisiae*. *Nucleic Acids Res.* **40**, 8646-8661 (2012).

115. Wu, S., Tutuncuoglu, B., Yan, K., Brown, H., Zhang, Y., Tan, D., Gamalinda, M., Yuan, Y., Li, Z., Jakovljevic, J., Ma, C., Lei, J., Dong, M.Q., Woolford, J.L., Jr. & Gao, N. Diverse roles of assembly factors revealed by structures of late nuclear pre-60S ribosomes. *Nature* **534**, 133-137 (2016).

116. Bassler, J. *et al.* A network of assembly factors is involved in remodeling rRNA elements during preribosome maturation. *J. Cell Biol.* **207**, 481-498 (2015).

117. Lebreton, A., Saveanu, C., Decourty, L., Jacquier, A. & Fromont-Racine, M. Nsa2 is an unstable, conserved factor required for the maturation of 27SB pre-rRNAs. *J. Biol. Chem.* **281**, 27099-27108 (2006).

118. de la Cruz, J., Sanz-Martínez, E. & Remacha, M. The essential WD-repeat protein Rsa4p is required for rRNA processing and intra-nuclear transport of 60S ribosomal subunits. *Nucleic Acids Res.* **33**, 5728-5739 (2005).

119. Saveanu, C., Bienvenu, D., Namane, A., Gleizes, P.E., Gas, N., Jacquier, A. & Fromont-Racine, M. Nog2p, a putative GTPase associated with pre-60S subunits and required for late 60S maturation steps. *EMBO J.* **20**, 6475-6484 (2001).

120. Bassler, J., Kallas, M. & Hurt, E. The NUG1 GTPase reveals and N-terminal RNA-binding domain that is essential for association with 60 S pre-ribosomal particles. *J. Biol. Chem.* **281**, 24737-24744 (2006).

121. Leidig, C., Thoms, M., Holdermann, I., Bradatsch, B., Berninghausen, O., Bange, G., Sinning, I., Hurt, E. & Beckmann, R. 60S ribosome biogenesis requires rotation of the 5S ribonucleoprotein particle. *Nat. Commun.* **5**, 3491 (2014).

122. Konikkat, S. & Woolford, J.L., Jr. Principles of 60S ribosomal subunit assembly emerging from recent studies in yeast. *Biochem J.* **474**, 195-214 (2017).

123. Kater, L., Mitterer, V., Thoms, M., Cheng, J., Berninghausen, O., Beckmann, R. & Hurt, E. Construction of the central protuberance and L1 stalk during 60S subunit biogenesis. *Mol. Cell* **79**, 615-628.e5 (2020).

124. Bassler, J., Kallas, M., Pertschy, B., Ulbrich, C., Thoms, M. & Hurt, E. The AAA-ATPase Rea1 drives removal of biogenesis factors during multiple stages of 60S ribosome assembly. *Mol. Cell* **38**, 712-721 (2010).

125. Thoms, M., Thomson, E., Bassler, J., Gnädig, M., Griesel, S. & Hurt, E. The exosome is recruited to RNA substrates through specific adaptor proteins. *Cell* **162**, 1029-1038 (2015).

126. Biedka, S., Wu, S., LaPeruta, A.J., Gao, N. & Woolford, J.L., Jr. Insights into remodeling events during eukaryotic large ribosomal subunit assembly provided by high resolution cryo-EM structures. *RNA Biol.* (2017).

127. Fuentes, J.L., Datta, K., Sullivan, S.M., Walker, A. & Maddock, J.R. *In vivo* functional characterization of the *Saccharomyces cerevisiae* 60S biogenesis GTPase Nog1. *Mol. Genet. Genomics* **278**, 105-123 (2007).

128. Lapik, Y.R., Misra, J.M., Lau, L.F. & Pestov, D.G. Restricting conformational flexibility of the switch II region creates a dominant-inhibitory phenotype in Obg GTPase Nog1. *Mol Cell. Biol.* **27**, 7735-7744 (2007).

129. Greber, B.J., Gerhardy, S., Leitner, A., Leibundgut, M., Salem, M., Boehringer, D., Leulliot, N., Aebersold, R., Panse, V.G. & Ban, N. Insertion of the biogenesis factor Rei1 probes the ribosomal tunnel during 60S maturation. *Cell* **164**, 91-102 (2016).

130. Ma, C., Wu, S., Li, N., Chen, Y., Yan, K., Li, Z., Zheng, L., Lei, J., Woolford, J.L., Jr. & Gao, N. Structural snapshot of cytoplasmic pre-60S ribosomal particles bound by Nmd3, Lsg1, Tif6 and Reh1. *Nat. Struct. Mol. Biol.* **24**, 214-220 (2017).

131. Zhang, J., Harnpicharnchai, P., Jakovljevic, J., Tang, L., Guo, Y., Oeffinger, M., Rout, M.P., Hiley, S.L., Hughes, T. & Woolford, J.L., Jr. Assembly factors Rpf2 and Rrs1 recruit 5S rRNA and ribosomal proteins rpL5 and rpL11 into nascent ribosomes. *Genes Dev.* **21**, 2580-2592 (2007).

132. Kressler, D., Bange, G., Ogawa, Y., Stjepanovic, G., Bradatsch, B., Pratte, D., Amlacher, S., Strauss, D., Yoneda, Y., Katahira, J., Sinning, I. & Hurt, E. Synchronizing nuclear import of ribosomal proteins with ribosome assembly. *Science* **338**, 666-671 (2012).

133. Calviño, F.R., Kharde, S., Ori, A., Hendricks, A., Wild, K., Kressler, D., Bange, G., Hurt, E., Beck, M. & Sinning, I. Symportin 1 chaperones 5S RNP assembly during ribosome biogenesis by occupying an essential rRNA-binding site. *Nat. Commun.* **6**, 6510 (2015).

134. Barrio-García, C., Thoms, M., Flemming, D., Kater, L., Berninghausen, O., Bassler, J., Beckmann, R. & Hurt, E. Architecture of the Rix1-Rea1 checkpoint machinery during pre-60S-ribosome remodeling. *Nat. Struct. Mol. Biol.* **23**, 37-44 (2016).

135. Pillon, M.C., Sobhany, M., Borgnia, M.J., Williams, J.G. & Stanley, R.E. Grc3 programs the essential endoribonuclease Las1 for specific RNA cleavage. *Proc. Natl. Acad. Sci. USA* **114**, E5530-E5538 (2017).

136. Pillon, M.C., Sobhany, M. & Stanley, R.E. Characterization of the molecular crosstalk within the essential Grc3/Las1 pre-rRNA processing complex. *RNA* **24**, 721-738 (2018).

137. Castle, C.D., Sardana, R., Dandekar, V., Borgianini, V., Johnson, A.W. & Denicourt, C. Las1 interacts with Grc3 polynucleotide kinase and is required for ribosome synthesis in *Saccharomyces cerevisiae*. *Nucleic Acids Res.* **41**, 1135-1150 (2013).

138. Schillewaert, S., Wacheul, L., Lhomme, F. & Lafontaine, D.L. The evolutionarily conserved protein Las1 is required for pre-rRNA processing at both ends of ITS2. *Mol. Cell. Biol.* **32**, 430-444 (2011).

139. Falk, S., Tants, J.N., Basquin, J., Thoms, M., Hurt, E., Sattler, M. & Conti, E. Structural insights into the interaction of the nuclear exosome helicase Mtr4 with the preribosomal protein Nop53. *RNA* **23**, 1780-1787 (2017).

140. Jackson, R.N., Klauer, A.A., Hintze, B.J., Robinson, H., van Hoof, A. & Johnson, S.J. The crystal structure of Mtr4 reveals a novel arch domain required for rRNA processing. *EMBO J.* **29**, 2205-2216 (2010).

141. Schuch, B., Feigenbutz, M., Makino, D.L., Falk, S., Basquin, C., Mitchell, P. & Conti, E. The exosome-binding factors Rrp6 and Rrp47 form a composite surface for recruiting the Mtr4 helicase. *EMBO J.* **33**, 2829-2846 (2014).

142. Kilchert, C., Wittmann, S. & Vasiljeva, L. The regulation and functions of the nuclear RNA exosome complex. *Nat. Rev. Mol. Cell. Biol.* **17**, 227-239 (2016).

143. LaCava, J., Houseley, J., Saveanu, C., Petfalski, E., Thompson, E., Jacquier, A. & Tollervey, D. RNA degradation by the exosome is promoted by a nuclear polyadenylation complex. *Cell* **121**, 713-724 (2005).

144. de la Cruz, J., Kressler, D., Tollervey, D. & Linder, P. Dob1p (Mtr4p) is a putative ATP-dependent RNA helicase required for the 3' end formation of 5.8S rRNA in *Saccharomyces cerevisiae*. *EMBO J.* **17**, 1128-1140 (1998).

145. Jankowsky, E. RNA helicases at work: binding and rearranging. *Trends Biochem. Sci.* **36**, 19-29 (2011).

146. Schuller, J.M., Falk, S., Fromm, L., Hurt, E. & Conti, E. Structure of the nuclear exosome captured on a maturing preribosome. *Science* **360**, 219-222 (2018).

147. Manikas, R.G., Thomson, E., Thoms, M. & Hurt, E. The K^+-dependent GTPase Nug1 is implicated in the association of the helicase Dbp10 to the immature peptidyl transferase centre during ribosome maturation. *Nucleic Acids Res.* **44**, 1800-1812 (2016).

148. Matsuo, Y., Granneman, S., Thoms, M., Manikas, R.G., Tollervey, D. & Hurt, E. Coupled GTPase and remodelling ATPase activities form a checkpoint for ribosome export. *Nature* **505**, 112-116 (2014).

149. Oeffinger, M. Joining the interface: a site for Nmd3 association on 60S ribosome subunits. *J. Cell Biol.* **189**, 1071-1073 (2010).

150. Sarkar, A., Pech, M., Thoms, M., Beckmann, R. & Hurt, E. Ribosome-stalk biogenesis is coupled with recruitment of nuclear-export factor to the nascent 60S subunit. *Nat. Struct. Mol. Biol.* **23**, 1074-1082 (2016).

151. Nerurkar, P., Altvater, M., Gerhardy, S., Schütz, S., Fischer, U., Weirich, C. & Panse, V.G. Eukaryotic ribosome assembly and nuclear export. *Int. Rev. Cell Mol. Biol.* **319**, 107-140 (2015).

152. Ho, J.H.-N., Kallstrom, G. & Johnson, A.W. Nascent 60S ribosomal subunits enter the free pool bound by Nmd3p. *RNA* **6**, 1625-1634 (2000).

153. Ho, J.H.-N., Kallstrom, G. & Johnson, A.W. Nmd3p is a Crm1p-dependent adapter protein for nuclear export of the large ribosomal subunit. *J. Cell Biol.* **151**, 1057-1066 (2000).

154. Sengupta, J., Bussiere, C., Pallesen, J., West, M., Johnson, A.W. & Frank, J. Characterization of the nuclear export adaptor protein Nmd3 in association with the 60S ribosomal subunit. *J. Cell Biol.* **189**, 1079-1086 (2010).

155. Hung, N.J., Lo, K.Y., Patel, S.S., Helmke, K. & Johnson, A.W. Arx1 is a nuclear export receptor for the 60S ribosomal subunit in yeast. *Mol. Biol. Cell* **19**, 735-744 (2008).

156. Yao, Y., Demoinet, E., Saveanu, C., Lenormand, P., Jacquier, A. & Fromont-Racine, M. Ecm1 is a new pre-ribosomal factor involved in pre-60S particle export. *RNA* **16**, 1007-1017 (2010).

157. Bradatsch, B., Katahira, J., Kowalinski, E., Bange, G., Yao, W., Sekimoto, T., Baumgartel, V., Boese, G., Bassler, J., Wild, K., Peters, R., Yoneda, Y., Sinning, I. & Hurt, E. Arx1 functions as an unorthodox nuclear export receptor for the 60S preribosomal subunit. *Mol. Cell* **27**, 767-779 (2007).

158. Bassler, J., Klein, I., Schmidt, C., Kallas, M., Thomson, E., Wagner, M.A., Bradatsch, B., Rechberger, G., Strohmaier, H., Hurt, E. & Bergler, H. The

conserved Bud20 zinc finger protein is a new component of the ribosomal 60S subunit export machinery. *Mol. Cell. Biol.* **32**, 4898-4912 (2012).

159. Hackmann, A., Gross, T., Baierlein, C. & Krebber, H. The mRNA export factor Npl3 mediates the nuclear export of large ribosomal subunits. *EMBO Rep.* **12**, 1024-1031 (2011).

160. Occhipinti, L., Chang, Y., Altvater, M., Menet, A.M., Kemmler, S. & Panse, V.G. Non-FG mediated transport of the large pre-ribosomal subunit through the nuclear pore complex by the mRNA export factor Gle2. *Nucleic Acids Res.* **41**, 8266-8279 (2013).

161. Yao, W., Roser, D., Kohler, A., Bradatsch, B., Bassler, J. & Hurt, E. Nuclear export of ribosomal 60S subunits by the general mRNA export receptor Mex67-Mtr2. *Mol. Cell* **26**, 51-62 (2007).

162. Yao, W., Lutzmann, M. & Hurt, E. A versatile interaction platform on the Mex67-Mtr2 receptor creates an overlap between mRNA and ribosome export. *EMBO J.* **27**, 6-16 (2008).

163. Moriggi, G., Nieto, B. & Dosil, M. Rrp12 and the Exportin Crm1 participate in late assembly events in the nucleolus during 40S ribosomal subunit biogenesis. *PLoS Genet.* **10**, e1004836 (2015).

164. Bradatsch, B., Leidig, C., Granneman, S., Gnadig, M., Tollervey, D., Bottcher, B., Beckmann, R. & Hurt, E. Structure of the pre-60S ribosomal subunit with nuclear export factor Arx1 bound at the exit tunnel. *Nat. Struct. Mol. Biol.* **19**, 1234-1241 (2012).

165. Lo, K.Y., Li, Z., Bussiere, C., Bresson, S., Marcotte, E.M. & Johnson, A.W. Defining the pathway of cytoplasmic maturation of the 60S ribosomal subunit. *Mol. Cell* **39**, 196-208 (2010).

166. Kappel, L., Loibl, M., Zisser, G., Klein, I., Fruhmann, G., Gruber, C., Unterweger, S., Rechberger, G., Pertschy, B. & Bergler, H. Rlp24 activates the AAA-ATPase Drg1 to initiate cytoplasmic pre-60S maturation. *J. Cell Biol.* **199**, 771-782 (2012).

167. Pertschy, B., Saveanu, C., Zisser, G., Lebreton, A., Tengg, M., Jacquier, A., Liebminger, E., Nobis, B., Kappel, L., van der Klei, I., Hogenauer, G., Fromont-Racine, M. & Bergler, H. Cytoplasmic recycling of 60S preribosomal factors depends on the AAA protein Drg1. *Mol. Cell. Biol.* **27**, 6581-6592 (2007).

168. Altvater, M., Chang, Y., Melnik, A., Occhipinti, L., Schütz, S., Rothenbusch, U., Picotti, P. & Panse, V.G. Targeted proteomics reveals compositional dynamics of 60S pre-ribosomes after nuclear export. *Mol. Syst. Biol.* **8**, 628 (2012).

169. Lebreton, A., Saveanu, C., Decourty, L., Rain, J.C., Jacquier, A. & Fromont-Racine, M. A functional network involved in the recycling of nucleocytoplasmic pre-60S factors. *J. Cell Biol.* **173**, 349-360 (2006).

170. Hung, N.J. & Johnson, A.W. Nuclear recycling of the pre-60S ribosomal subunit-associated factor Arx1 depends on Rei1 in *Saccharomyces cerevisiae*. *Mol. Cell. Biol.* **26**, 3718-3727 (2006).

171. Demoinet, E., Jacquier, A., Lutfalla, G. & Fromont-Racine, M. The Hsp40 chaperone Jjj1 is required for the nucleo-cytoplasmic recycling of preribosomal factors in *Saccharomyces cerevisiae*. *RNA* **13**, 1570-1581 (2007).

172. Meyer, A.E., Hoover, L.A. & Craig, E.A. The cytosolic J-protein, Jjj1, and Rei1 function in the removal of the pre-60 S subunit factor Arx1. *J. Biol. Chem.* **285**, 961-968 (2010).

173. Greber, B.J., Boehringer, D., Montellese, C. & Ban, N. Cryo-EM structures of Arx1 and maturation factors Rei1 and Jjj1 bound to the 60S ribosomal subunit. *Nat. Struct. Mol. Biol.* **19**, 1228-1233 (2012).

174. Parnell, K.M. & Bass, B.L. Functional redundancy of yeast proteins Reh1 and Rei1 in cytoplasmic 60S subunit maturation. *Mol. Cell. Biol.* **29**, 4014-4023 (2009).

175. Rodríguez-Mateos, M., Abia, D., García-Gómez, J.J., Morreale, A., de la Cruz, J., Santos, C., Remacha, M. & Ballesta, J.P.G. The amino terminal domain from Mrt4 protein can functionally replace the RNA binding domain of the ribosomal P0 protein. *Nucleic Acids Res.* **37**, 3514-3521 (2009).

176. Kemmler, S., Occhipinti, L., Veisu, M. & Panse, V.G. Yvh1 is required for a late maturation step in the 60S biogenesis pathway. *J. Cell Biol.* **186**, 863-880 (2009).

177. Lo, K.Y., Li, Z., Wang, F., Marcotte, E.M. & Johnson, A.W. Ribosome stalk assembly requires the dual-specificity phosphatase Yvh1 for the exchange of Mrt4 with P0. *J. Cell Biol.* **186**, 849-862 (2009).

178. Kargas, V. *et al.* Mechanism of completion of peptidyltransferase centre assembly in eukaryotes. *eLife* **8**, e44904 (2019).

179. Sulima, S.O., Gulay, S.P., Anjos, M., Patchett, S., Meskauskas, A., Johnson, A.W. & Dinman, J.D. Eukaryotic rpL10 drives ribosomal rotation. *Nucleic Acids Res.* **42**, 2049-2063 (2014).

180. Hedges, J., West, M. & Johnson, A.W. Release of the export adapter, Nmd3p, from the 60S ribosomal subunit requires Rpl10p and the cytoplasmic GTPase Lsg1p. *EMBO J.* **24**, 567-579 (2005).

181. Fernández-Pevida, A., Rodríguez-Galán, O., Díaz-Quintana, A., Kressler, D. & de la Cruz, J. Yeast ribosomal protein L40 assembles late into precursor 60S ribosomes and is required for their cytoplasmic maturation. *J. Biol. Chem.* **287**, 38390-38407 (2012).

182. Malyutin, A.G., Musalgaonkar, S., Patchett, S., Frank, J. & Johnson, A.W. Nmd3 is a structural mimic of eIF5A, and activates the cpGTPase Lsg1 during 60S ribosome biogenesis. *EMBO J.* **36**, 854-868 (2017).

183. Bécam, A.M., Nasr, F., Racki, W.J., Zagulski, M. & Herbert, C.J. Ria1p (Ynl163c), a protein similar to elongation factors 2, is involved in the biogenesis of the 60S subunit of the ribosome in *Saccharomyces cerevisiae*. *Mol. Genet. Genomics* **266**, 454-462 (2001).

184. Senger, B., Lafontaine, D.L., Graindorge, J.S., Gadal, O., Camasses, A., Sanni, A., Garnier, J.M., Breitenbach, M., Hurt, E. & Fasiolo, F. The nucle(ol)ar Tif6p and Efl1p are required for a late cytoplasmic step of ribosome synthesis. *Mol. Cell* **8**, 1363-1373 (2001).

185. Menne, T.F., Goyenechea, B., Sanchez-Puig, N., Wong, C.C., Tonkin, L.M., Ancliff, P.J., Brost, R.L., Costanzo, M., Boone, C. & Warren, A.J. The Shwachman-Bodian-Diamond syndrome protein mediates translational activation of ribosomes in yeast. *Nat. Genet.* **39**, 486-495 (2007).

186. Finch, A.J. *et al.* Uncoupling of GTP hydrolysis from eIF6 release on the ribosome causes Shwachman-Diamond syndrome. *Genes Dev.* **25**, 917-929 (2011).

187. Graindorge, J.S., Rousselle, J.C., Senger, B., Lenormand, P., Namane, A., Lacroute, F. & Fasiolo, F. Deletion of EFL1 results in heterogeneity of the 60 S GTPase-associated rRNA conformation. *J. Mol. Biol.* **352**, 355-369 (2005).

188. Weis, F., Giudice, E., Churcher, M., Jin, L., Hilcenko, C., Wong, C.C., Traynor, D., Kay, R.R. & Warren, A.J. Mechanism of eIF6 release from the nascent 60S ribosomal subunit. *Nat. Struct. Mol. Biol.* **22**, 914-919 (2015).

189. Lecompte, O., Ripp, R., Thierry, J.C., Moras, D. & Poch, O. Comparative analysis of ribosomal proteins in complete genomes: an example of reductive evolution at the domain scale. *Nucleic Acids Res.* **30**, 5382-5390 (2002).

190. Costanzo, M. *et al.* The genetic landscape of a cell. *Science* **327**, 425-431 (2010).

191. Chan, C.T., Pang, Y.L., Deng, W., Babu, I.R., Dyavaiah, M., Begley, T.J. & Dedon, P.C. Reprogramming of tRNA modifications controls the oxidative stress response by codon-biased translation of proteins. *Nat. Commun.* **3**, 937 (2012).

192. Kim, S.J. & Strich, R. Rpl22 is required for IME1 mRNA translation and meiotic induction in S. cerevisiae. *Cell Div.* **11**, 10 (2016).

193. Abrhamova, K., Nemcko, F., Libus, J., Prevorovsky, M., Halova, M., Puta, F. & Folk, P. Introns provide a platform for intergenic regulatory feedback of RPL22 paralogs in yeast. *PLoS One* **13**, e0190685 (2018).

194. Maitra, N., He, C., Blank, H.M., Tsuchiya, M., Schilling, B., Kaeberlein, M., Aramayo, R., Kennedy, B.K. & Polymenis, M. Translational control of one-carbon metabolism underpins ribosomal protein phenotypes in cell division and longevity. *Elife* **9**, e53127 (2020).

195. Kawashima, T., Douglass, S., Gabunilas, J., Pellegrini, M. & Chanfreau, G.F. Widespread use of non-productive alternative splice sites in *Saccharomyces cerevisiae*. *PLoS Genet.* **10**, e1004249 (2014).

196. Gabunilas, J. & Chanfreau, G. Splicing-mediated autoregulation modulates Rpl22p expression in *Saccharomyces cerevisiae*. *PLoS Genet.* **12**, e1005999 (2016).

197. Parenteau, J., Durand, M., Morin, G., Gagnon, J., Lucier, J.F., Wellinger, R.J., Chabot, B. & Elela, S.A. Introns within ribosomal protein genes regulate the production and function of yeast ribosomes. *Cell* **147**, 320-331 (2011).

198. Steffen, K.K., MacKay, V.L., Kerr, E.O., Tsuchiya, M., Hu, D., Fox, L.A., Dang, N., Johnston, E.D., Oakes, J.A., Tchao, B.N., Pak, D.N., Fields, S., Kennedy, B.K. & Kaeberlein, M. Yeast life span extension by depletion of 60S ribosomal subunits is mediated by Gcn4. *Cell* **133**, 292-302 (2008).

199. Cao, B., Fang, Z., Liao, P., Zhou, X., Xiong, J., Zeng, S. & Lu, H. Cancer-mutated ribosome protein L22 (RPL22/eL22) suppresses cancer cell survival by blocking p53-MDM2 circuit. *Oncotarget* **8**, 90651-90661 (2017).

200. Houmani, J.L., Davis, C.I. & Ruf, I.K. Growth-promoting properties of Epstein-Barr virus EBER-1 RNA correlate with ribosomal protein L22 binding. *J. Virol.* **83**, 9844-9853 (2009).

201. Minervini, C.F., Berloco, M.F., Marsano, R.M. & Viggiano, L. The ribosomal protein RpL22 interacts in vitro with 5'-UTR sequences found in some *Drosophila melanogaster* transposons. *Genes* **13**, 305 (2022).

202. Gietz, D., St. Jean, A., Woods, R.A. & Schiestl, R.H. Improved method for high efficiency transformation of intact yeast cells. *Nucleic Acids Res.* **20**, 1425 (1992).

203. Sambrook, J., Fritsch, E.F. & Maniatis, T. *Molecular cloning: a laboratory manual*, (Cold Spring Harbor Laboratory Press, Cold Spring Harbor, N. Y., 1989).

204. Kaiser, C., Michaelis, S. & Mitchell, A. *Methods in yeast genetics: a Cold Spring Harbor Laboratory Course Manual*, (Cold Spring Harbor Laboratory Press, Cold Spring Harbor, N. Y., 1994).

205. Salas-Marco, J. & Bedwell, D.M. Discrimination between defects in elongation fidelity and termination efficiency provides mechanistic insights into translational readthrough. *J. Mol. Biol.* **348**, 801-815 (2005).

206. Keeling, K.M., Lanier, J., Du, M., Salas-Marco, J., Gao, L., Kaenjak-Angeletti, A. & Bedwell, D.M. Leaky termination at premature stop codons antagonizes nonsense-mediated mRNA decay in *S. cerevisiae*. *RNA* **10**, 691-703 (2004).

207. Kressler, D., de la Cruz, J., Rojo, M. & Linder, P. Fal1p is an essential DEAD-box protein involved in 40S-ribosomal-subunit biogenesis in *Saccharomyces cerevisiae*. *Mol. Cell. Biol.* **17**, 7283-7294 (1997).

208. Ausubel, F.M., Brent, R., Kingston, R.E., Moore, D.D., Seidman, J.G., Smith, J.A. & Struhl, K. *Saccharomyces cerevisiae*. in *Current Protocols in Molecular Biology* 13.0.1-13.14.17 (John Wiley & Sons, Inc., New York, N. Y., 1994).

209. Venema, J., Planta, R.J. & Raué, H.A. *In vivo* mutational analysis of ribosomal RNA in *Saccharomyces cerevisiae*. in *Protein synthesis: Methods and Protocols* (ed. Martin, R.) 257-270 (Humana Press, Totowa, N. J., 1998).

210. Kressler, D., de la Cruz, J., Rojo, M. & Linder, P. Dbp6p is an essential putative ATP-dependent RNA helicase required for 60S-ribosomal-subunit assembly in *Saccharomyces cerevisiae*. *Mol. Cell. Biol.* **18**, 1855-1865 (1998).

211. García-Gómez, J.J., Lebaron, S., Froment, C., Monsarrat, B., Henry, Y. & de la Cruz, J. Dynamics of the putative RNA helicase Spb4 during ribosome assembly in *Saccharomyces cerevisiae*. *Mol. Cell. Biol.* **31**, 4156-4164 (2011).

212. Gietz, R.D. & Sugino, A. New yeast-*Escherichia coli* shuttle vectors constructed with *in vitro* mutagenized yeast genes lacking six-base pair restriction sites. *Gene* **74**, 527-534 (1988).

213. Ulbrich, C., Diepholz, M., Bassler, J., Kressler, D., Pertschy, B., Galani, K., Böttcher, B. & Hurt, E. Mechanochemical removal of ribosome biogenesis factors from nascent 60S ribosomal subunits. *Cell* **138**, 911-922 (2009).

214. Belk, J.P., He, F. & Jacobson, A. Overexpression of truncated Nmd3p inhibits protein synthesis in yeast. *RNA* **5**, 1055-1070 (1999).

215. Wawiórka, L., Molestak, E., Szajwaj, M., Michalec-Wawiórka, B., Molon, M., Borkiewicz, L., Grela, P., Boguszewska, A. & Tchórzewski, M. Multiplication of ribosomal P-stalk proteins contributes to the fidelity of translation. *Mol. Cell. Biol.* **37**, e00060-17 (2017).

216. Martín-Villanueva, S., Fernández-Fernández, J., Rodríguez-Galán, O., Fernández-Boraita, J., Villalobo, E. & de la Cruz, J. Role of the 40S beak ribosomal protein eS12 in ribosome biogenesis and function in *Saccharomyces cerevisiae*. *RNA Biol.* **17**, 1271-1276 (2020).

217. Rossler, I., Weigl, S., Fernández-Fernández, J., Martín-Villanueva, S., Strauss, D., Hurt, E., de la Cruz, J. & Pertschy, B. The C-terminal tail of ribosomal protein Rps15 is engaged in cytoplasmic pre-40S maturation. *RNA Biol.* **19**, 560-574 (2022).

218. de la Cruz, J., Karbstein, K. & Woolford, J.L., Jr. Functions of ribosomal proteins in assembly of eukaryotic ribosomes *in vivo*. *Annu. Rev. Biochem.* **84**, 93-129 (2015).

219. Gadal, O., Strauss, D., Kessl, J., Trumpower, B., Tollervey, D. & Hurt, E. Nuclear export of 60S ribosomal subunit depends on Xpo1p and requires a nuclear export

sequence-containing factor, Nmd3p, that associates with the large subunit protein Rpl10p. *Mol. Cell. Biol.* **21**, 3405-3415 (2001).

220. Peisker, K., Braun, D., Wolfle, T., Hentschel, J., Funfschilling, U., Fischer, G., Sickmann, A. & Rospert, S. Ribosome-associated complex binds to ribosomes in close proximity of Rpl31 at the exit of the polypeptide tunnel in yeast. *Mol. Biol. Cell* **19**, 5279-5288 (2008).

221. Meyer, A.E., Hung, N.J., Yang, P., Johnson, A.W. & Craig, E.A. The specialized cytosolic J-protein, Jjj1, functions in 60S ribosomal subunit biogenesis. *Proc. Natl. Acad. Sci. USA* **104**, 1558-1563 (2007).

222. O'Leary, M.N. *et al.* The ribosomal protein Rpl22 controls ribosome composition by directly repressing expression of its own paralog, Rpl22l1. *PLoS Genet.* **9**, e1003708 (2013).

223. Micic, J., Rodríguez-Galán, O., Babiano, R., Fitzgerald, F., Fernández-Fernández, J., Zhang, Y., Gao, N., Woolford, J.L. & de la Cruz, J. Ribosomal protein eL39 is important for maturation of the nascent polypeptide exit tunnel and proper protein folding during translation. *Nucleic Acids Res.* **50**, 6453-6473 (2022).

224. Gerhardy, S., Oborska-Oplova, M., Gillet, L., Borner, R., van Nues, R., Leitner, A., Michel, E., Petkowski, J.J., Granneman, S., Sigel, R.K.O., Aebersold, R. & Panse, V.G. Puf6 primes 60S pre-ribosome nuclear export at low temperature. *Nat. Commun.* **12**, 4696 (2021).

225. Saveanu, C., Namane, A., Gleizes, P.E., Lebreton, A., Rousselle, J.C., Noaillac-Depeyre, J., Gas, N., Jacquier, A. & Fromont-Racine, M. Sequential protein association with nascent 60S ribosomal particles. *Mol. Cell. Biol.* **23**, 4449-4460 (2003).

226. Simoff, I., Moradi, H. & Nygard, O. Functional characterization of ribosomal protein L15 from *Saccharomyces cerevisiae*. *Curr. Genet.* **55**, 111-125 (2009).

227. Dong, Z., Jiang, H., Liang, S., Wang, Y., Jiang, W. & Zhu, C. Ribosomal protein L15 is involved in colon carcinogenesis. *Int. J. Med. Sci.* **16**, 1132-1141 (2019).

228. Ebright, R.Y. *et al.* Deregulation of ribosomal protein expression and translation promotes breast cancer metastasis. *Science* **367**, 1468-1473 (2020).

229. Li, Y., Gong, Y., Ma, J. & Gong, X. Overexpressed circ-RPL15 predicts poor survival and promotes the progression of gastric cancer via regulating miR-502-3p/OLFM4/STAT3 pathway. *Biomed. Pharmacother.* **127**, 110219 (2020).

230. Ma, Y., Xue, H., Wang, W., Yuan, Y. & Liang, F. The miR-567/RPL15/TGF-beta/Smad axis inhibits the stem-like properties and chemo-resistance of gastric cancer cells. *Transl Cancer Res* **9**, 3539-3549 (2020).

231. Wang, H., Zhao, L.N., Li, K.Z., Ling, R., Li, X.J. & Wang, L. Overexpression of ribosomal protein L15 is associated with cell proliferation in gastric cancer. *BMC Cancer* **6**, 91 (2006).

232. Wu, Z., Sun, H., Liu, W., Zhu, H., Fu, J., Yang, C., Fan, L., Wang, L., Liu, Y., Xu, W., Li, J. & Jin, H. Circ-RPL15: a plasma circular RNA as novel oncogenic driver to promote progression of chronic lymphocytic leukemia. *Leukemia* **34**, 919-923 (2020).

233. Yan, T.T., Fu, X.L., Li, J., Bian, Y.N., Liu, D.J., Hua, R., Ren, L.L., Li, C.T., Sun, Y.W., Chen, H.Y., Fang, J.Y. & Hong, J. Downregulation of RPL15 may predict poor survival and associate with tumor progression in pancreatic ductal adenocarcinoma. *Oncotarget* **6**, 37028-37042 (2015).

234. Wlodarski, M.W. *et al.* Recurring mutations in RPL15 are linked to hydrops fetalis and treatment independence in Diamond-Blackfan anemia. *Haematologica* **103**, 949-958 (2018).

235. Brachmann, C.B., Davies, A., Cost, G.J., Caputo, E., Li, J., Hieter, P. & Boeke, J.D. Designer deletion strains derived from *Saccharomyces cerevisiae* S288C: a useful set of strains and plasmids for PCR-mediated gene disruption and other applications. *Yeast* **14**, 115-132 (1998).

236. Schütz, S., Fischer, U., Altvater, M., Nerurkar, P., Pena, C., Gerber, M., Chang, Y., Caesar, S., Schubert, O.T., Schlenstedt, G. & Panse, V.G. A RanGTP-independent mechanism allows ribosomal protein nuclear import for ribosome assembly. *eLife* **3**, e03473 (2014).

237. Jakob, S., Ohmayer, U., Neueder, A., Hierlmeier, T., Pérez-Fernández, J., Hochmuth, E., Deutzmann, R., Griesenbeck, J., Tschochner, H. & Milkereit, P. Interrelationships between yeast ribosomal protein assembly events and transient ribosome biogenesis factors interactions in early pre-ribosomes. *PLoS One* **7**, e32552 (2012).

238. Braun, C.M., Hackert, P., Schmid, C.E., Bohnsack, M.T., Bohnsack, K.E. & Pérez-Fernández, J. Pol5 is required for recycling of small subunit biogenesis factors and for formation of the peptide exit tunnel of the large ribosomal subunit. *Nucleic Acids Res.* **48**, 405-420 (2020).

239. Jakovljevic, J., Ohmayer, U., Gamalinda, M., Talkish, J., Alexander, L., Linnemann, J., Milkereit, P. & Woolford, J.L., Jr. Ribosomal proteins L7 and L8 function in concert with six A_3 assembly factors to propagate assembly of domains I and II of 25S rRNA in yeast 60S ribosomal subunits. *RNA* **18**, 1805-1822 (2012).

240. Helser, T.L., Baan, R.A. & Dahlberg, A.E. Characterization of a 40S ribosomal subunit complex in polyribosomes of *Saccharomyces cerevisiae* treated with cycloheximide. *Mol. Cell. Biol.* **1**, 51-57 (1981).

241. Rotenberg, M., Moritz, M. & Woolford, J.L., Jr. Depletion of *Saccharomyces cerevisiae* ribosomal protein L16 causes a decrease in 60S ribosomal subunits and formation of half-mer polysomes. *Genes Dev.* **2**, 160-172 (1988).

242. Eisinger, D.P., Dick, F.A. & Trumpower, B.L. Qsr1p, a 60S ribosomal subunit protein, is required for joining of 40S and 60S subunits. *Mol. Cell. Biol.* **17**, 5136-5145 (1997).

243. Fringer, J.M., Acker, M.G., Fekete, C.A., Lorsch, J.R. & Dever, T.E. Coupled release of eukaryotic translation initiation factors 5B and 1A from 80S ribosomes following subunit joining. *Mol. Cell. Biol.* **27**, 2384-2397 (2007).

244. Foiani, M., Cigan, A.M., Paddon, C.J., Harashima, S. & Hinnebusch, A.G. GCD2, a translational repressor of the *GCN4* gene, has a general function in the initiation of protein synthesis in *Saccharomyces cerevisiae*. *Mol. Cell. Biol.* **11**, 3203-3216 (1991).

245. Ramos-Sáenz, A., González-Álvarez, D., Rodríguez-Galán, O., Rodríguez-Gil, A., Gaspar, S.G., Villalobo, E., Dosil, M. & de la Cruz, J. Pol5 is an essential ribosome biogenesis factor required for 60S ribosomal subunit maturation in *Saccharomyces cerevisiae*. *RNA* **25**, 1561-1575 (2019).

246. Espinar-Marchena, F., Rodríguez-Galán, O., Fernández-Fernández, J., Linnemann, J. & de la Cruz, J. Ribosomal protein L14 contributes to the early assembly of 60S ribosomal subunits in *Saccharomyces cerevisiae*. *Nucleic Acids Res.* **46**, 4715-4732 (2018).

247. Babiano, R. & de la Cruz, J. Ribosomal protein L35 is required for 27SB pre-rRNA processing in *Saccharomyces cerevisiae Nucleic Acids Res.* **38**, 5177-5192 (2010).

248. Thomson, E. & Tollervey, D. Nop53p is required for late 60S ribosome subunit maturation and nuclear export in yeast. *RNA* **11**, 1215-1224 (2005).

249. Milkereit, P., Gadal, O., Podtelejnikov, A., Trumtel, S., Gas, N., Petfalski, E., Tollervey, D., Mann, M., Hurt, E. & Tschochner, H. Maturation and intranuclear transport of pre-ribosomes requires Noc proteins. *Cell* **105**, 499-509 (2001).

250. Abdelhaleem, M. Do human RNA helicases have a role in cancer? *Biochim. Biophys. Acta* **1704**, 37-46 (2004).

251. Wan, K., Yabuki, Y. & Mizuta, K. Roles of Ebp2 and ribosomal protein L36 in ribosome biogenesis in *Saccharomyces cerevisiae*. *Curr. Genet.* **61**, 31-41 (2014).

252. Pöll, G., Braun, T., Jakovljevic, J., Neueder, A., Jakob, S., Woolford, J.L., Jr., Tschochner, H. & Milkereit, P. rRNA maturation in yeast cells depleted of large ribosomal subunit proteins. *PLoS One* **4**, e8249 (2009).

253. Babiano, R., Gamalinda, M., Woolford, J.L., Jr. & de la Cruz, J. *Saccharomyces cerevisiae* ribosomal protein L26 is not essential for ribosome assembly and function. *Mol. Cell. Biol.* **32**, 3228-3241 (2012).

254. Gamalinda, M., Ohmayer, U., Jakovljevic, J., Kumcuoglu, B., Woolford, J., Mbom, B., Lin, L. & Woolford, J.L., Jr. A hierarchical model for assembly of eukaryotic 60S ribosomal subunit domains. *Genes Dev.* **28**, 198-210 (2014).

255. Yusupova, G. & Yusupov, M. High-resolution structure of the eukaryotic 80S ribosome. *Annu. Rev. Biochem.* **83**, 467-486 (2014).

256. Rodríguez-Mateos, M., García-Gómez, J.J., Francisco-Velilla, R., Remacha, M., de la Cruz, J. & Ballesta, J.P.G. Role and dynamics of the ribosomal protein P0 and its related *trans*-acting factor Mrt4 during ribosome assembly in *Saccharomyces cerevisiae*. *Nucleic Acids Res.* **37**, 7519-7532 (2009).

257. Bautista-Santos, A. & Zinker, S. The P1/P2 Protein Heterodimers Assemble to the Ribosomal Stalk at the Moment When the Ribosome Is Committed to Translation but Not to the Native 60S Ribosomal Subunit in *Saccharomyces cerevisiae*. *Biochemistry* **53**, 4105-4112 (2014).

258. Kressler, D., Rojo, M., Linder, P. & de la Cruz, J. Spb1p is a putative methyltransferase required for 60S ribosomal subunit biogenesis in *Saccharomyces cerevisiae*. *Nucleic Acids Res.* **27**, 4598-4608 (1999).

259. Bassler, J., Grandi, P., Gadal, O., Lessmann, T., Petfalski, E., Tollervey, D., Lechner, J. & Hurt, E. Identification of a 60S preribosomal particle that is closely linked to nuclear export. *Mol. Cell* **8**, 517-529 (2001).

260. Adams, C.C., Jakovljevic, J., Roman, J., Harnpicharnchai, P. & Woolford, J.L., Jr. *Saccharomyces cerevisiae* nucleolar protein Nop7p is necessary for biogenesis of 60S ribosomal subunits. *RNA* **8**, 150-165 (2002).

261. Granneman, S., Petfalski, E. & Tollervey, D. A cluster of ribosome synthesis factors regulate pre-rRNA folding and 5.8S rRNA maturation by the Rat1 exonuclease. *EMBO J.* **30**, 4006-4019 (2011).

262. Krogan, N.J. *et al.* High-definition macromolecular composition of yeast RNA-processing complexes. *Mol. Cell* **13**, 225-239 (2004).

263. Zhang, W. *et al.* The functional landscape of mouse gene expression. *J Biol* **3**, 21 (2004).

264. Talkish, J., Campbell, I.W., Sahasranaman, A., Jakovljevic, J. & Woolford, J.L., Jr. Ribosome assembly factors Pwp1 and Nop12 are important for folding of 5.8S rRNA during ribosome biogenesis in *Saccharomyces cerevisiae*. *Mol. Cell. Biol.* **34**, 1863-1877 (2014).

265. Ohmayer, U., Gil-Hernández, A., Sauert, M., Martín-Marcos, P., Tamame, M., Tschochner, H., Griesenbeck, J. & Milkereit, P. Studies on the coordination of ribosomal protein assembly events involved in processing and stabilization of yeast early large ribosomal subunit precursors. *PLoS One* **10**, e0143768 (2015).

266. Rai, J., Parker, M.D., Huang, H., Choy, S., Ghalei, H., Johnson, M.C., Karbstein, K. & Stroupe, M.E. An open interface in the pre-80S ribosome coordinated by ribosome assembly factors Tsr1 and Dim1 enables temporal regulation of Fap7. *RNA* **27**, 221-233 (2021).

267. Martín-Marcos, P., Gil-Hernández, A. & Tamame, M. Wide mutational analysis to ascertain the functional roles of eL33 in ribosome biogenesis and translation initiation. *Curr. Genet.* **68**, 619-644 (2022).

268. Nakai, K. & Kanehisa, M. A knowledge base for predicting protein localization sites in eukaryotic cells. *Genomics* **14**, 897-911 (1992).

269. Chu, S., Archer, R.H., Zengel, J.M. & Lindahl, L. The RNA of RNase MRP is required for normal processing of ribosomal RNA. *Proc. Natl. Acad. Sci. USA* **91**, 659-663 (1994).

270. Chamberlain, J.R., Lee, Y., Lane, W.S. & Engelke, D.R. Purification and characterization of the nuclear RNase P holoenzyme complex reveals extensive subunit overlap with RNase MRP. *Genes Dev.* **12**, 1678-1690 (1998).

271. Shimoji, K., Jakovljevic, J., Tsuchihashi, K., Umeki, Y., Wan, K., Kawasaki, S., Talkish, J., Woolford, J.L., Jr. & Mizuta, K. Ebp2 and Brx1 function cooperatively in 60S ribosomal subunit assembly in *Saccharomyces cerevisiae*. *Nucleic Acids Res.* **40**, 4574-4588 (2012).

272. Wehner, K.A. & Baserga, S.J. The sigma(70)-like motif: a eukaryotic RNA binding domain unique to a superfamily of proteins required for ribosome biogenesis. *Mol. Cell* **9**, 329-339 (2002).

273. Wu, K., Wu, P. & Aris, J.P. Nucleolar protein Nop12p participates in synthesis of 25S rRNA in *Saccharomyces cerevisiae*. *Nucleic Acids Res.* **29**, 2938-2949 (2001).

274. Sahasranaman, A., Dembowski, J., Strahler, J., Andrews, P., Maddock, J. & Woolford, J.L., Jr. Assembly of *Saccharomyces cerevisiae* 60S ribosomal subunits: role of factors required for 27S pre-rRNA processing. *EMBO J.* **30**, 4020-4032 (2011).

275. Pestov, D.G., Stockelman, M.G., Strezoska, Z. & Lau, L.F. *ERB1*, the yeast homolog of mammalian *Bop1*, is an essential gene required for maturation of the 25S and 5.8S ribosomal RNAs. *Nucleic Acids Res.* **29**, 3621-3630 (2001).

276. Gadal, O., Strauss, D., Petfalski, E., Gleizes, P.E., Gas, N., Tollervey, D. & Hurt, E. Rlp7p is associated with 60S preribosomes, restricted to the granular component of the nucleolus, and required for pre-rRNA processing. *J. Cell Biol.* **157**, 941-951 (2002).

277. Dunbar, D.A., Dragon, F., Lee, S.J. & Baserga, S.J. A nucleolar protein related to ribosomal protein L7 is required for an early step in large ribosomal subunit biogenesis. *Proc. Natl. Acad. Sci. USA* **97**, 13027-13032 (2000).

278. Ripmaster, T.L., Vaughn, G.P. & Woolford, J.L., Jr. A putative ATP-dependent RNA helicase involved in *Saccharomyces cerevisiae* ribosome assembly. *Proc. Natl. Acad. Sci. USA* **89**, 11131-11135 (1992).

279. Oeffinger, M., Leung, A., Lamond, A., Tollervey, D. & Lueng, A. Yeast Pescadillo is required for multiple activities during 60S ribosomal subunit synthesis. *RNA* **8**, 626-636 (2002).

280. Horsey, E.W., Jakovljevic, J., Miles, T.D., Harnpicharnchai, P. & Woolford, J.L., Jr. Role of the yeast Rrp1 protein in the dynamics of pre-ribosome maturation. *RNA* **10**, 813-827 (2004).

281. Gamalinda, M. & Woolford, J.L., Jr. Deletion of L4 domains reveals insights into the importance of ribosomal protein extensions in eukaryotic ribosome assembly. *RNA* **20**, 1725-1731 (2014).

282. Espinar-Marchena, F.J., Fernández-Fernández, J., Rodríguez-Galán, O., Fernández-Pevida, A., Babiano, R. & de la Cruz, J. Role of the yeast ribosomal protein L16 in ribosome biogenesis. *FEBS J.* **283**, 2968-2985 (2016).

283. Martín-Marcos, P., Hinnebusch, A.G. & Tamame, M. Ribosomal protein L33 is required for ribosome biogenesis, subunit joining, and repression of *GCN4* translation. *Mol. Cell. Biol.* **27**, 5968-5985 (2007).

284. Linnemann, J., Poll, G., Jakob, S., Ferreira-Cerca, S., Griesenbeck, J., Tschochner, H. & Milkereit, P. Impact of two neighbouring ribosomal protein clusters on biogenesis factor binding and assembly of yeast late small ribosomal subunit precursors. *PLoS One* **14**, e0203415 (2019).

285. Talkish, J., Biedka, S., Jakovljevic, J., Zhang, J., Tang, L., Strahler, J.R., Andrews, P.C., Maddock, J.R. & Woolford, J.L., Jr. Disruption of ribosome assembly in yeast blocks cotranscriptional pre-rRNA processing and affects the global hierarchy of ribosome biogenesis. *RNA* **22**, 852-866 (2016).

286. Biedka, S., Micic, J., Wilson, D., Brown, H., Diorio-Toth, L. & Woolford, J.L., Jr. Hierarchical recruitment of ribosomal proteins and assembly factors remodels nucleolar pre-60S ribosomes. *J. Cell Biol.* **217**, 2503-2518 (2018).

287. Burlacu, E., Lackmann, F., Aguilar, L.C., Belikov, S., Nues, R.V., Trahan, C., Hector, R.D., Dominelli-Whiteley, N., Cockroft, S.L., Wieslander, L., Oeffinger, M. & Granneman, S. High-throughput RNA structure probing reveals critical folding events during early 60S ribosome assembly in yeast. *Nat. Commun.* **8**, 714 (2017).

288. Osheim, Y.N., French, S.L., Keck, K.M., Champion, E.A., Spasov, K., Dragon, F., Baserga, S.J. & Beyer, A.L. Pre-18S ribosomal RNA is structurally compacted into the SSU processome prior to being cleaved from nascent transcripts in *Saccharomyces cerevisiae*. *Mol. Cell* **16**, 943-954 (2004).

289. Khoshnevis, S., Liu, X., Dattolo, M.D. & Karbstein, K. Rrp5 establishes a checkpoint for 60S assembly during 40S maturation. *RNA* **25**, 1164-1176 (2019).

290. Dez, C., Froment, C., Noaillac-Depeyre, J., Monsarrat, B., Caizergues-Ferrer, M. & Henry, Y. Npa1p, a component of very early pre-60S ribosomal particles, associates with a subset of small nucleolar RNPs required for peptidyl transferase center modification. *Mol. Cell. Biol.* **24**, 6324-6337 (2004).

291. Sun, C. & Woolford, J.L., Jr. The yeast *NOP4* gene product is an essential nucleolar protein required for pre-rRNA processing and accumulation of 60S ribosomal subunits. *EMBO J.* **13**, 3127-3135 (1994).

292. Gamalinda, M., Jakovljevic, J., Babiano, R., Talkish, J., de la Cruz, J. & Woolford, J.L., Jr. Yeast polypeptide exit tunnel ribosomal proteins L17, L35 and L37 are necessary to recruit late-assembling factors required for 27SB pre-rRNA processing. *Nucleic Acids Res.* **41**, 1965-1983 (2013).

293. Peculis, B.A. & Greer, C.L. The structure of the ITS2-proximal stem is required for pre-rRNA processing in yeast. *RNA* **4**, 1610-1622 (1998).

294. Henry, Y., Wood, H., Morrissey, J.P., Petfalski, E., Kearsey, S. & Tollervey, D. The 5' end of yeast 5.8S rRNA is generated by exonucleases from an upstream cleavage site. *EMBO J.* **13**, 2452-2463 (1994).